AN INVESTIGATION OF SHIP RELATED MOTION AND ITS EFFECT ON TURBULENCE MEASUREMENTS

Patrick Timothy Welsh

NAVAL POSTGRADUATE SCHOOL

Monterey, California

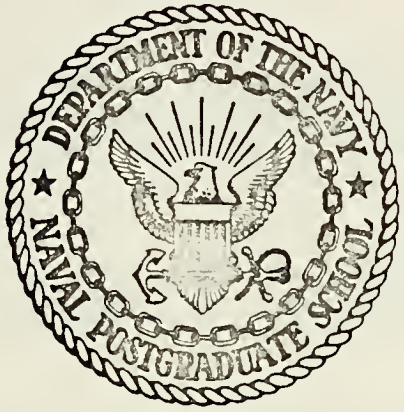

THESIS

AN INVESTIGATION OF SHIP RELATED MOTION

AND

ITS EFFECT ON TURBULENCE MEASUREMENTS

by

Patrick Timothy Welsh

Thesis Advisor: Kenneth L. Davidson

March 1974

REPORT

AN INVESTIGATION OF SHIP RELATED MOTION AND ITS EFFECT ON TURBULENCE MEASUREMENTS

by

Patrick Timothy Welsh
Lieutenant, United States Navy
B.S., United States Naval Academy, 1969

Submitted in partial fulfillment of the
requirements for the degree of

MASTER OF SCIENCE IN METEOROLOGY

from the

NAVAL POSTGRADUATE SCHOOL
March 1974

ABSTRACT

This study follows the development and initial employment of piezo-resistive accelerometers as ship motion sensors. The spectral results are discussed as they relate to concurrent measurements of wind fluctuation and temperature variance data. Both analog and digital Fourier analysis were performed. Results include co-spectra, quad-spectra, and phase and coherence plots. Biasing of mean parameters by pitching effects are also discussed.

TABLE OF CONTENTS

I. INTRODUCTION

The purpose of this study was to develop measurement procedures for shipboard motion and to analyze resulting data for information about platform motion effects on turbulence measurements. The shipboard motions of interest included the large scale motion associated with the waves, intermediate scales associated with heavy equipment vibration, and high frequency motions associated with vibrations of the instrument mast.

The results of this study are necessary in evaluations of different approaches for making turbulence measurements from a ship. In the past, turbulence measurements have been primarily made from land stations or stable overwater platforms. Open-ocean turbulence data are scarce because of the difficulties in describing turbulence properties from shipboard measurements.

This study is a part of a larger investigation being conducted by an interdisciplinary group at the Naval Postgraduate School on optical wave (laser) propagation in the marine boundary layer. The primary objective of the group is to relate optical propagation to the measureable properties of atmospheric turbulence. The area of concentration is to define the properties and effects unique to the marine environment. Since these effects depend upon turbulence properties related to the wind, temperature, humidity and wave conditions, a subgroup was formed to conduct micrometeorological observational experiments.

The purpose of the boundary layer investigation is to gather the data necessary to define the state of atmospheric turbulence during the propagation experiments. For this it is necessary to make both turbulence and profile measurements from a ship. During these experiments the ship is located along the propagation path.

The scarcity of actual data that can be used to verify existing boundary layer theory requires further empirical examination. While present boundary layer theory is primarily based on overland results, there is reason to believe that the turbulent regime of the marine boundary layer may differ significantly from that found in land-based studies, due to water wave effects.

This study is directly concerned with measurement problems encountered from unstable platforms, specifically ships. The phases in the study were the development of the measurement system, the measurement of motion during a turbulence experiment, and analysis of the results.

II. TURBULENCE MEASUREMENT CONSIDERATIONS

Parameters used in boundary layer descriptions include the wind shear stress parameter (U_*) and the heat flux parameter (T_*). The first parameter is a direct derivative of the mean flux of horizontal momentum in the vertical direction ($-\overline{u'w'}$) which is related to the vertical wind shear (du/dz). The second is also related to the vertical temperature gradient ($d\theta/dz$). The emphasis in this study is primarily on the wind shear stress parameter (U_*).

The wind shear stress parameter appears in the following expressions for the wind profile and wind gradient:

$$\overline{U} = \frac{U_*}{k} [\mathrm{Ln}(z/z_o)] \tag{1}$$

and

$$\frac{d\overline{U}}{dz} = \frac{U_*}{kz} \tag{2}$$

where $\overline{U}$ is the mean horizontal wind at height (z) over the surface of characteristic roughness length (z_o). The constant of proportionality (k) is the Von Karman constant.

Generally these expressions and other similar expressions have been formulated or evaluated with actual measured fluxes. This has been done almost exclusively from land experiments or from stable marine platforms. Such comparisons cannot be made from shipboard systems due to the unacceptable error induced by tilt angles as small as one degree to the vertical axis when measuring vertical fluxes.

However, on the basis of the Kolomogorov hypothesis for the spectral distribution of velocity variance and on the basis of the turbulent kinetic energy balance expression, one can obtain estimates of the

dissipation of turbulent kinetic energy (ε) and the dissipation of temperature variance (ε_θ) which can then be related to the fluxes.

Dissipation estimates are part of the Kolomogorov's hypothesis, i.e. there exists, in wave number space, a separate region between the frequencies which generate and dissipate turbulent kinetic energy. In this region, referred to as the inertial subrange, neither generation nor dissipation occurs. Turbulent kinetic energy is transferred to higher frequency disturbances until it is dissipated by viscous forces.

From this hypothesis, a -5/3 power law for the inertial subrange of wind fluctuation spectra was suggested (Figure 1). The equation has the form

$$\phi(k) = C \varepsilon^{2/3} k^{-5/3} \tag{3}$$

where $\phi(k)$ is the power spectrum of wind fluctuations; ε is dissipation of turbulent kinetic energy; k is the wave number of the disturbance within the inertial subrange, and C is a constant.

There is another relation for estimating . It is based on the wave number (k_o) which corresponds to the upper frequency limit of the inertial subrange as illustrated in Figure 1. The relation between and the wave number corresponding to the upper limit of inertial subrange is:

$$\frac{k_o \overline{U}}{2\pi} = \left(\frac{\gamma^3}{\varepsilon}\right)^{1/4} \tag{4}$$

Both relations should be fully exploited for best results, and both require accurate description of spectral properties. Further discussion is available in Johnston (1974).

The dissipation rate (ε) can also be related to stability parameters and the stress parameter (U_*) by the equation:

$$\varepsilon = \frac{U_*^3}{kz} \left[{}_m\left(\frac{Z}{L}\right) - \frac{Z}{L}\right] \tag{5}$$

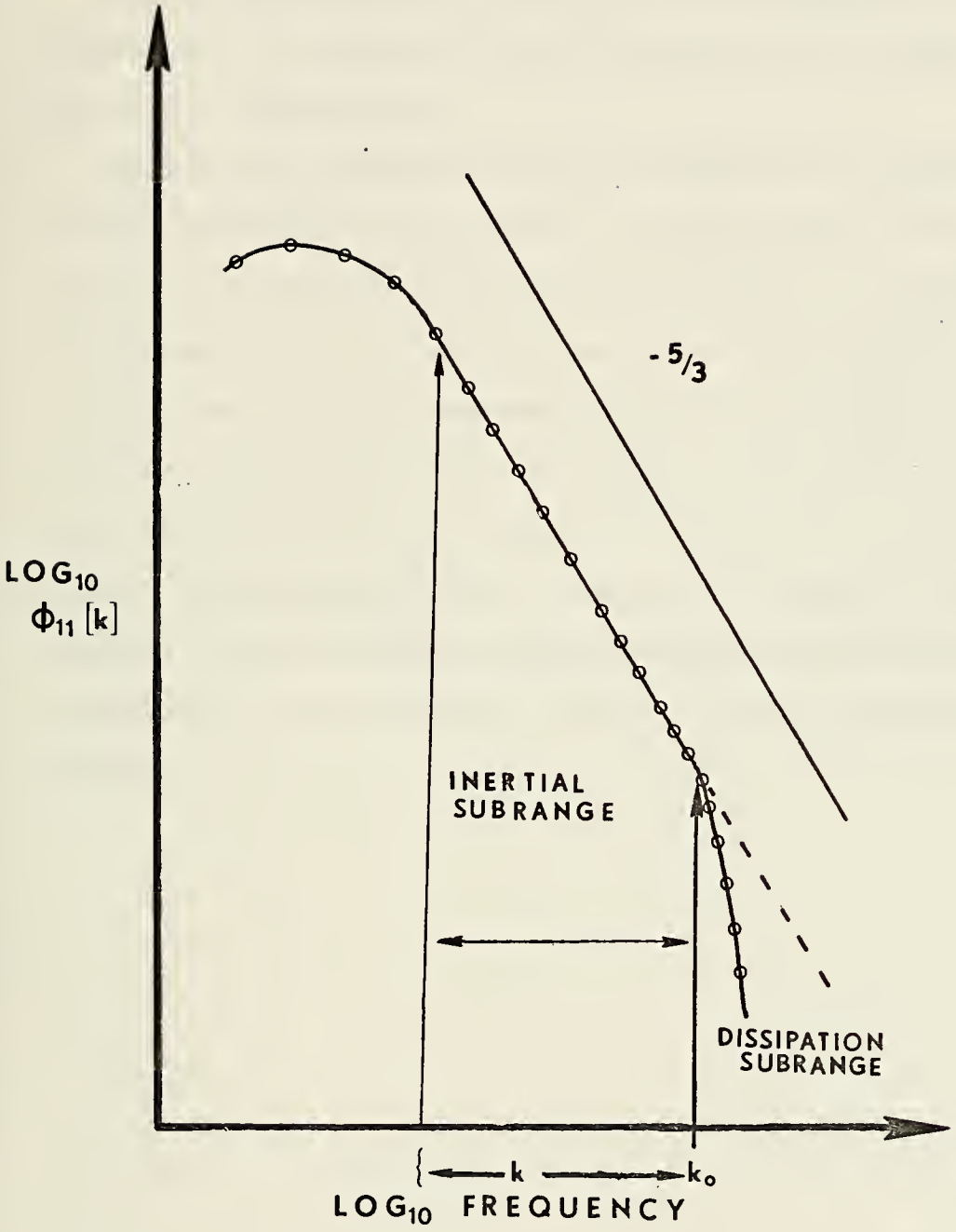

Figure 1. Turbulence Regime in Wavenumber Space.

where $\phi_m(\frac{Z}{L})$ is an empirically derived stability function dependent on the air-sea temperature difference. L is the MONIN-OBUKOV stability length.

Similar expressions exist which relate the dissipation of temperature variance (ε_θ) to larger scale thermal properties of the boundary layer, but are not discussed here.

The key in an approach in which flux estimates are obtained from dissipation estimates is the ability to obtain accurate descriptions of the spectra associated with wind fluctuations (u'), and temperature fluctuations (t'). With good spectral data reliable estimates of ε and ε_θ can be made. Initial experiments aboard the R/V Acania yielded velocity spectra which appeared contaminated due to ship-related motion and thus demonstrated the need for this study. Figure 2 illustrates the results of unpublished studies by Kasales (1973) aboard R/V Acania. The recurrent spikes and improper slope of produced spectra required the development of a sensor system to check the origin of such spectral deviation.

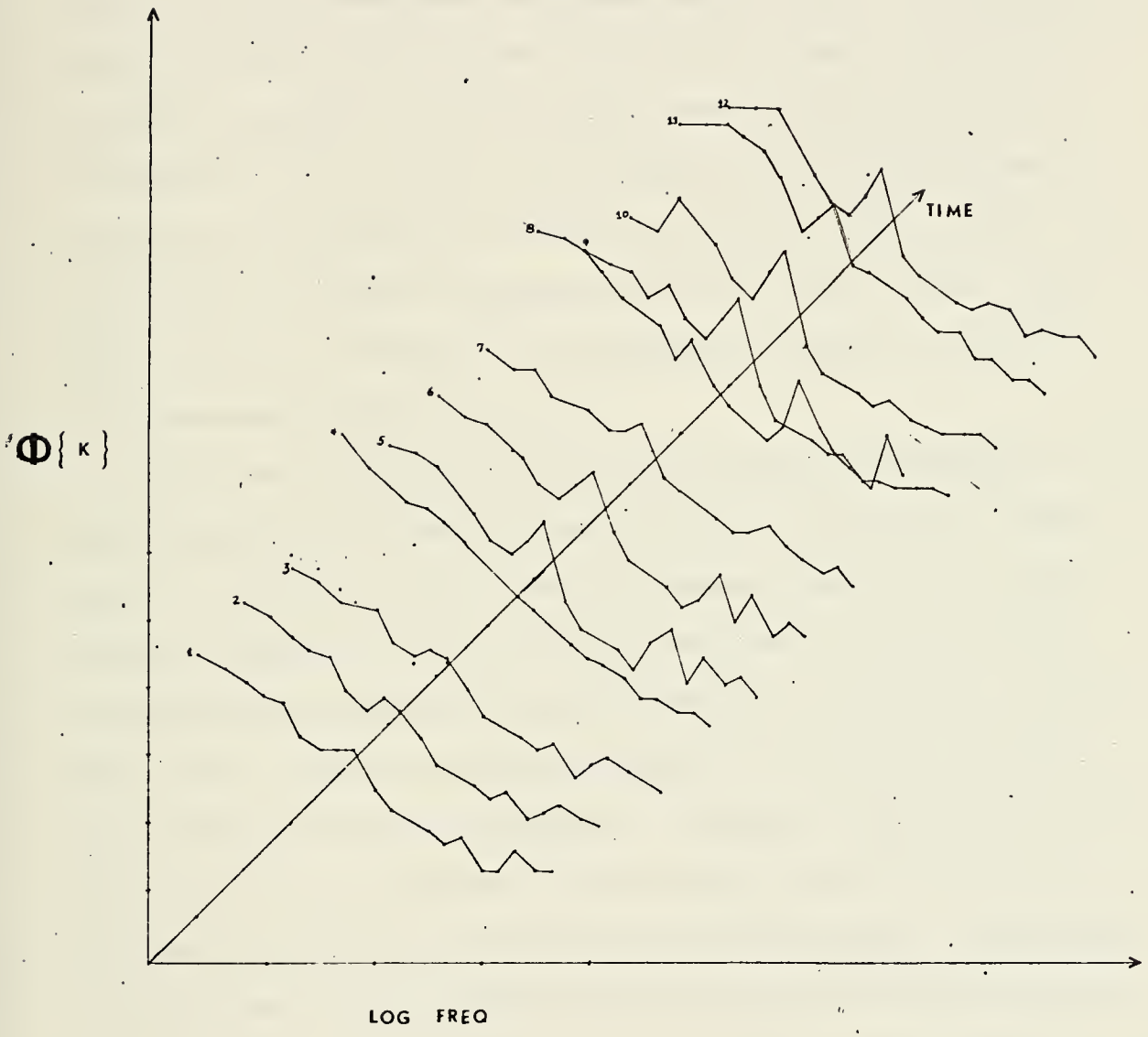

Figure 2. Kasales Wind Fluctuation Spectra.

III. DEVELOPMENT OF MEASUREMENT SYSTEM

A. SUMMARY OF DEVELOPMENT

The experiment, which commenced on 13 September 1973 and lasted ten days, was the final phase of a continuous program of observational research and sensor development which began early in 1973. The plan to examine ship motion was initiated in July 1973. Sensor availability with only two months of lead time proved to be a limiting factor in the experiment. Other meteorological sensors such as quartz thermometers were in procurement processes for six months or more. Some had been used in previous experiments and on the earlier cruise to San Nicholas Island. Other sensors and systems were being used on shipboard experiments for the first time.

A field test of a piezoresistive accelerometer was performed in early August after preliminary sensor evaluation. The reason for the test was to check the sensor's very low frequency response and also to estimate its signal to noise level. For the test, one piezoresistive accelerometer was taken aboard the R/V Acania for an afternoon cruise in Monterey Bay. The test was hindered somewhat due to spray associated with pitching in large swell conditions. However, sufficient data were recorded to verify a satisfactory low frequency response to the wave field and to verify that there was sufficient signal level. The particular accelerometer used in this test had less than half the rated signal level of the sensor ultimately used, and also had a higher resonant frequency.

The selection of the desired sensor, and the construction of the conditioning unit were begun after completion of the shipboard feasibility trial. Procurement was expedited yet all development tasks were completed only slightly more than a week before the experiment.

Calibration was limited due to time available and the necessity for syttem check-out. Calibration information from tests by the manufacturer on each of the six instruments was available and were depended on heavily. In particular, response changes with frequency had to be accepted. However, the manufacturer's signal level calibrations could not be used due to a change in the excitation voltage supplied to the accelerometer by a modified conditioning unit. Calibration of signal levels were completed prior to installation aboard the R/V Acania.

B. SELECTION CRITERIA

Several criteria were defined as being important in the final selection of the instrument to be used as the motion sensor. Factors which later proved to be most important were signal output level, cost, and availability as well as range of frequency response. Both gyroscopes and accelerometers were included in the initial consideration. Gyroscopic systems would have been most valuable in interpreting low frequency motion. They also would have provided inherent stable orientations of the axes. However, they were either too large or too expensive for use in this experiment. A typical cost would have been in excess of thirty thousand dollars for a triaxial prepackaged system, and a lease would have been about five thousand dollars for the necessary time frame.

After tests on the sensitivity of the instrument on board the R/V Acania, (described previously), the piezoresistive accelerometer was chosen. Its advantages were its very small size, weight, and linear

response over a broad frequency range. The piezoresistive transducer consists of a seismic mass and four semiconductor crystals which support the mass, two in tension and two in compression, Figure 3. The resistance of the crystalline material changes with a change in stress on the crystal. In a bridge circuit, the resistance change produces a signal voltage. Any acceleration of the mass along its axis of support by the crystals will cause a change in crystal stress. The lack of dependence on crystal support except along a single axis provides directional sensitivity with only a small transverse sensitivity. The resulting signal voltage in a bridge circuit is directly proportional to the acceleration, and is sensitive even to very low frequency or steady state accelerations such as gravity.

The thermal effects on the sensitivity of the accelerometer were not as critical as first envisioned. Thermal effects must be considered whenever a resistance type sensor is being used. Tests indicated a deviation of less than three percent from the measurement of the manufacturer's rated (75°F) temperature over a range from 0 to 160°F. During the experiment the maximum temperature variation was nine Fahrenheit degrees which occurred over several data periods. A thermal zero shift due to temperature changes was noticeable in analog traces extending over periods of hours. This was associated with diurnal temperature variations.

Gravity contamination proved to be the most serious problem, as was expected. Depending on the axis of orientation the change in the component if gravitational acceleration due to the axial tilting would exceed the value of the translational acceleration. In particular, a beam sea produces roll of the R/V Acania often in excess of ten degrees, hence the component of the gravitational acceleration can exceed the actual

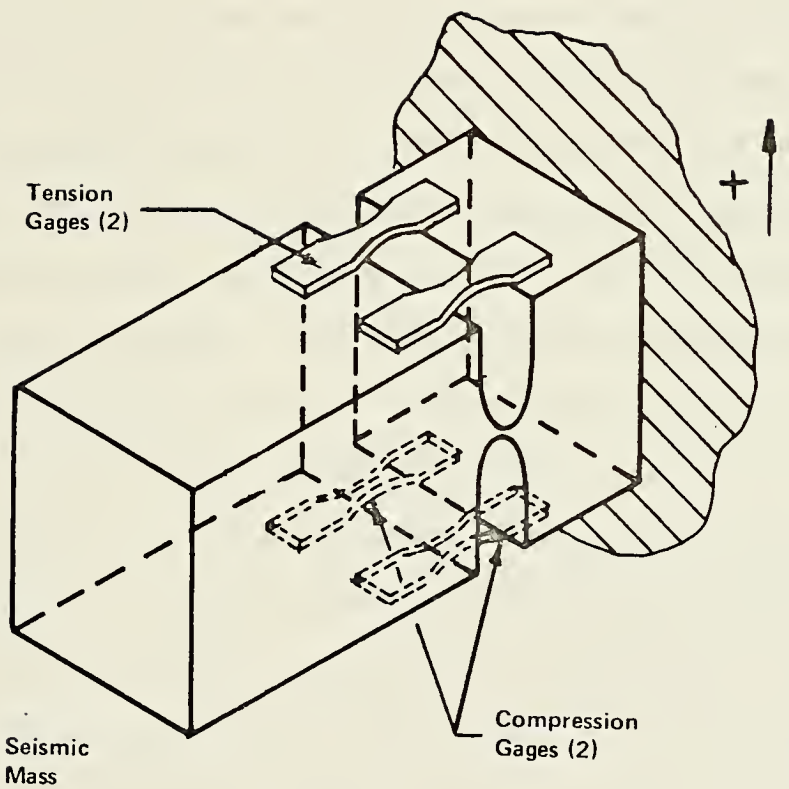

Figure 3. Model Diagram for a Piezoresistive Accelerometer.

lateral acceleration. However this effect is expected to occur only within a narrow low frequency spectral band. Because of the gravity effect, pitch is generally a more reliable axis for low frequency accelerometer data. This is fortunate since the ship was headed into the wind and sea during measurements in order to obtain better sampling of the wind field. Thus, the motion due to pitch was greater than that due to roll. Gravity contamination limited quantitative analysis of wave and ship interaction frequencies for this study. This could probably be overcone by different mounting arrangement, such as mentioned by Miyake (1970).

Integration of the accelerometer data was not a serious problem. Analog integration was performed and the results were excellent for low frequency study. Such integration is a form of low pass filtering. This would seem to nullify the advantage of the broader frequency spectrum, however, this is not the case. Assuming a relatively small number of sinusoidal Fourier components, which when integrated keep the same frequency but shift in phase, it does not matter if the accelerations are integrated or not for spectral analysis studies.

The piezoresistive accelerometers were selected in part because of their availability. Fortunately those available from the supplier covered the expected frequency range and had a high signal to acceleration ratio. The problem bandwidth versus signal level was minimized. In this regard, the minimum bandwidth necessary should be such that the signal level will sufficiently exceed noise.

It is characteristic of the device that the resonant frequency (F_r) determines the bandwidth. Two easy estimates of acceptable bandwidth are the four percent error point of one-fifth of resonant frequency,

and the half power (-3 db) point of one-half resonant frequency. Graphical plots of frequency response normalized by resonant frequency (relative frequency response) can be found in Appendix A.

Another important consideration was the susceptibility of the sensors to shock damage due to dropping or metal to metal contact. In fact, one of the six sensors used in this study failed in spite of special shock blocking included by the manufacturer, and careful handling by the experimenter.

Without regard to the long-term zero shift previously mentioned, the reproducibility of measurements was better than one percent in calibration runs and approached three digit accuracy for four sensors out of six. This calibration accuracy exceeded that of all instruments used in the experiment with the exception of the quartz thermometers. Post experimental calibration was not successful due to recording and conditioning gain problems during the experiment.

C. CONDITIONING OF SIGNALS

The accelerometers required additional components before voltage signals could be recorded. Two primary considerations were that the signal had to be amplified from a few millivolts up to the order of one volt, and that the Wheatstone bridge circuit had to be completed. Although a system was available from the manufacturer, construction of a bridge system for six accelerometers was accomplished at the Naval Postgraduate School.

The Wheatstone bridge in this system was located in two sepatate parts and joined by the cables. The side of the bridge corresponding to the accelerometer changes resistance (in the manner previously described) in response to the excitation voltage allowing a varying current

to flow through one-half of the bridge circuit. The other half of the bridge circuit consistes of a matched pair of 1.7 K ohm resistors.

Additional bridge components consisted of a 10 K ohm current limiting resistor, a balance potentiometer for nulling the steady state current and the excitation power supply. The power supply was solid state controlled and had a direct current output of five volts.

The manufacturer's rated excitation voltage for the accelerometers was twice that supplied by the conditioning unit which was used. This resulted in a signal level degradation by a factor of nearly three from that specified for the sensor. Instead of signal levels of over 30 millivolts per g (gravity force) unamplified, voltages were of the order of 10 to 12 millivolts per g. Bridge signals were amplified by a solid state millivolt amplifier with resistors matched for a hundredfold gain, but limited by a variable resistor used as an output attenuator. The signal voltage was that which existed between this resistor and ground. It was amplified by gains of from 30 to 60 before recording.

A diagram of the accelerometer-cable-conditioning unit is shown as Figure 4. Unfortunately, the conditioning unit was inadvertently decalibrated during a tape recorder change. This also was complicated by recorder calibration problems.

D. MOUNTING CONSIDERATIONS

The accelerometer triads were mounted during the experiment at the base of the mast 2.54 m above the waterline and at the highest level of meteorological instruments approximately 14.42 m, Figure 5. The lower mounting was envisioned primarily as a pitch and roll mounting with the hope that it would also measure any specific hull vibrations transferred to the mast through its mountings. The upper mounting was designed

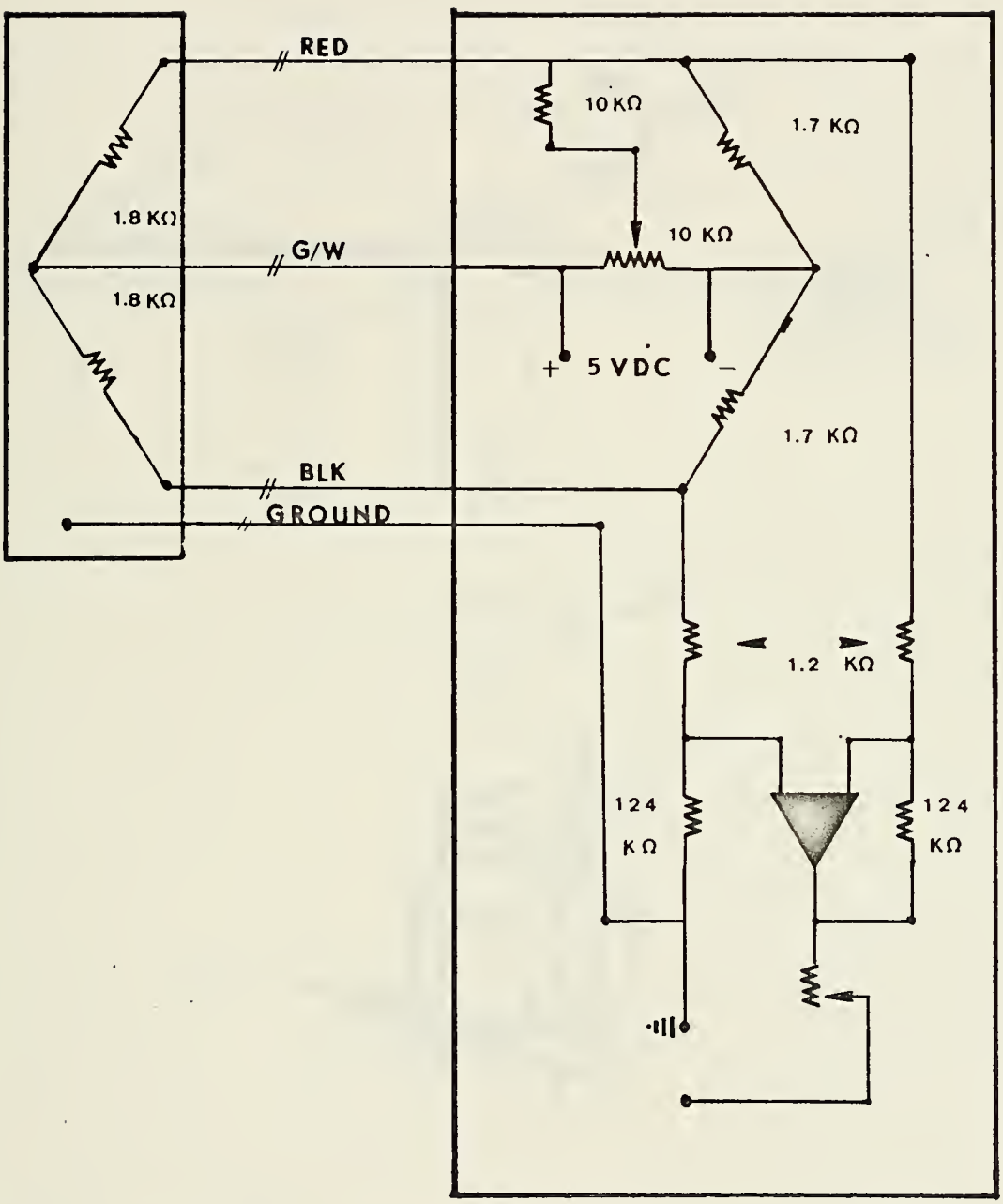

Figure 4. Circuit Diagram for the Measurement System.

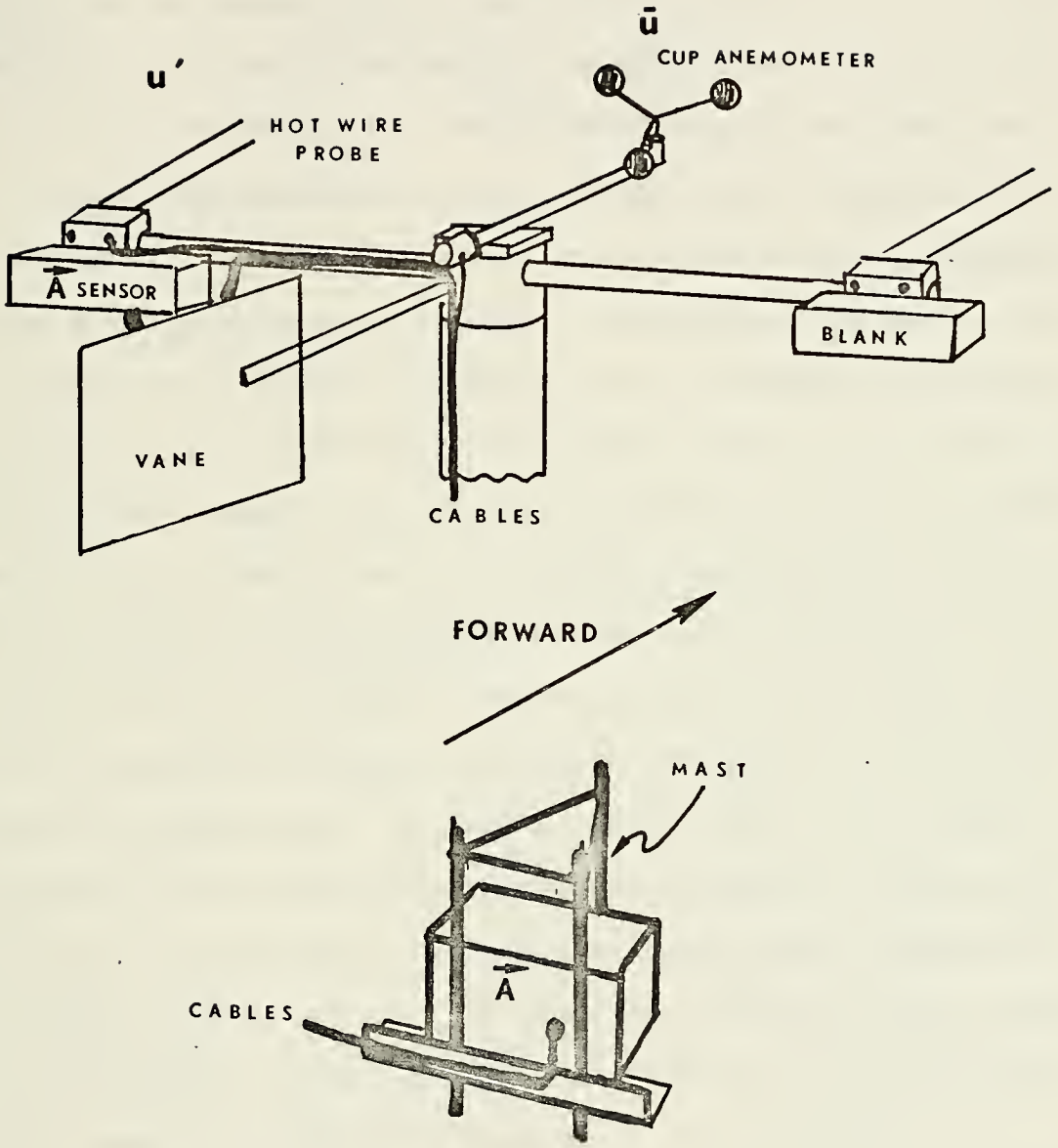

Figure 5. Vane Assembly for Upper Level, Mast Mounting at Lower Level.

to describe as exactly as possible the vibrations to which the wind fluctuations probe was subjected, with the secondary objective of showing by comparison with the lower sensor, any mast structure deviations from solid body motion. Few deviations due to mast motion were expected for low frequencies because of guy wires attached to the mast at two levels. The lattice structure of the mast was expected to contribute some unique high frequency vibrations not found in the spectra of the lower sensor.

Special considerations were made to insure proper mounting of the accelerometers. To give the greatest reproduction of motion the mounting system had to be as rigid as possible. In this regard the upper triad of sensors were mounted in an aluminum casing and directly connected to the wind fluctuation probe assembly by tapping screws into the base block of the probe assembly. This was done to maximize the correlation between the vibrations sensed by the wind fluctuation probe and those sensed by the accelerometer group. Aluminum was chosen as the material for the container since both the size of the casing and its weight could affect the wind resistance and balance of the vane assembly which aligned the probe with the mean wind. To minimize these effects a second casing of the same size with added internal weight was added to the opposite side of the vane probe assembly. The vane with both casings attached was at the highest level on the mast. Accelerations at that level were compared with the wind fluctuation spectra at that level as well as with accelerations measured at deck level, Figure 6.

The lower sensor package was constructed of dressed one-inch lumber and was eight inches square and nine inches deep. It was waterproofed with a jam lid, silicone rubber sealant and waterproof canvas tape.

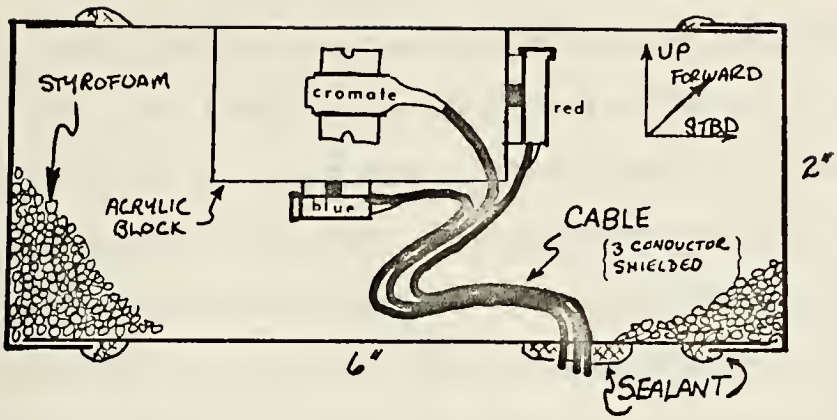

UPPER LEVEL

MOUNTING

LOWER LEVEL

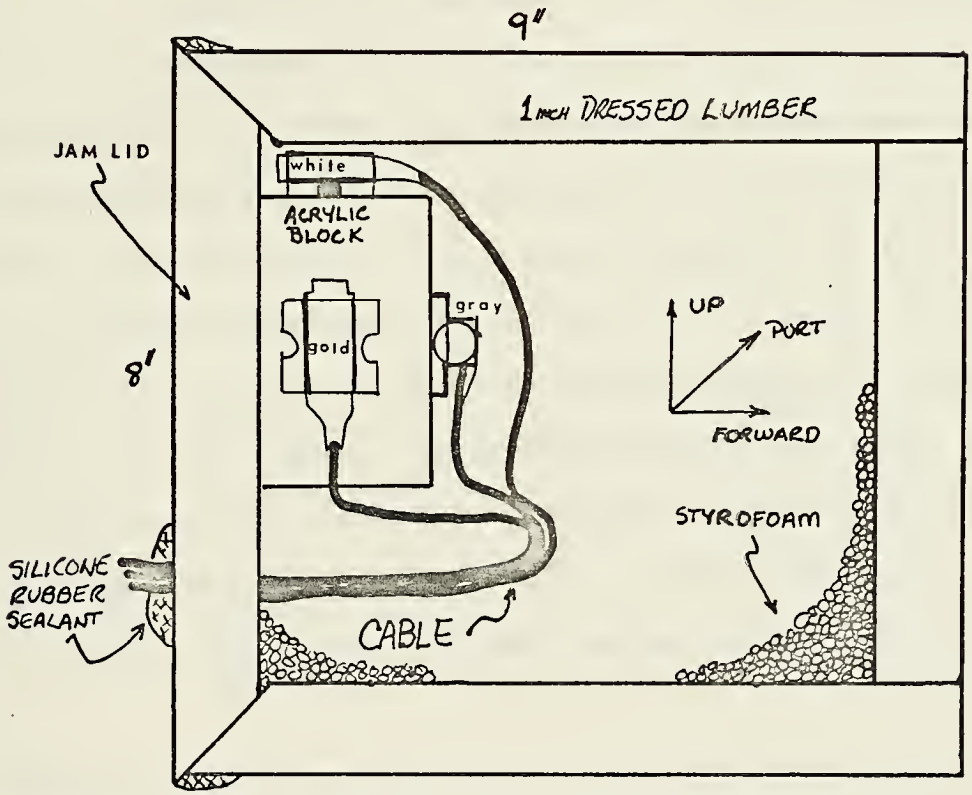

Figure 6. Internal Casing Configurations.

Mounting was on angle iron about four inches off the deck surface to prevent pooling of water, and additionally rigidized with nylon strapping tape. The lower triad was aligned with the ship's centerline.

Internally, both mountings were similar with emphasis on rigidity and thermal insulation. The purpose of the latter was to reduce the effect temperature changes associated with solar radiation, relative wind shifts which would change the ventilation of the casing surface, and possibly turbulent temperature fluctuations. One procedure used to reduce temperature changes was to paint both casings white. Additionally each set of three sensors was mounted on an acrylic block with one sensor on each of three mutually perpendicular faces.

Acrylic plastic is solid and is therefore good for vibration transmission. It is also a poor heat conductor which provided extra thermal protection over metallic blocks. The surface of the acrylic can be buffed very smooth and suffers less deformation damage than wood surfaces. The buffing provided a good contact and minimal warping of the accelerometer face. Unfortunately the acrylic proved to be too brittle to allow tapping holes for mounting screws so the accelerometers were mounted on double sided tape as a compromise rather than permanently affix them with epoxy glue. This measure proved satisfactory because of the small sensor weight along with the additional support from styrofoam pellets which filled the cavities providing the final thermal insulation. The acrylic block was then glued to the outer casing, and the casings were sealed.

Cabling was attached permanently with waterproofed connections to each accelerometer. The cable was a triaxial-grounded shield type. Cables were 200 feet in length. The cables from upper and lower sensor

packages were strung from the foredeck of the R/V Acania to the dry laboratory where they were connected to the conditioning unit. Cables were color coded with respect to sensors and conditioning amplifiers during calibration and were not changed during the experiment.

Initial shipboard checkout during the very calm conditions of early morning indicated that one sensor had failed during installation. Therefore the deck mounted triad of sensors was reoriented to exclude the fore and aft accelerations in favor of pitch and roll accelerations.

IV. THE EXPERIMENT

A. SUMMARY OF THE INSTRUMENT SUITE

The observational experiment was conducted aboard the R/V Acania, Figure (7), operated by the Department of Oceanography. The ship is over 48 meters in length, has 6.5 meter beam and has a draft of 2.7 meters.

The complete instrument suite consisted of groups of meteorological instruments mounted at several levels on a 50-foot mast on the foredeck of the ship and a short mast at the bow. Additionally, a sea-surface temperature probe was trailed from a boom amidships.

The optical portion of the experiment included a gyro-stabilized helium neon laser mounted in the wet laboratory. The laser receiving equipment was located on the northwest tip of San Nicolas Island.

The mean parameter components of the meteorological instrument suite included cup anemometers for mean wind measurements, hygrosensors for humidity measurements, and quartz thermometers for mean temperature readings. Additional information on these sensors has been provided by Cavanaugh (1974).

Fluctuations in temperature and velocity were measured with hot-wire type sensors used with different overheat characteristics. Further discussion of these is provided by Johnston (1974). Photographs of instrument arrays appear in Appendix B.

B. RECORDING OF DATA

Conditioned signals were recorded on a Sangamo FM 14-channel tape recorder. Difficulties with each of three tape recorders on board the R/V Acania during the experiment reduced the amount of usable data to small portions of each data tape and, additionally, limited the longest

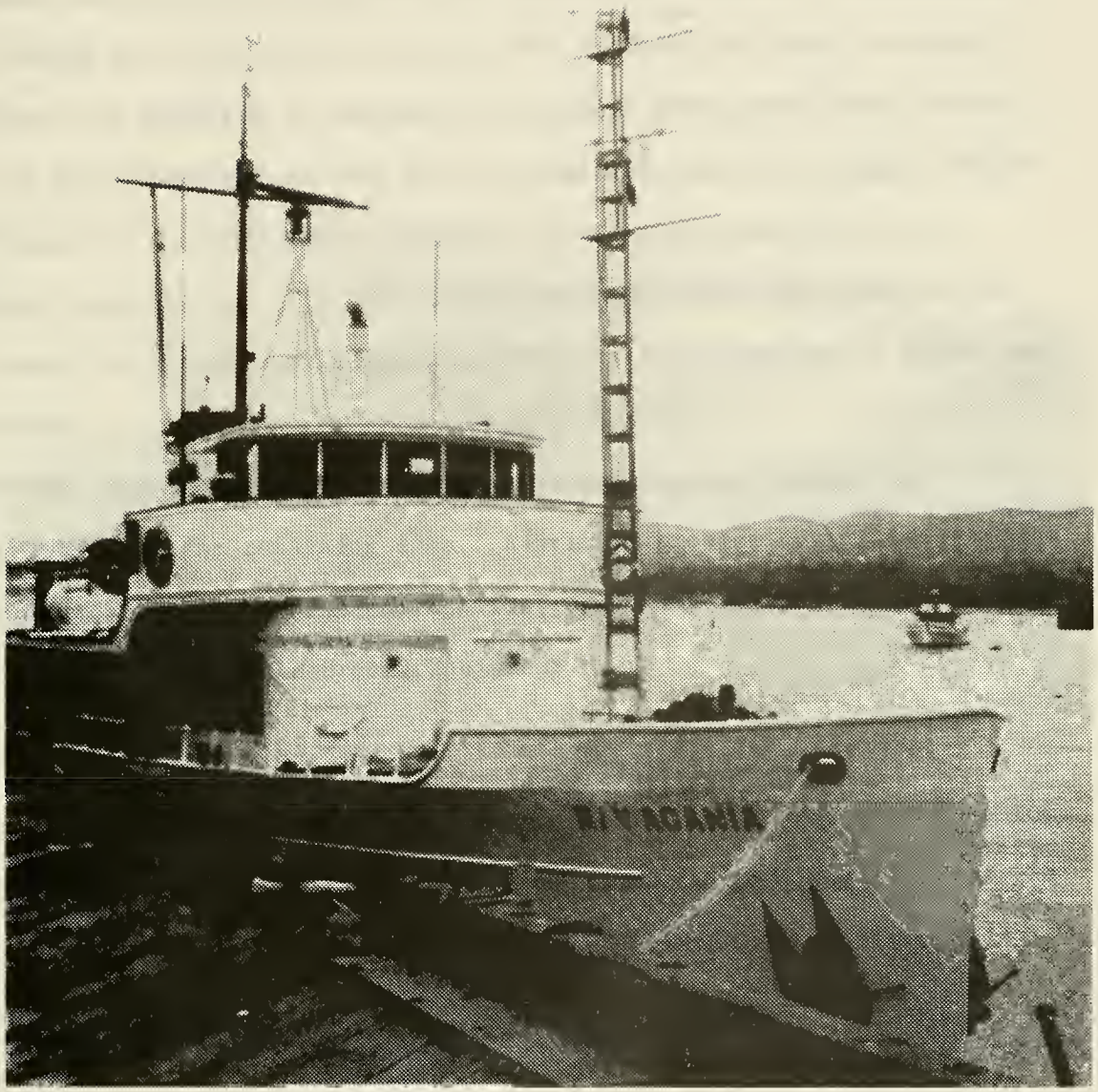

Figure 7. R/V Acania with meteorological mast
(Stem mast not shown)

data period available to 20 minutes. However, sufficient periods of data were available from a variety of recording periods with different mean conditions to meet most experimental objectives.

A difficulty encountered after the data were gathered was that the recorder used could not reproduce the data on all channels at all available speeds since playback amplifiers did not have the speed circuitry required. In addition an intermittent capstan drive oscillation caused loss of large sections of data due to large spurious noise signals which blanketed the recorded data. Finally, it was discovered that tape recorder channels had different gains associated with them, and had not been marked for proper replacement so that exact calibration of signal was impossible.

These conditioning and recording problems greatly reduced the quantitative value of the remaining data. A primary problem during the experiment proved to be equipment malfunction, which may occur during shipboard use of sophisticated electronic equipment.

C. THE OBSERVATIONAL PHASE

The transit from Monterey Bay to San Nicolas Island was the beginning of the data collection segment of the experiment. During the transit the instrument signals were monitored on an oscilloscope. Winds from the stern blew exhaust gases over the sensor arrays during this phase, and precluded measurement of the turbulent regime. This effect and superstructure wind interference greatly limit the allowable directions of relative wind for representative turbulence measurements while underway.

A strip chart record was made of the output of the five functioning accelerometers during the transit, prior to the arrival at San Nicolas Island.

The ship anchored on the night of 19 September 1973, in 10 fathoms of water about 1600 yards from the shoreline of San Nicolas Island. The anchorage was on the northwest side of the island and allowed unlimited fetch to the winds which were from the northwest, Figure (8). The kelp moderated the smaller wind waves, and water depth probably increased the swell height.

On the morning of 20 September 1973, data collection from all systems was begun. Unfortunately, the tape recorder used for the accelerometer data began to act erratically and attempts to locate the problem were unsuccessful beyond isolation of the problem to a card in the power supply. The problem was later determined to be a cracked component.

Fortunately channels were available on the recorder used to record wind and temperature fluctuation data and they were used. Coincident recording enabled examination time correlation and phase information between these two sets of data. If possible, this should be done on future studies.

D. SUMMARY OF MEASUREMENTS

Acceleration measurements were made with five sensors (one failed very early in the experiment) mounted in groups of three and two at the two levels. All three upper level sensors and the lower roll and pitch sensors lasted through the five days of constant use and rough sea conditions. Due to large direct current offset voltages with respect to signal output much data was lost due to the fact that the tape recorder was preset with insufficient voltage limits. Fortunately, the usable data were those which were recorded simultaneously with velocity and temperature data (when available).

The time frames and parameters available as well as descriptions of

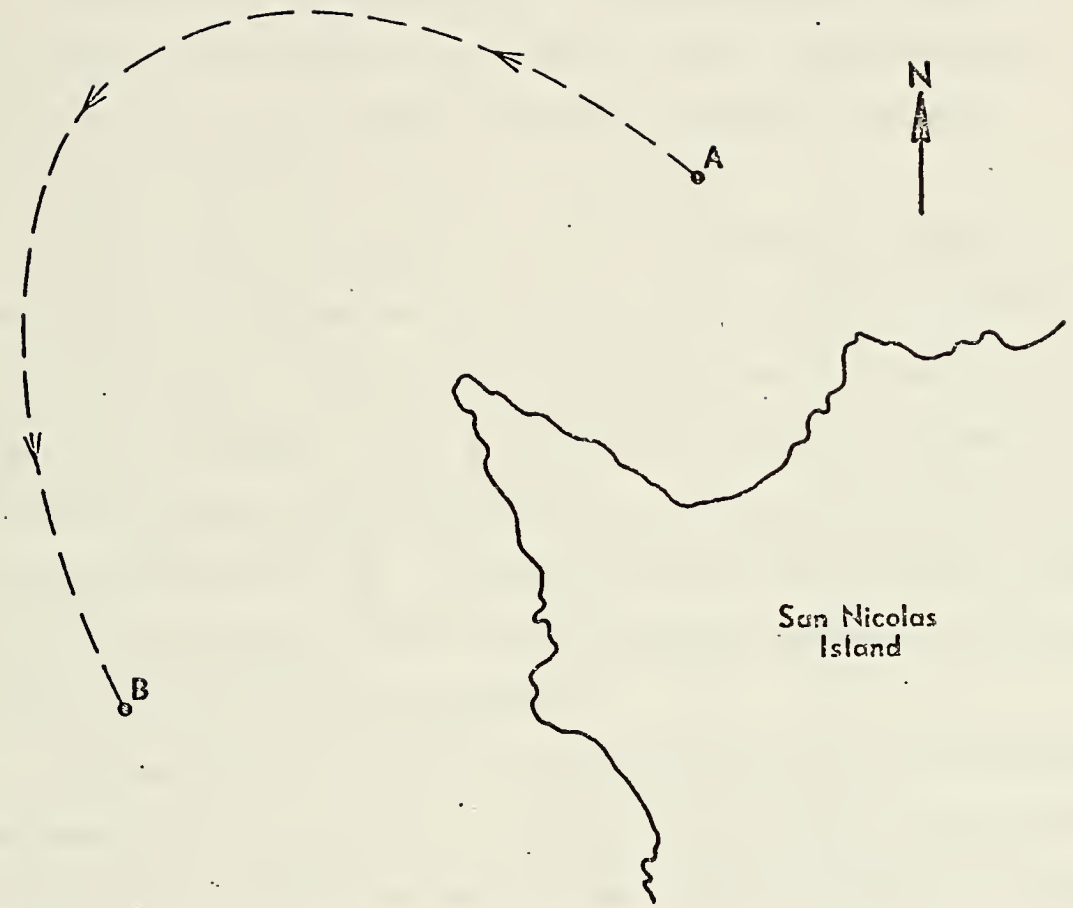

Figure 8. North End, San Nicolas Island

mean conditions (from Cavanaugh, 1974) appear in Appendix C. Only a small portion of the available data was analyzed due to long analysis procedures necessary to proceed from the original analog signals to the final digital computer output.

E. ANALYSIS PROCEDURES

Analysis procedures consisted of a post-cruise strip playback of all analog tapes for preliminary analyses of the data, digitalization of selected time periods, digital processing of the data from seven- to nine-track tape, and Fourier analysis to yield spectra.

In the first step, analog signals were played back at high speeds and the output were displayed on an eight-channel strip-chart recorder run at a very slow speed. This yielded an overview of the data available for analysis. One segment of such a recording is included as Figure (9) where data include wind fluctuation (u'), temperature fluctuation (t'), and accelerometer data (A). Coincident mean data were recorded by hand at 10-minute intervals. This provided 10-minute averages of winds, with median values for the other variables.

Time segments with usable data were restricted due to the recording problems previously mentioned. The length of continuous data periods was limited to about 20 minutes and precluded sequential studies of overlapping time frames.

Data were reproduced with the same tape recorder used to record the data, but only after some repairs had been effected. Prior to conversion a gain of 50 was applied to the input signals, and one channel of the accelerometer data was integrated.

The integration was done in order to relate low frequency ship related motion in a relative velocity to fluctuation measured by the velocity

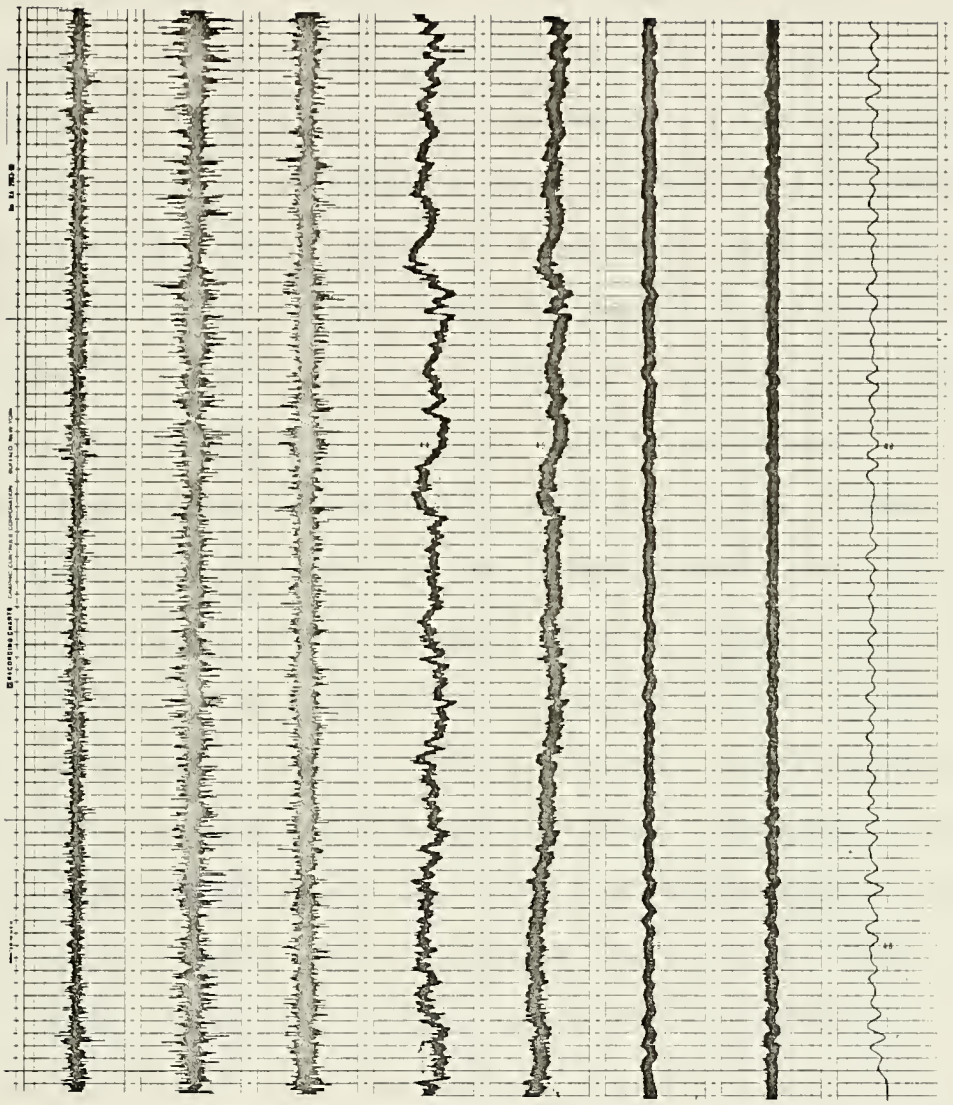

Figure 9. Fluctuation variable signals. From left, 3(u'), 2(t'), 2($\vec{A}$), and integrated accelerometer.

fluctuation sensors.

During the digital conversion, velocity signals were low-pass filtered at 400 Hertz in order to remove spurious spikes. Direct current offsets were also nulled. It is thought that an integrated signal for one time frame (run 3) was influenced by an improper null adjustment.

One of the problems associated with multiple processing of data is the addition of noise. High frequency noise is added due to non-linear electrical responses. Power supply noises and their harmonies are also cumulative. Spurious spikes can result from connectors and these multiply as the number of equipment interfaces increase. All such noise signals contaminate the final spectra. A direct input to an analog fast Fourier transform device (spectrum analyzer) would lessen many of these problems.

Analog to digital conversion was performed on the Naval Postgraduate School SDS 9300 analog/digital hybrid computer system. These procedures have been detailed by Jones (1971) and Johnston (1974) and yield a seven-track digital tape. This must be converted to a nine-track tape for use in the IBM 360 system digital computer. Several minutes of computer time are required per conversion. Data from this experiment produced 13 digital tapes. The seven- to nine-track tape conversion is described in the W. R. Church Computer Center, Technical Note No. 0211-08.

The nine-track digital tape was processed with a version of the University of British Columbia Fourier Transform program which has been adapted for use at the Naval Postgraduate School. It is used to compute complex Fourier coefficients which are used to describe spectra evergy distribution. Final output requires another program which takes the tabular coefficients as input and converts them to power and cross-spectra which are then output in final form on a Cal-Comp plotter.

Johnson (1974) has described the procedures used on this experiment to obtain the final spectra.

V. RESULTS

A primary outcome of this experiment was that the developmental system functioned properly throughout the experiment, giving data which could be compared to the fluctuation parameters. The results from the observational experiment include strip chart recordings, analog variance spectra, and digital variance spectra, cospectra, quad-spectra as well as phase and coherence spectra. These various results were examined for correlations between the accelerometer data and the wind fluctuation data.

A. STRIP CHART RESULTS

Strip chart results were useful for the interpretations. This fact is illustrated by the strip chart sections in Figure 9 which show accelerometer outputs, at low chart speed, in comparison with the wind fluctuations (u') and temperature fluctuations (t') signals. Figure 10 illustrates the relation between signals fron the five accelerometers. An examination of the same signal reproduced at higher chart speeds shows that high-frequency components were different between sensors, Figures 11 and 12.

Other strip chart recordings suggest significant correlations between the single low frequency wind fluctuation signal available and the integrated vertical accelerometer signal. This relationship is most evident for larger motion oscillations, and less significant for small motions. Figure 13 illustrates this phenomenon for a section of the strip chart. The correlation is further evident between the vertical accelerometer data and wind fluctuation data both of which had been high-pass filtered

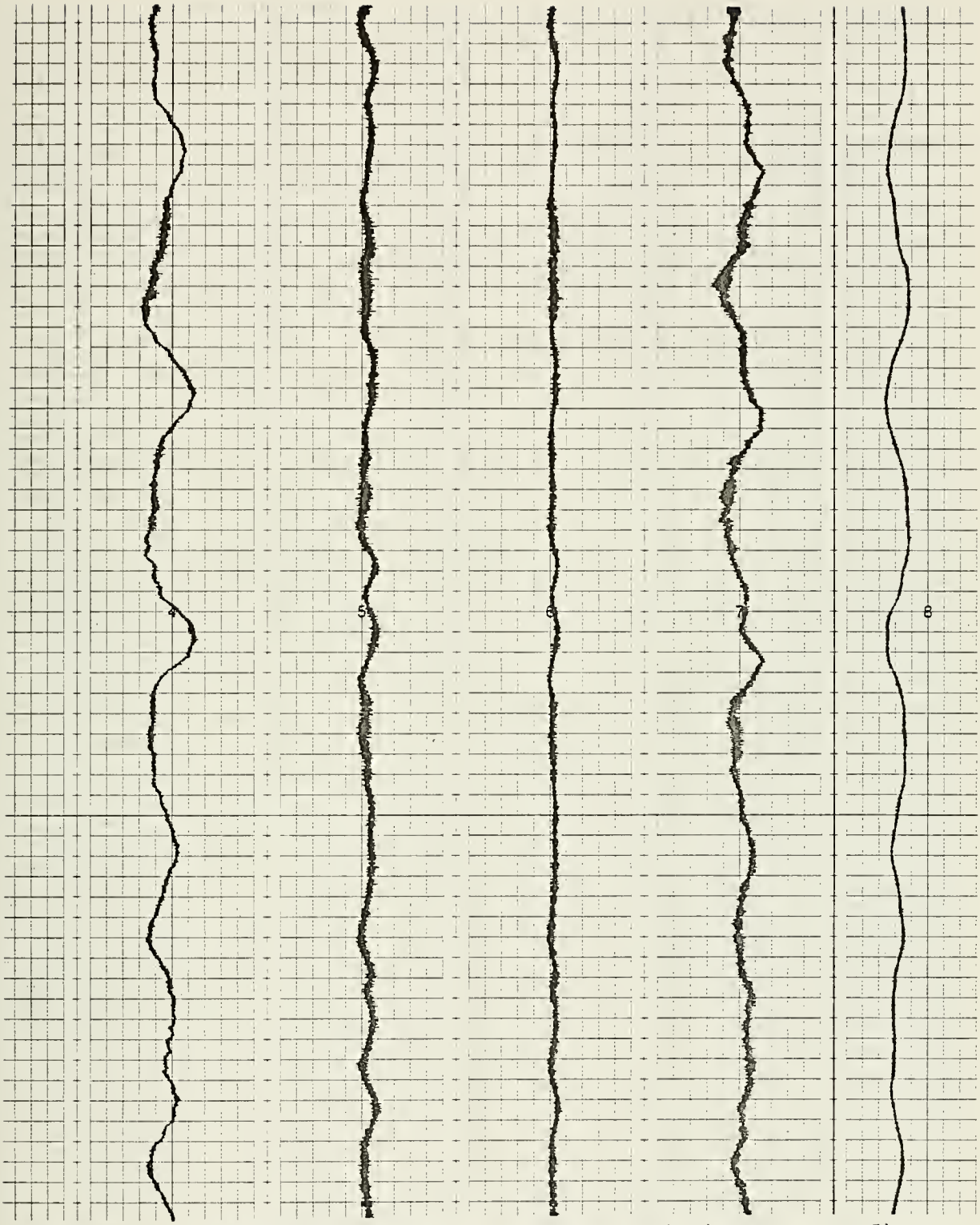

Figure 10. Accelerometer signals (low frequencies) 4)upper vert, 5) upper lat, 6) upper fore-aft, 7) pitch, 8) roll, speed:1mm/sec.

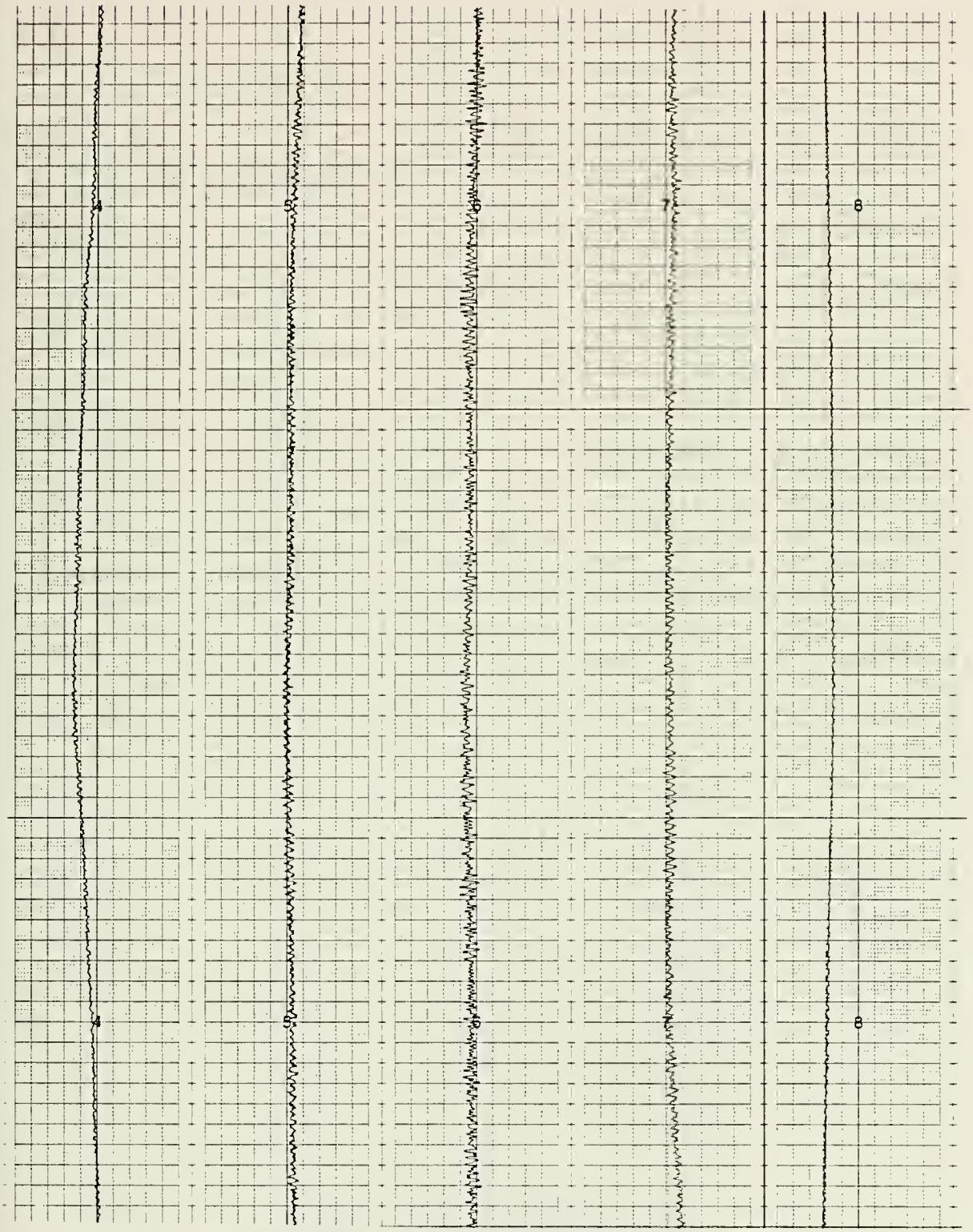

Figure 11. Accelerometer signal (inertial frequencies) 10mm/sec.

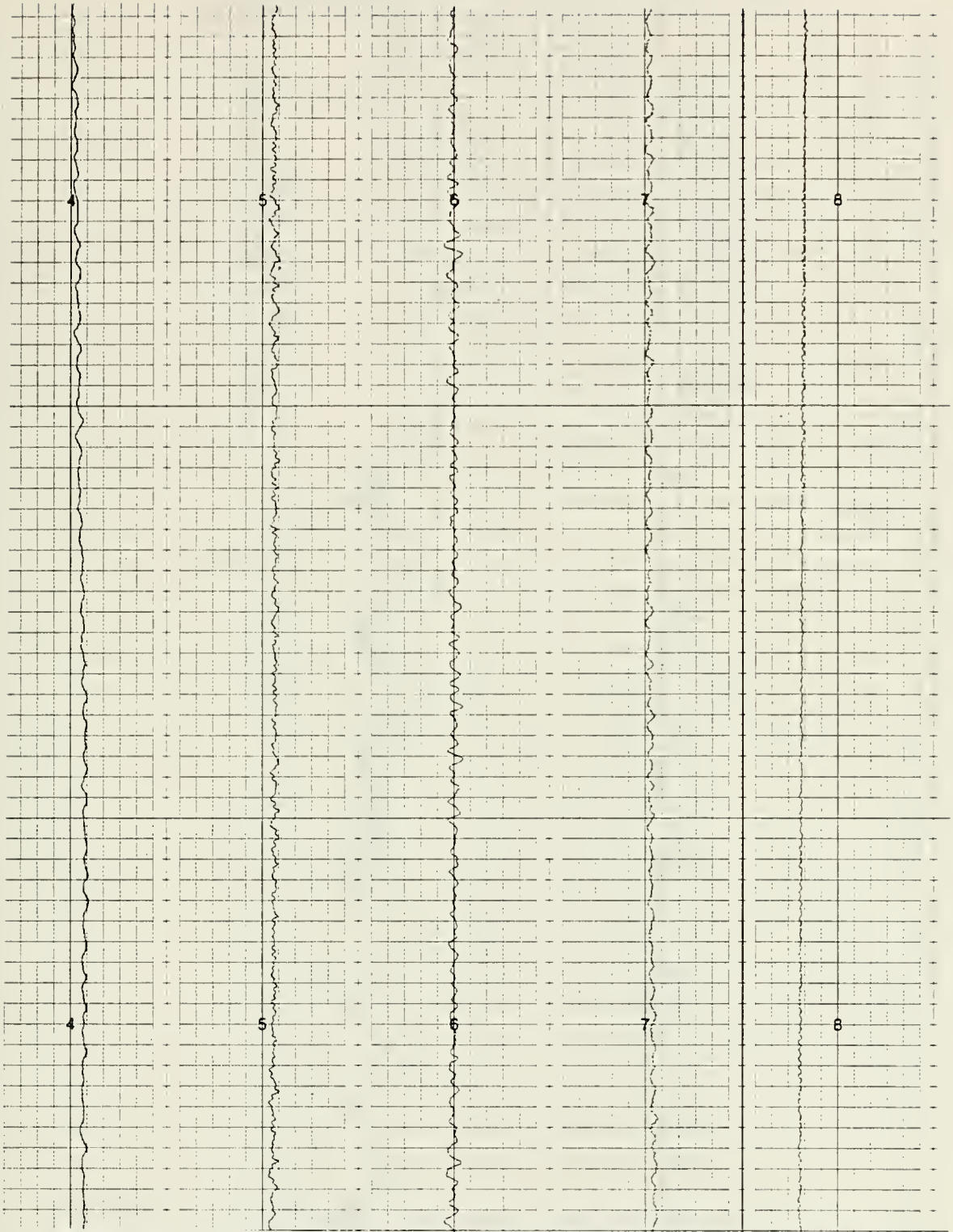

Figure 12. Accelerometer signal (high frequencies) - 50 mm/sec.

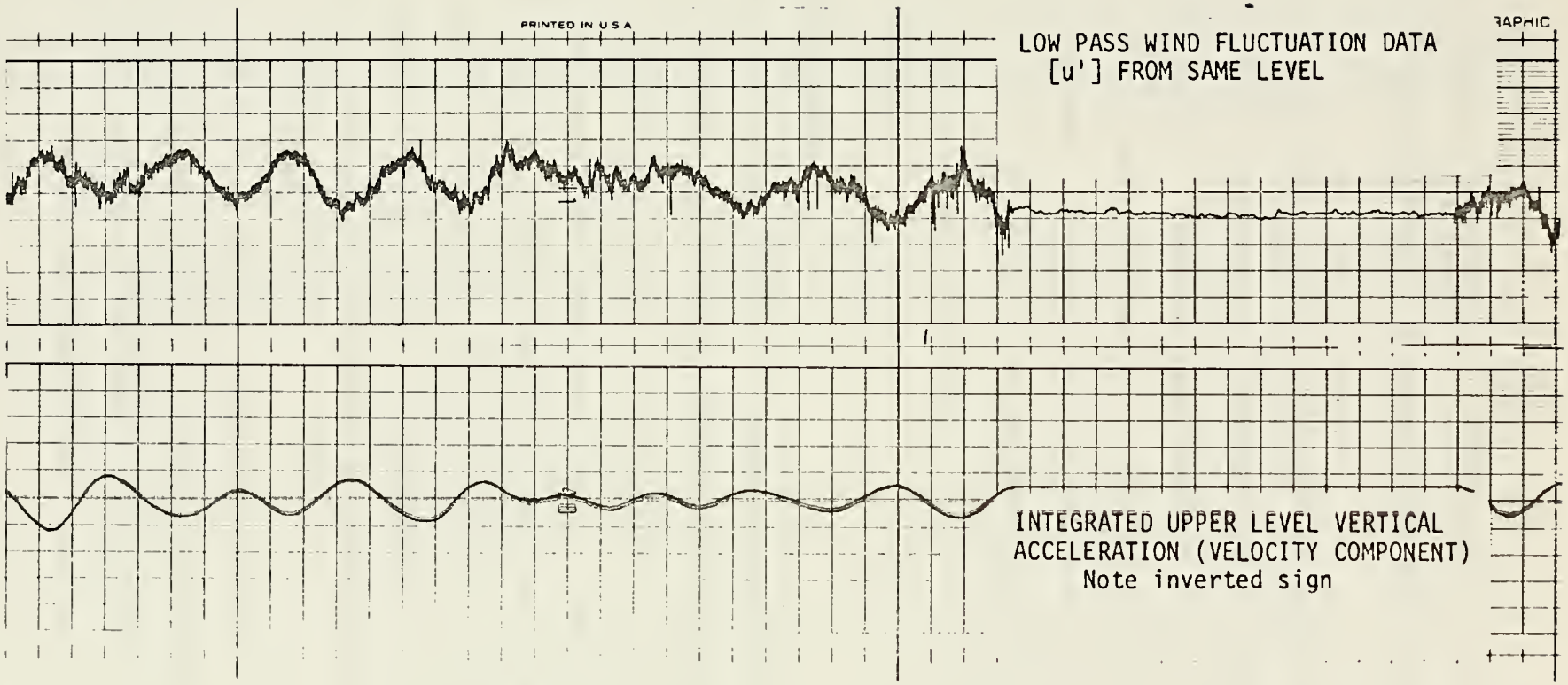

Figure 13. Wind fluctuation data compared with integrated upper vertical acceleration data.

at ten Hz. Although the signal was high-pass filtered there is still evidence of some energy due to low frequency ship's motion. This is only evident for very large signal levels. Figure 14 shows this low frequency coupling.

The sections of strip-chart recording which were included in this section were those which revealed the low frequency motion effects on the wind fluctuation sensor. There were only two strip chart records with the proper gain and speed relationships to make the evidence visible. Unfortunately, low frequency correlation analysis of spectra could not be accomplished due to a combination of the digitization rate and block size limitations in the computer code. Spectral results are described in the following section.

B. ANALOG SPECTRAL RESULTS

Analog spectra were obtained from an x-y plotter connected to a SPECTRAL DYNAMICS MODEL SD-301C Real Time Analyzer and SD-309 Ensemble Averager, available during the cruise. The x-y plotter was used to make spectral plots in nearly real time. Many such plots made on 20 September 1973. Unfortunately, for the available spectra, the system was not properly calibrated so that scales are not consistent. However, decade values could be marked so frequency can be estimated. Variance spectral plots of the velocity (u') obtained by this method are presented in Figures 15, 16, 17, and 18.

Accelerometer spectra from the upper triad appear in Figure 19. It is interesting to note the coincidence of spectral spikes among the three sensors. Especially significant is the fact that the predominant spike is many decibels larger than the secondary spikes. The frequency associated with the predominant spike is 54 Hertz. A similar plot of spectra

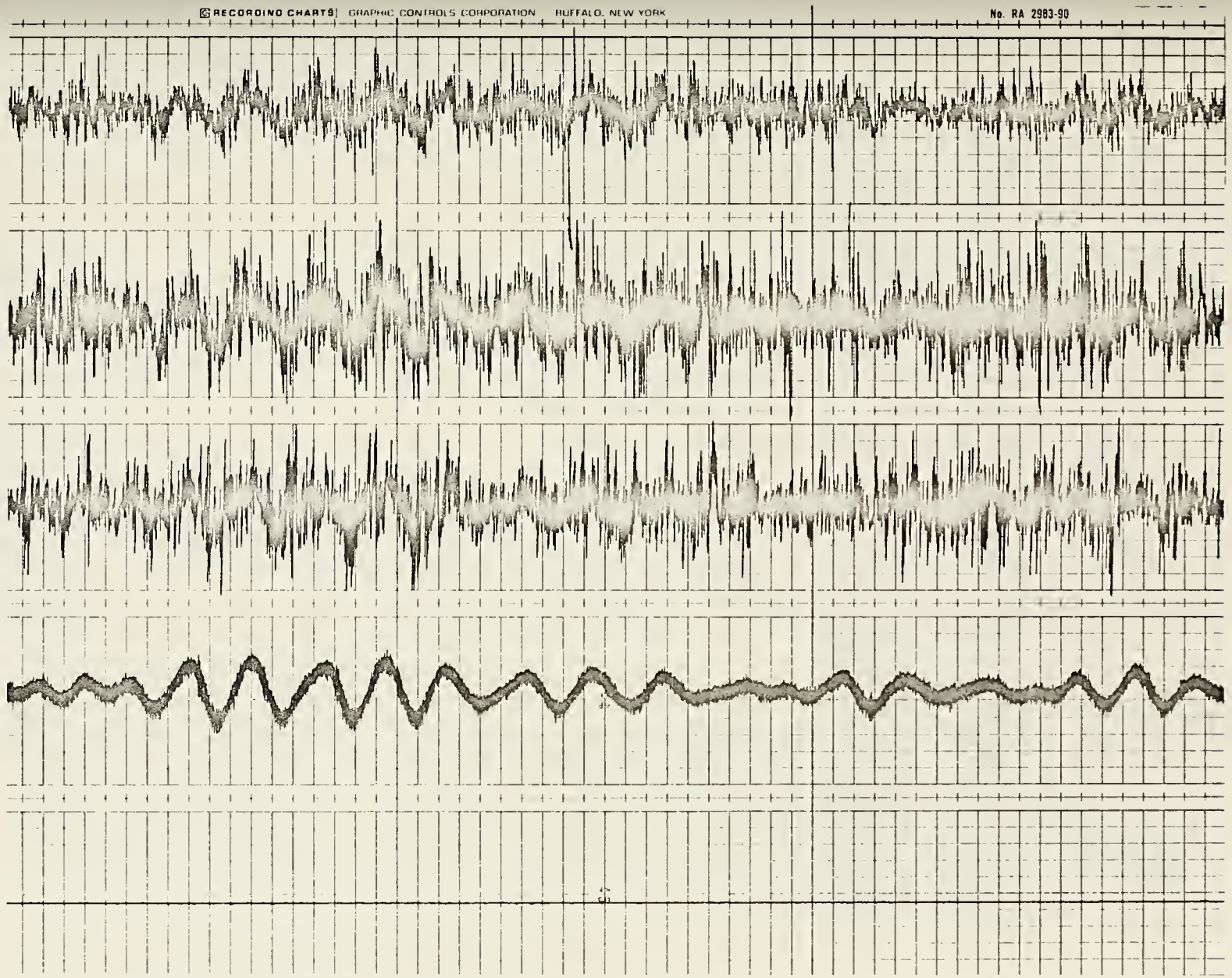

Figure 14. Filtered wind data compared with upper vertical acceleration data.

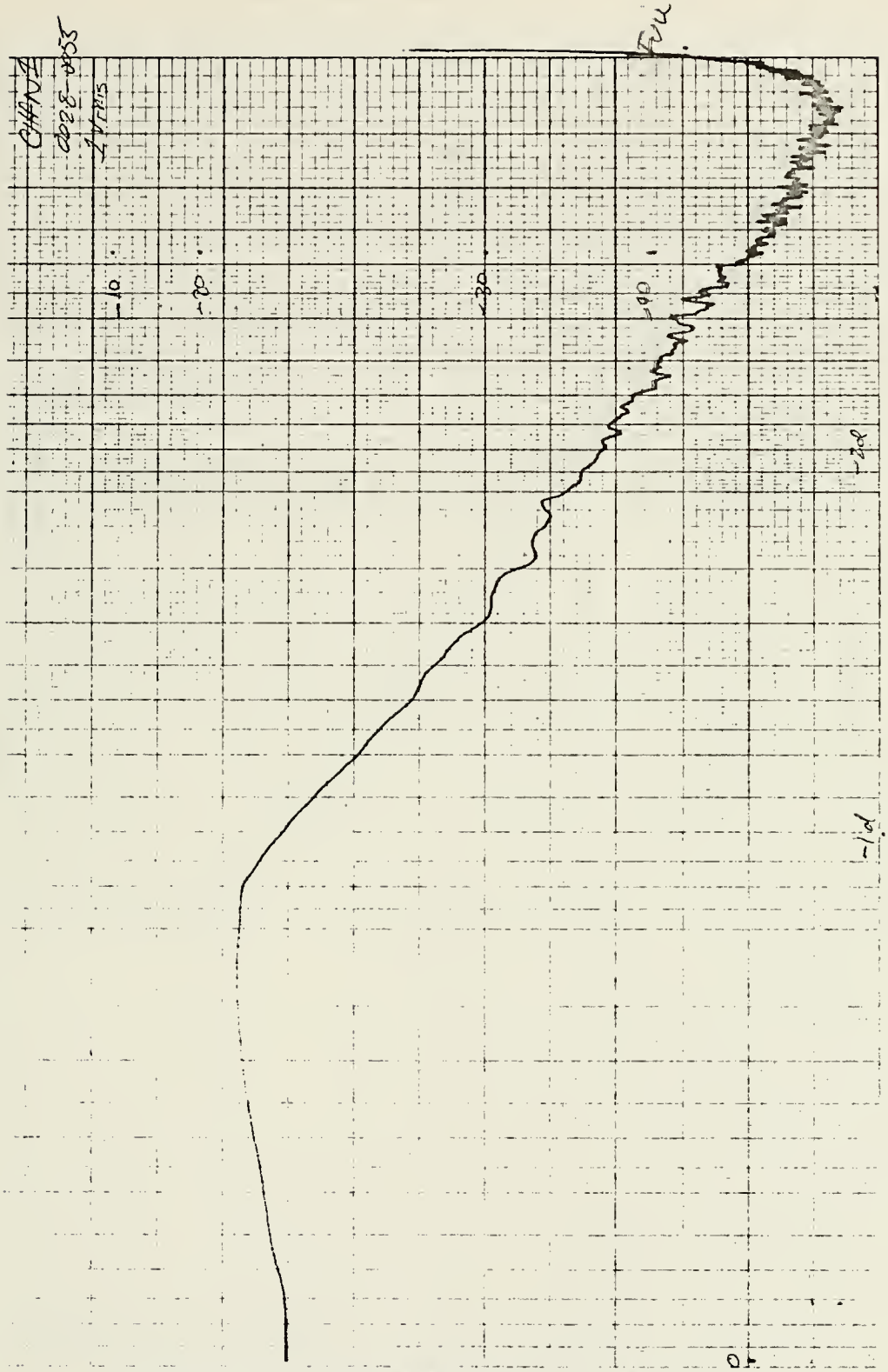

Figure 15. Analog spectrum of u', level (1).

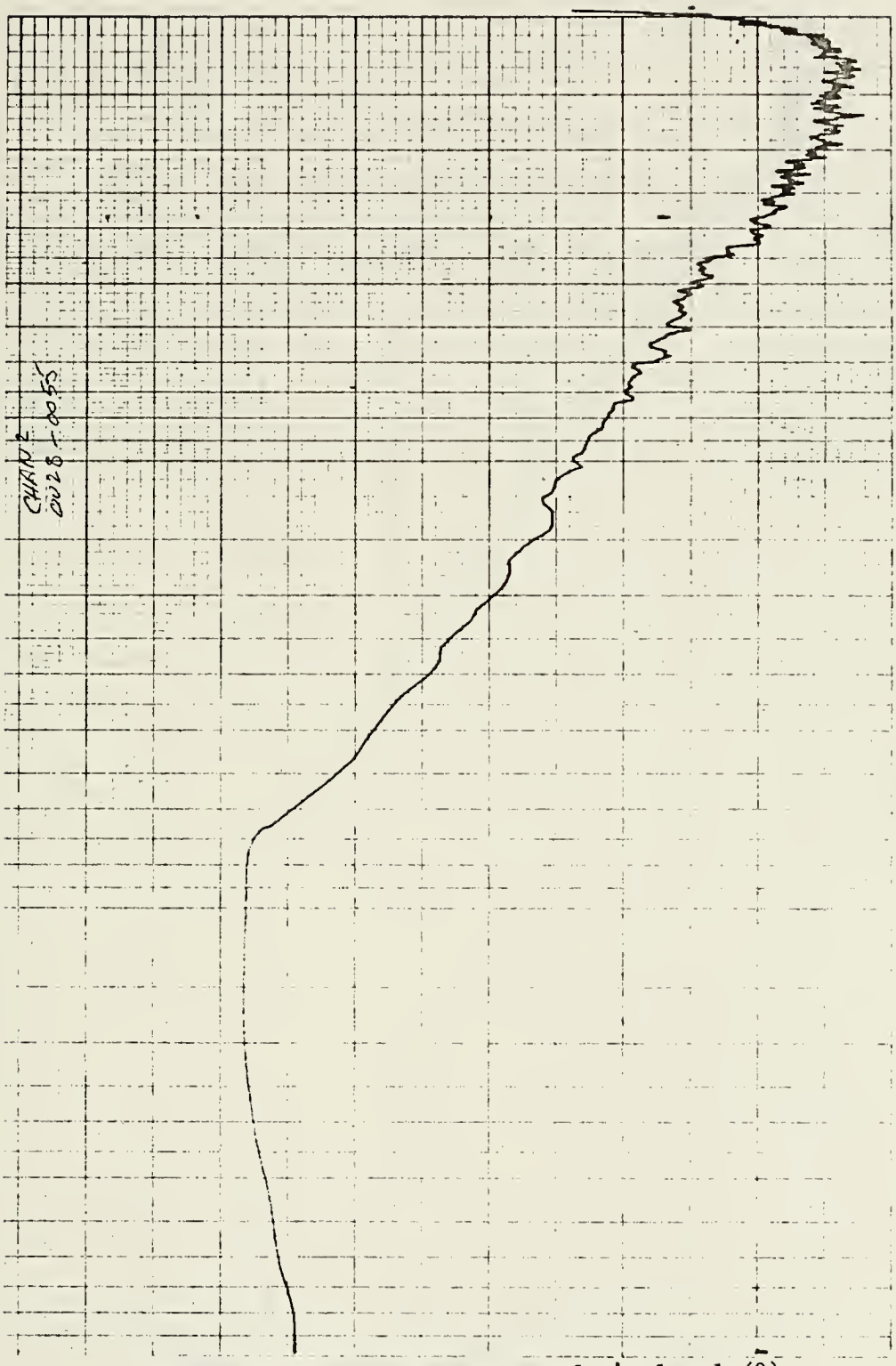

Figure 16. Analog spectrum of u', level (2).

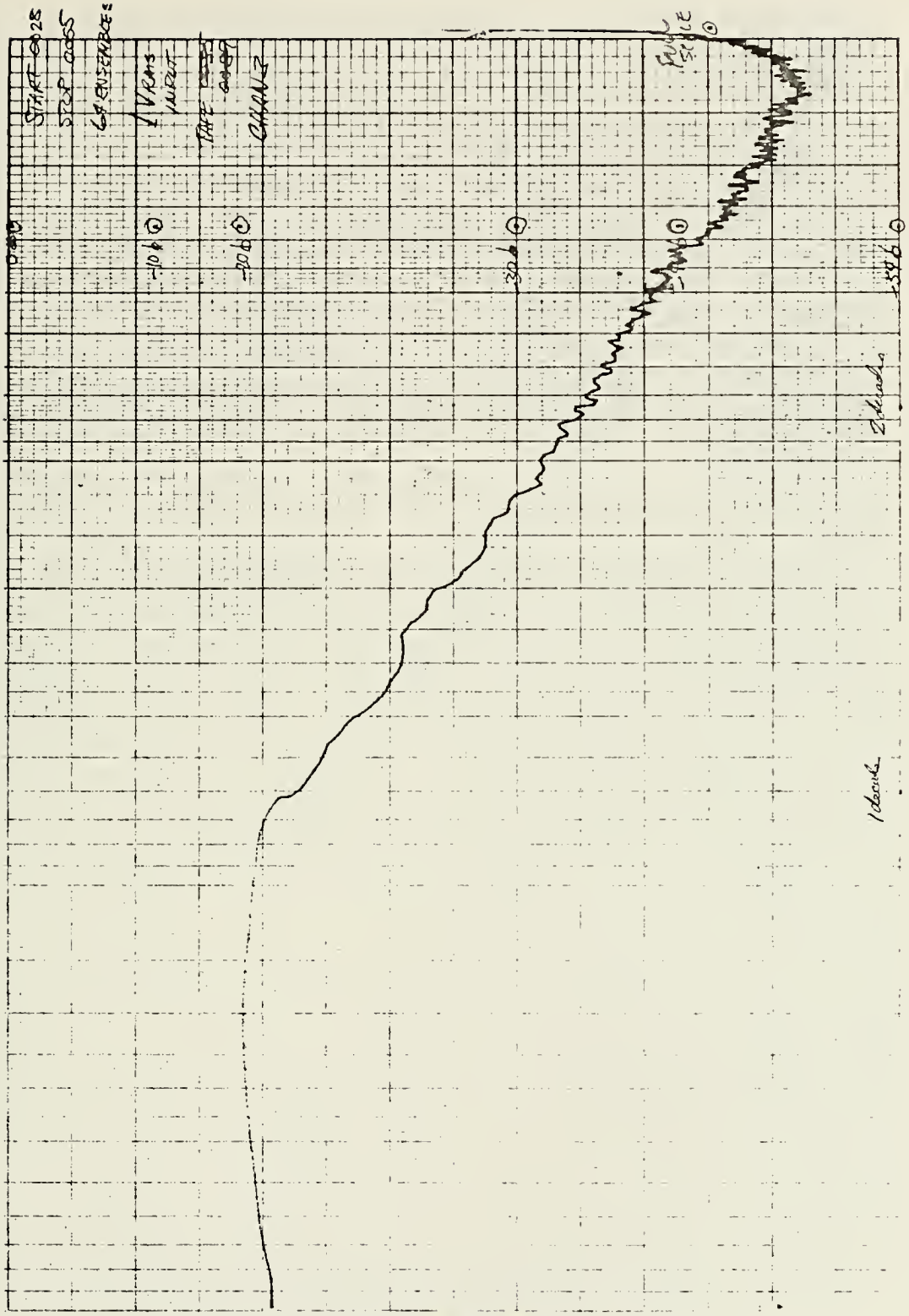

Figure 17. Analog Spectrum of u', level (3).

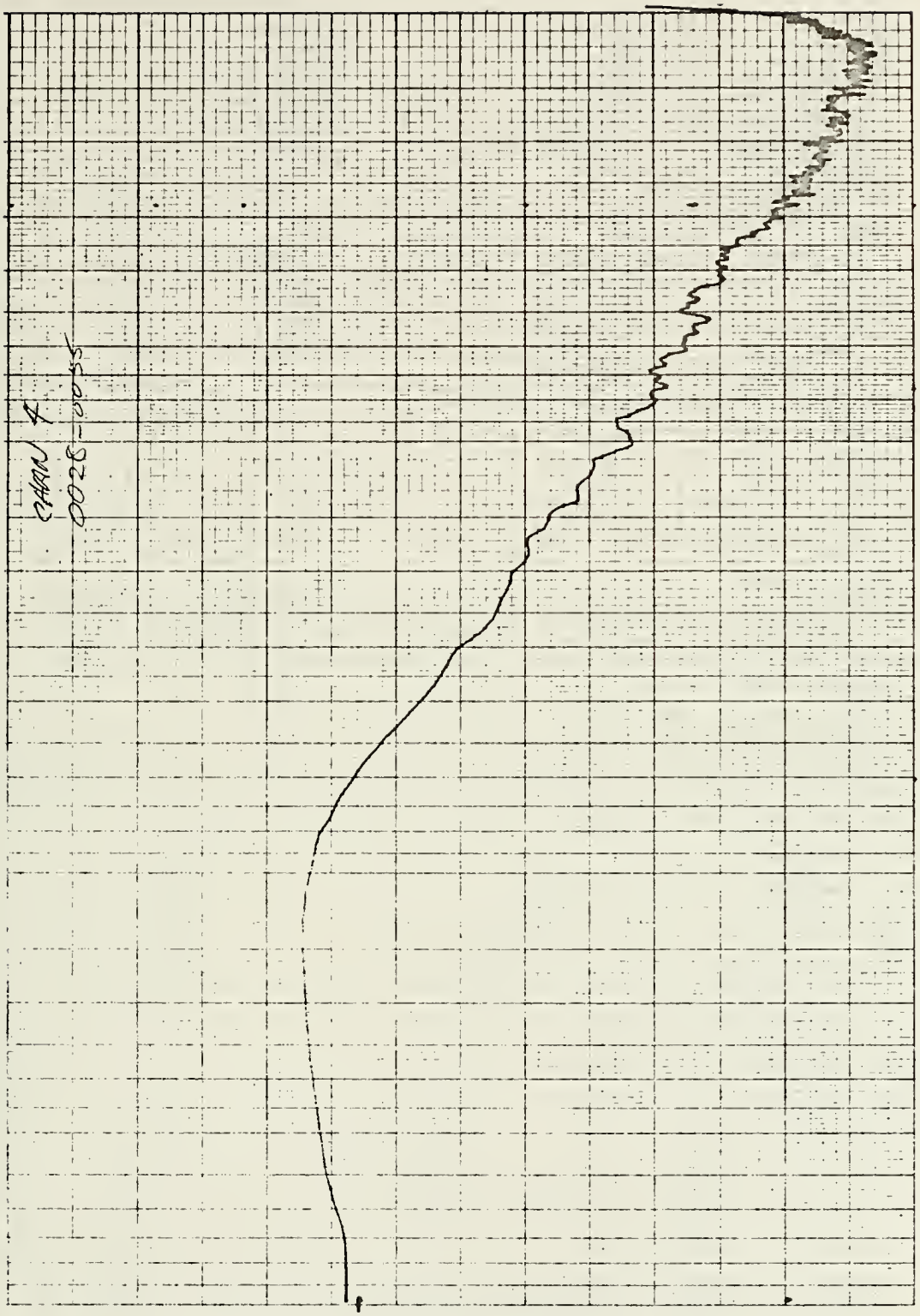

Figure 18. Analog spectrum of u', level (4).

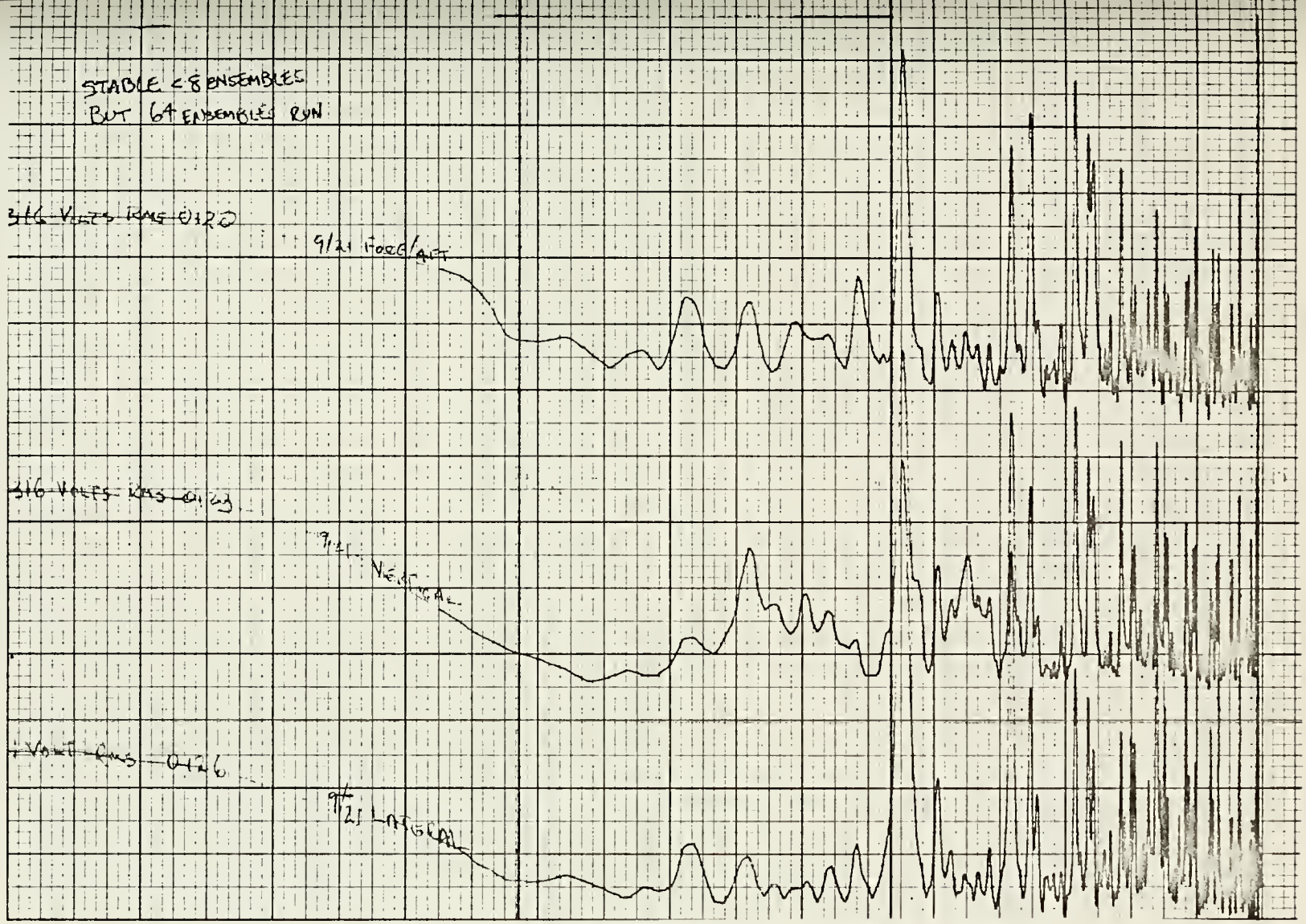

Figure 19. Analog Spectra of Upper Triad Accelerometer Signals.

for the lower two sensors does not have the striking resemblance of the upper triad plot. However, dissimilar spikes and differences in shape are evident in Figure 20. A tabular listing of significant spikes according to frequency is given in Table I below.

TABLE I

FREQUENCIES OF 500 HZ SPECTRUM

264.5	120.0	30.0
211.5	105.0	24.5
173.5	54.0	16.5
158.5	39.5	11.5

Spectral differences are evident in combined spectral plots of the accelerometers and the u' sensors. The predominance of spikes found in the accelerometer spectrum is barely discernable in the wind variance spectrum. The predicted decreasing spectrum of the inertial subrange with its associated -5/3 slope is clearly seen in Figure 21.

C. DIGITAL SPECTRAL RESULTS

Digital spectral results differed slightly in appearance from analog spectral results due to the different bandwidths in the two computations. Digital spectra were obtained for three data periods in order to make visual comparisons between spikes in the wind variance spectra and accelerometer spectra. The accelerometer spectra have the same form for all these runs; the upper triad sensors with the analog integration of the vertical accelerometer as the fourth spectrum. Combined spectra are illustrated in Figure 22.

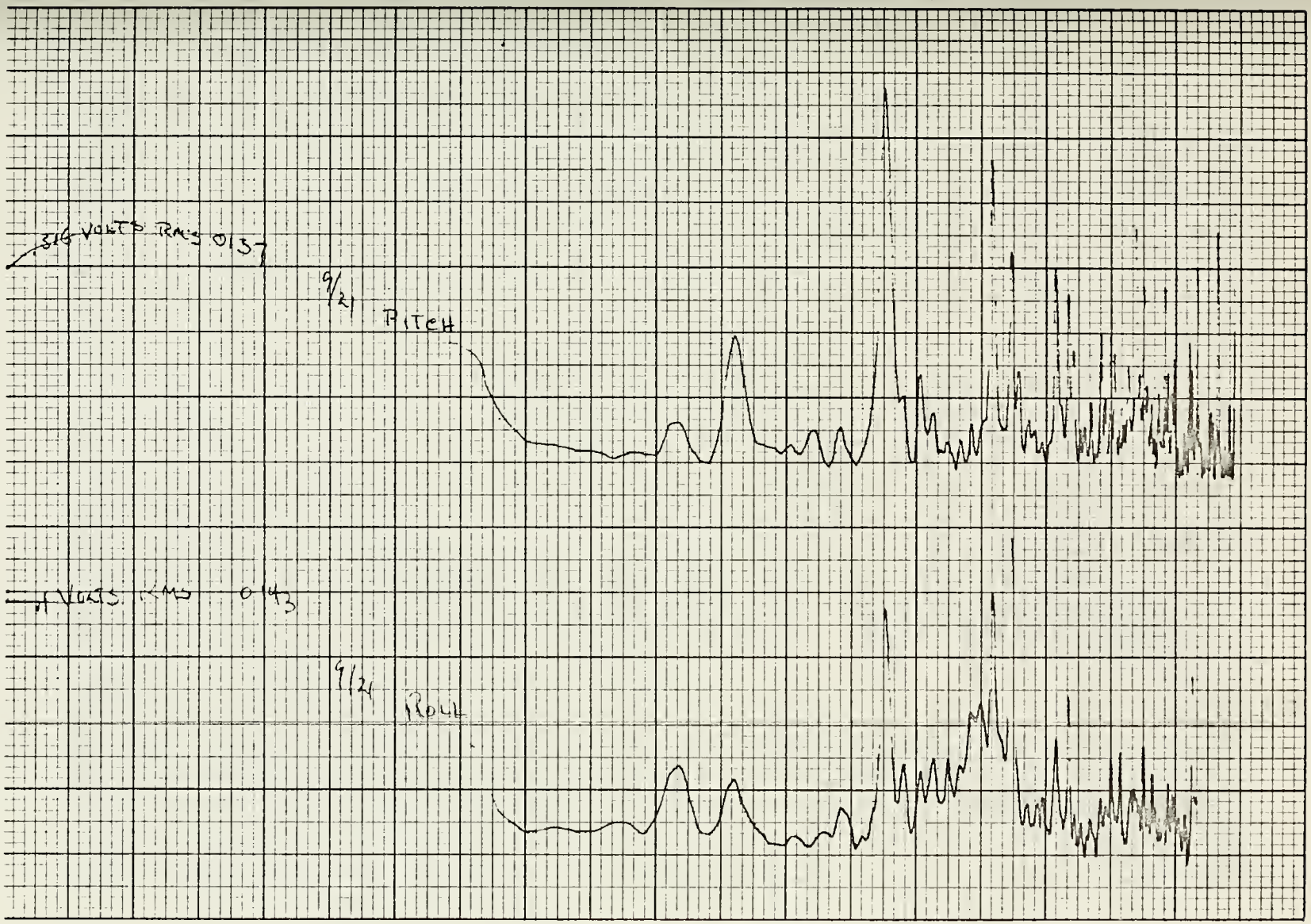

Figure 20. Analog Spectra of Pitch and Roll Accelerometer Signals.

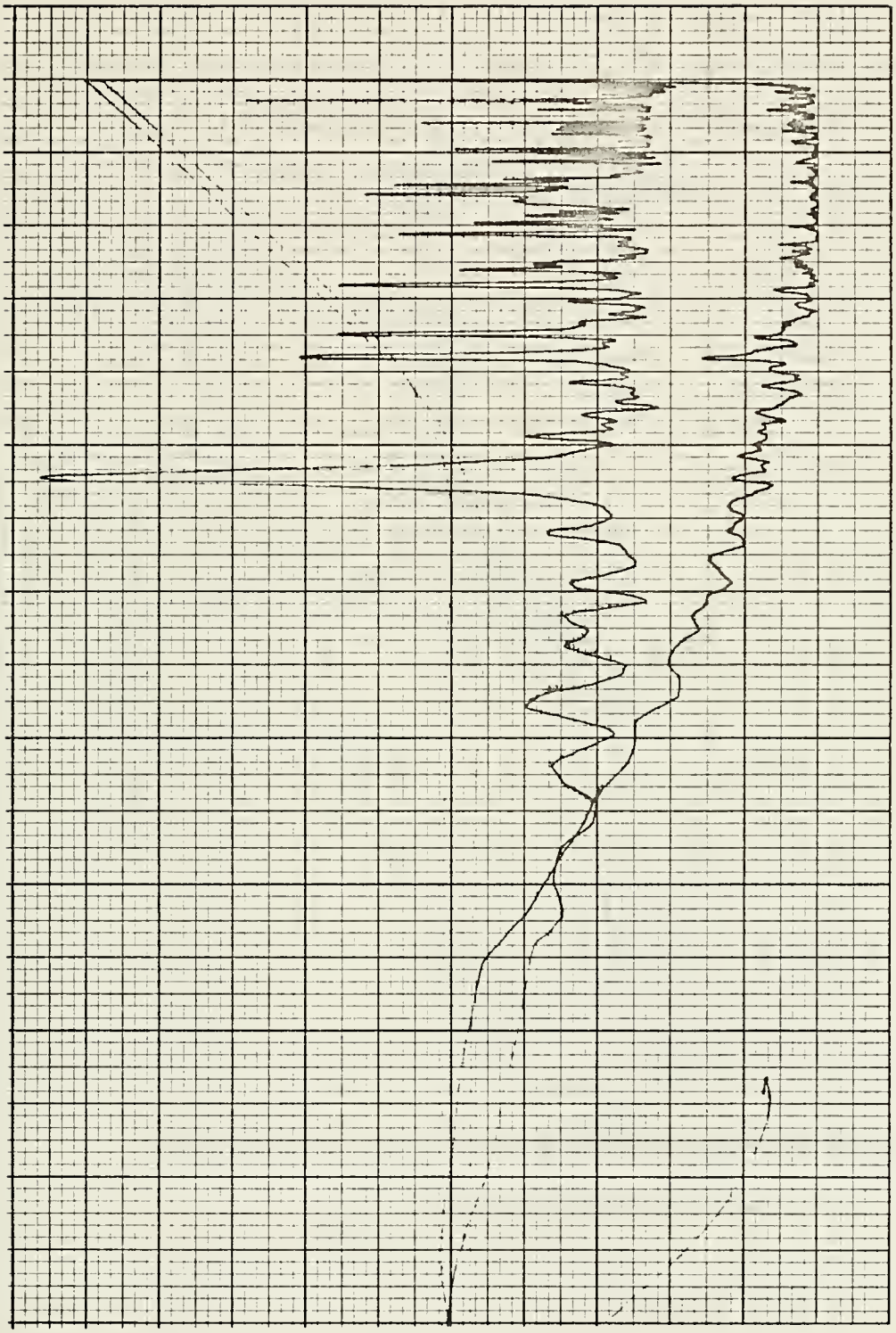

Figure 21. Analog Spectral Shapes (not to same scale).

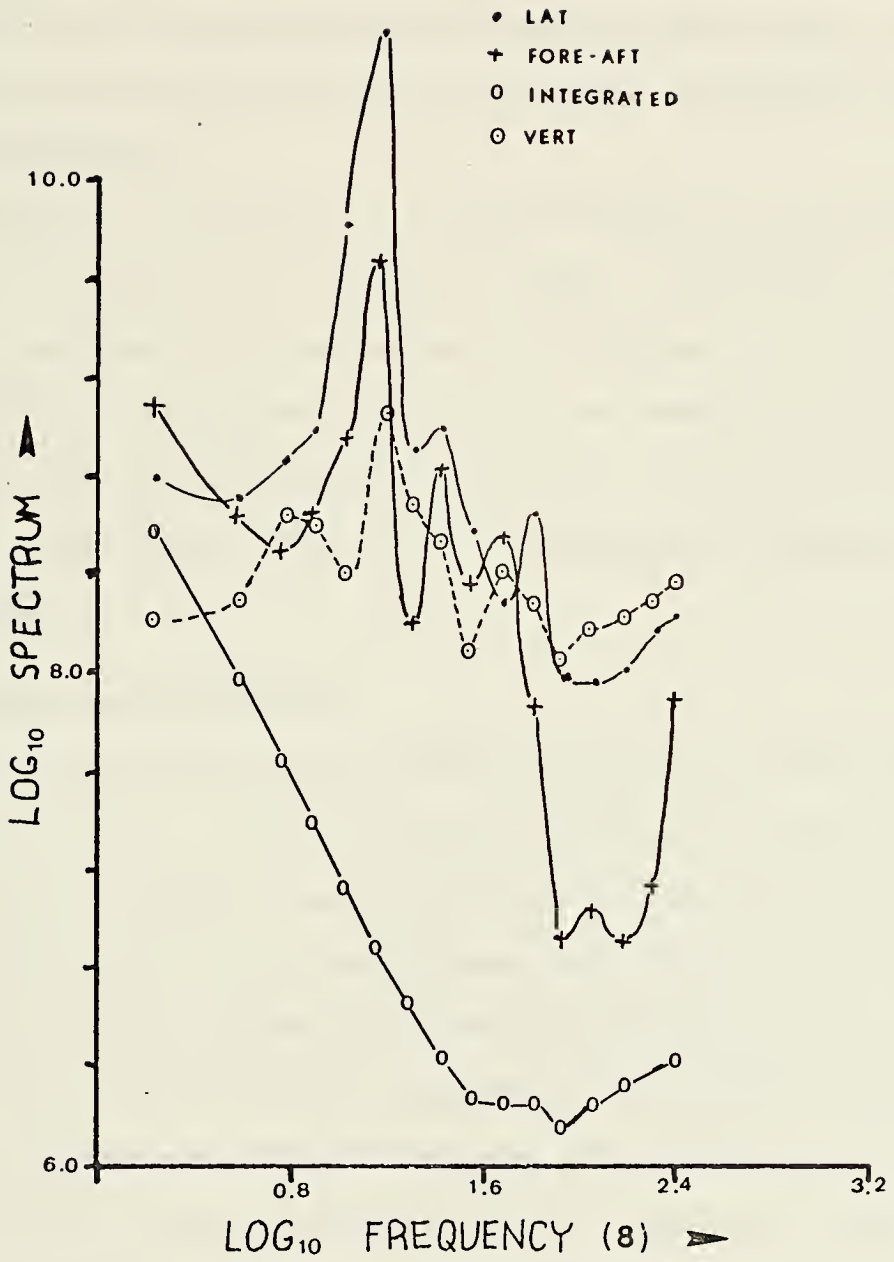

Figure 22. Combined Digital Accelerometer Spectra.

In comparison with the analog spectra, there is less representation of detail in the digital spectra. Although the detail could be obtained by digital means, it would be at a significant cost in computer time and core storage. It may be further contraindicated since larger bandwidths would tend to smooth any sharp vibration induced spike. Digital spectra for the data runs (2), (3), and (8) appear as Figures 23, 24, and 25, respectively.

The latter run, Figures 25a - d, which contained the only unfiltered u' data, was selected for most detailed analysis. The objective was to see if functional relationships could be established. For this examination, cospectra, quad-spectra, phase, and coherence spectra were computed. These are interpreted below for phase relationships between the three accelerometer signals as well as the wind and temperature variance data.

D. ADDITIONAL DIGITAL SPECTRA

Three wind variance spectra and three accelerometer apectra appear in Figures 26 to 31. From the co-spectra, quad-spectra, phase and coherence plots, conclusions can be drawn about the relation of the turbulent wind variance and the accelerometer data. It is noted that the integrated acceleration shows strong relationship with the wind fluctuation on basis of the co-spectra, quad-spectra, and coherence spectra for the lowest frequency band. Such similarity is notably absent in the region from 30 to 50 Hz in all four plots, concurring with the idea that dissipation rate (ε) can be estimated at these wave numbers without much ship motion effect. Figures 32 to 35 illustrate this effect.

Additionally the phase shows a remarkably constant phase, near zero, for frequencies above 60 Hz, while the coherence values rise almost


LOG10 SPECTRUM (M/SEC**2**2/HERTZ)
5.5
6.0
6.5
7.0
7.5
0.0
0.8
1.6
2.4
3.2
LOG10 FREQUENCY
INTEGRATED UPPER LEVEL VERT ACC (2)

Figure 23.


LOG10 SPECTRUM (M/SEC**2**2/HERTZ)
12.2
11.2
10.2
9.2
8.2
7.2
0.0
0.8
1.6
2.4
3.2
LOG10 FREQUENCY
INTEGRATED UPPER LEVEL VERT ACC (3)

Figure 24.

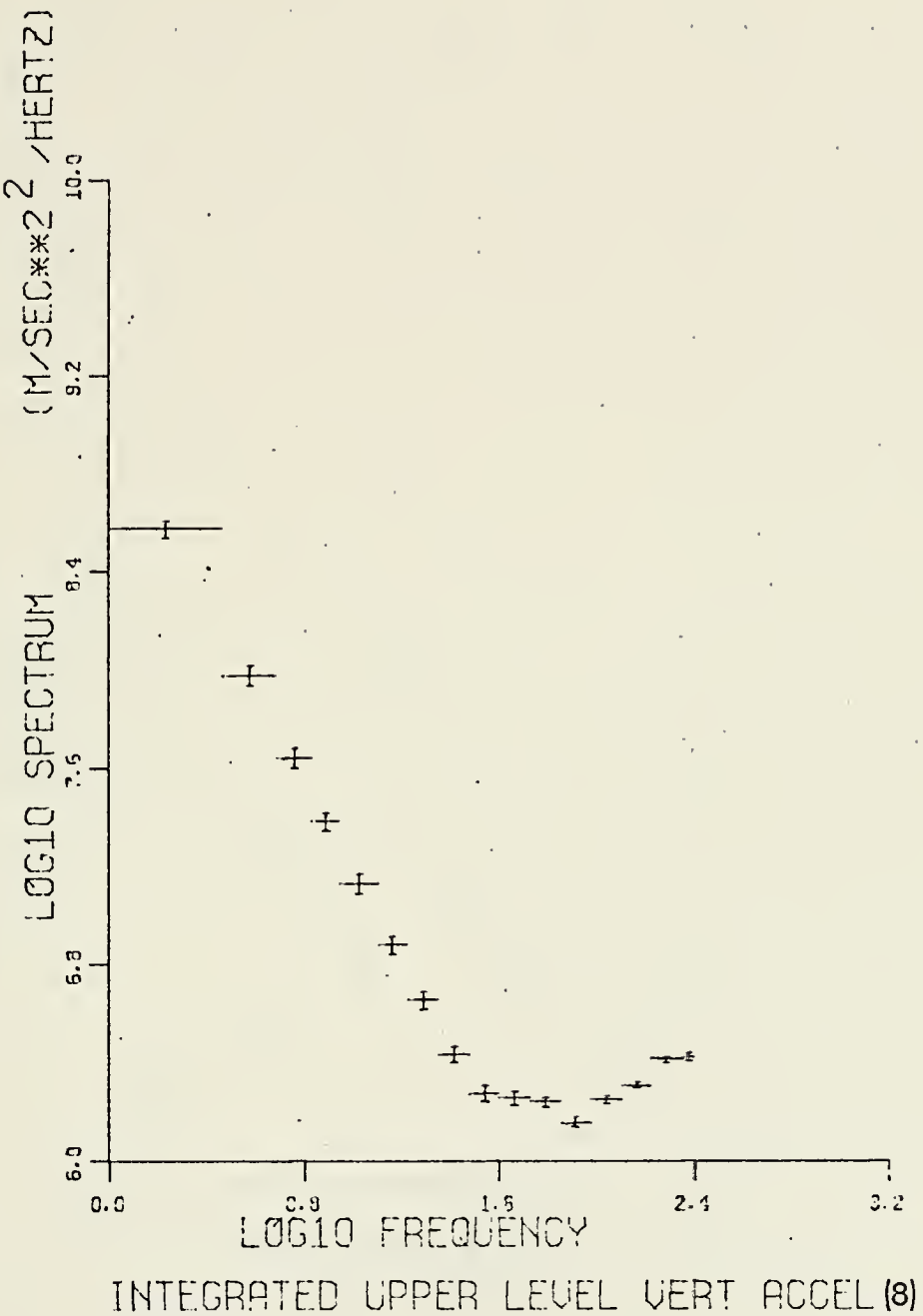
LOG10 SPECTRUM (M/SEC**2 **2 /HERTZ)
10.0
9.2
8.4
7.6
6.8
6.0
0.0
0.8
1.6
2.4
3.2
LOG10 FREQUENCY
INTEGRATED UPPER LEVEL VERT ACCEL (8)

Figure 25a.

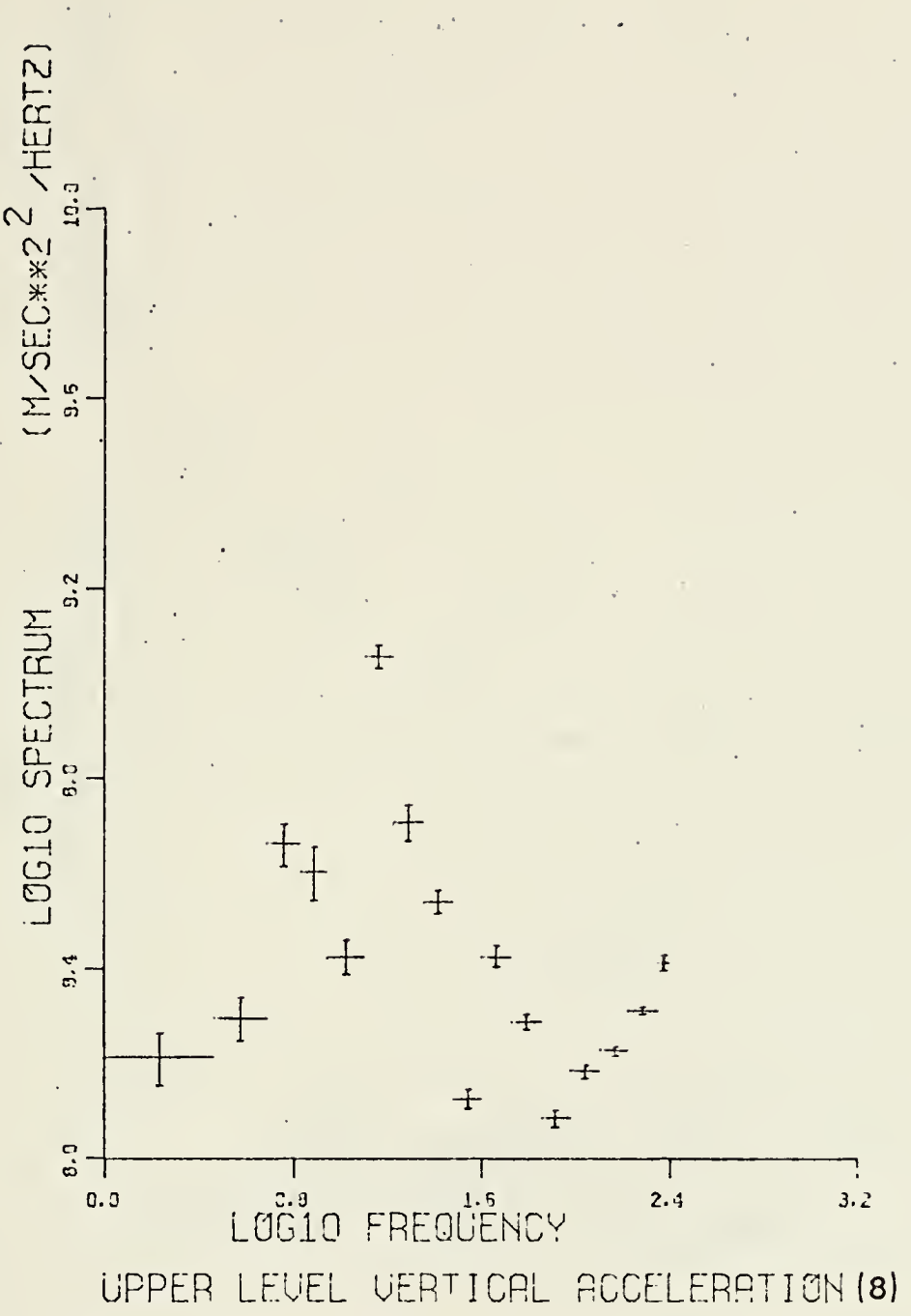
LOG10 SPECTRUM (M/SEC**2**2/HERTZ)
10.0
9.6
9.2
8.8
8.4
8.0
0.0
0.8
1.6
2.4
3.2
LOG10 FREQUENCY
UPPER LEVEL VERTICAL ACCELERATION (8)

Figure 25b.

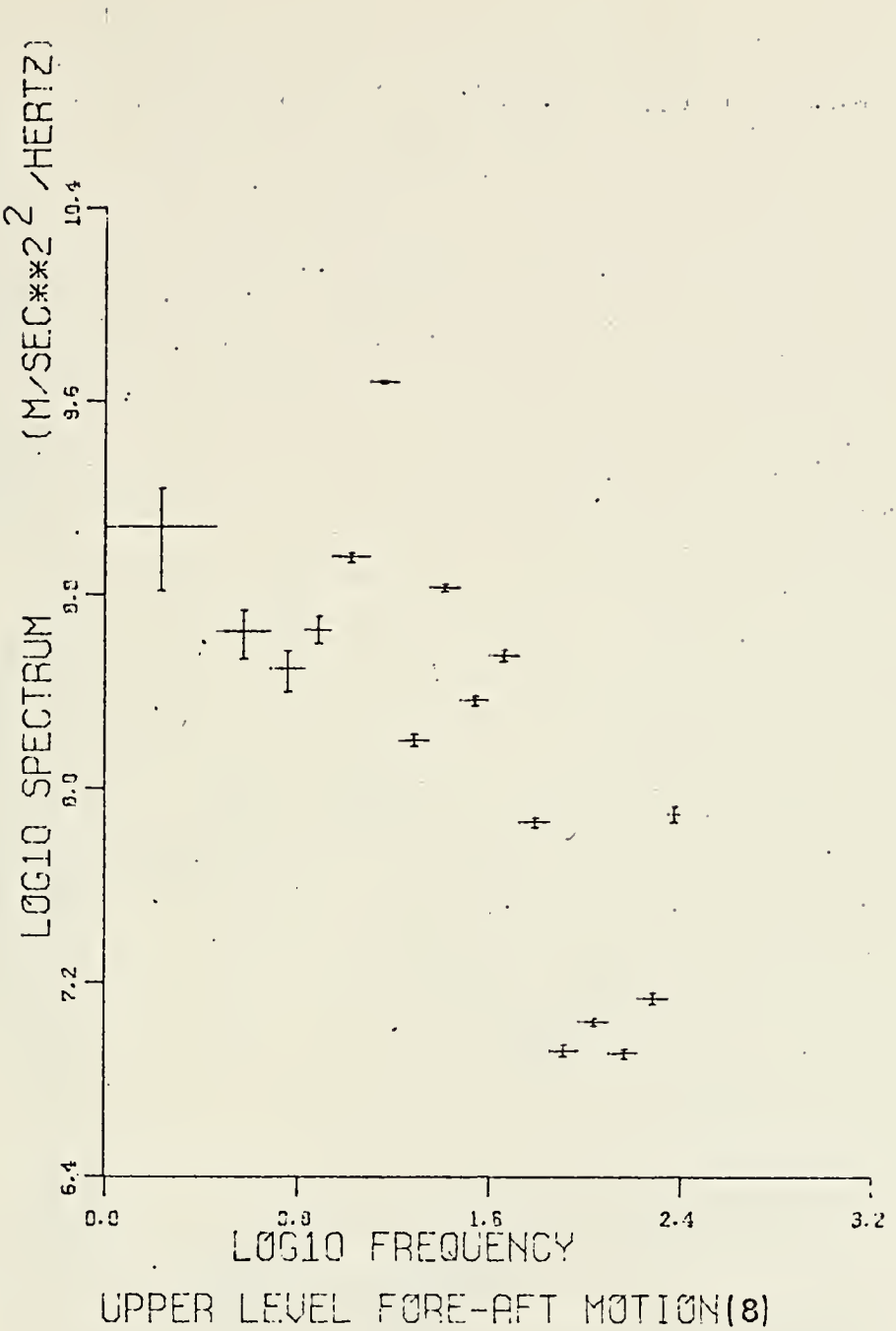
LOG10 SPECTRUM (M/SEC**2)**2/HERTZ)
10.4
9.6
8.8
8.0
7.2
6.4
0.0
0.8
1.6
2.4
3.2
LOG10 FREQUENCY
UPPER LEVEL FORE-AFT MOTION(8)

Figure 25c.

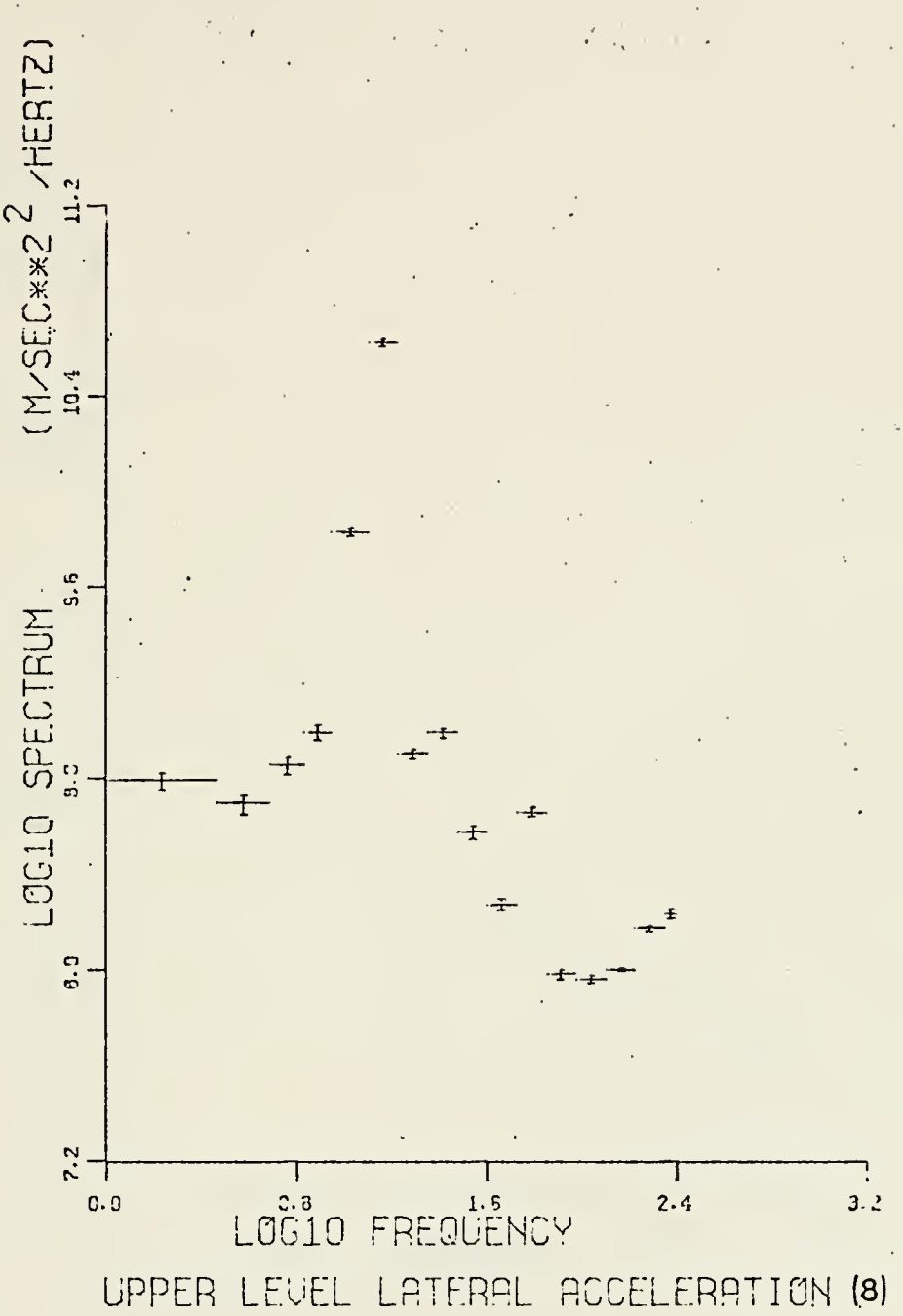
LOG10 SPECTRUM (M/SEC**2 **2 /HERTZ)
11.2
10.4
9.6
8.8
8.0
7.2
0.0
0.8
1.6
2.4
3.2
LOG10 FREQUENCY
UPPER LEVEL LATERAL ACCELERATION (8)

Figure 25d.


LOG10 SPECTRUM (UNITS**2/HERTZ)
10.5
9.5
8.5
7.5
6.5
5.5
0.5
1.0
1.5
2.0
2.5
LOG10 FREQUENCY
U' LEVEL 1

Figure 26.


LOG10 SPECTRUM (UNITS 2/HERTZ)
11.2
10.4
9.6
8.8
8.0
7.2
0.5
1.0
1.5
2.0
2.5
LOG10 FREQUENCY
U' LEVEL 2

Figure 27.


LOG10 SPECTRUM (UNITS**2/HERTZ)
11.2
10.4
9.6
8.8
8.0
7.2
0.5
1.0
1.5
2.0
2.5
LOG10 FREQUENCY
U' LEVEL 3

Figure 28.

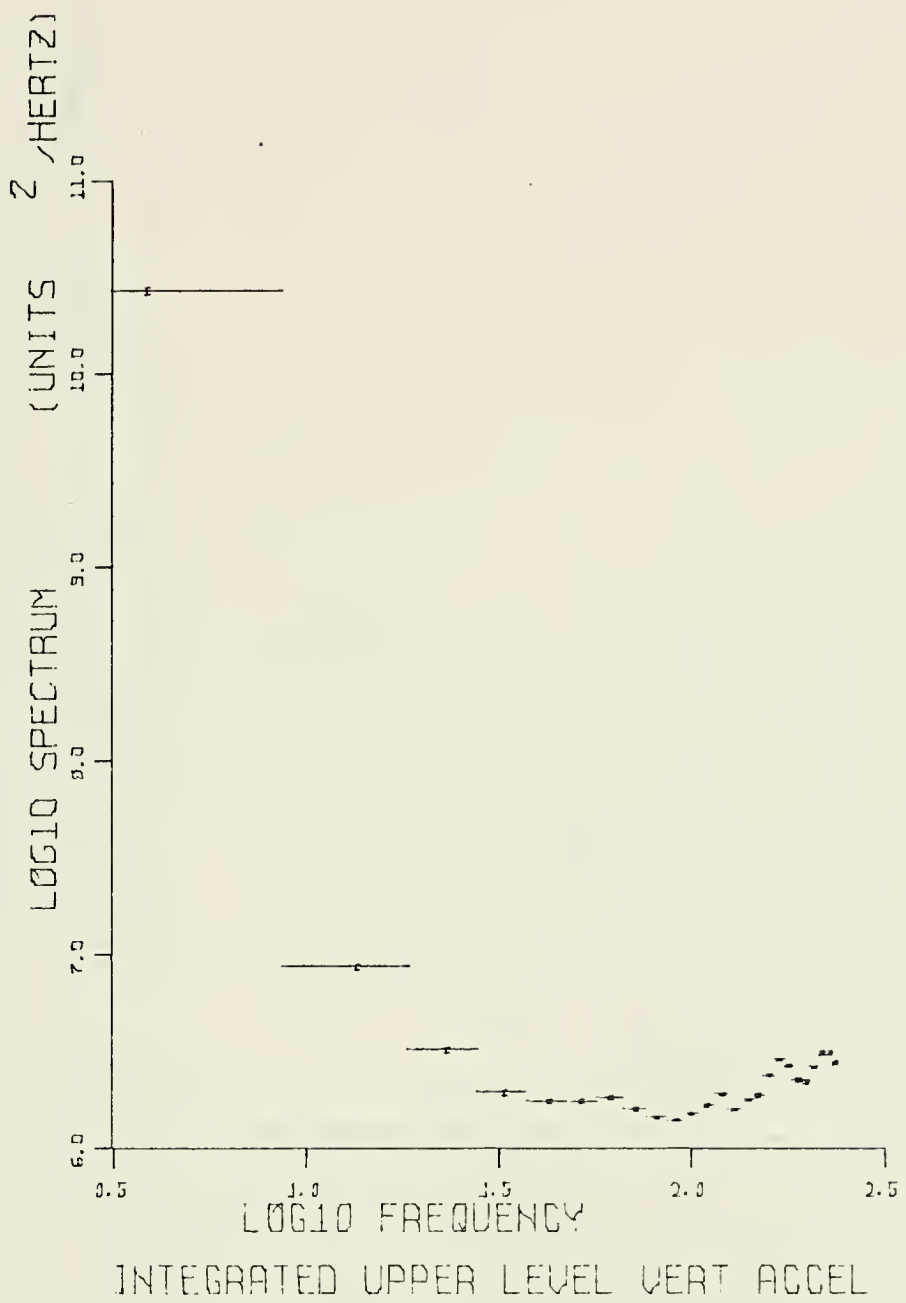
LØG10 SPECTRUM (UNITS 2 /HERTZ)
11.0
10.0
9.0
8.0
7.0
6.0
0.5
1.0
1.5
2.0
2.5
LØG10 FREQUENCY
INTEGRATED UPPER LEVEL VERT ACCEL

Figure 29.

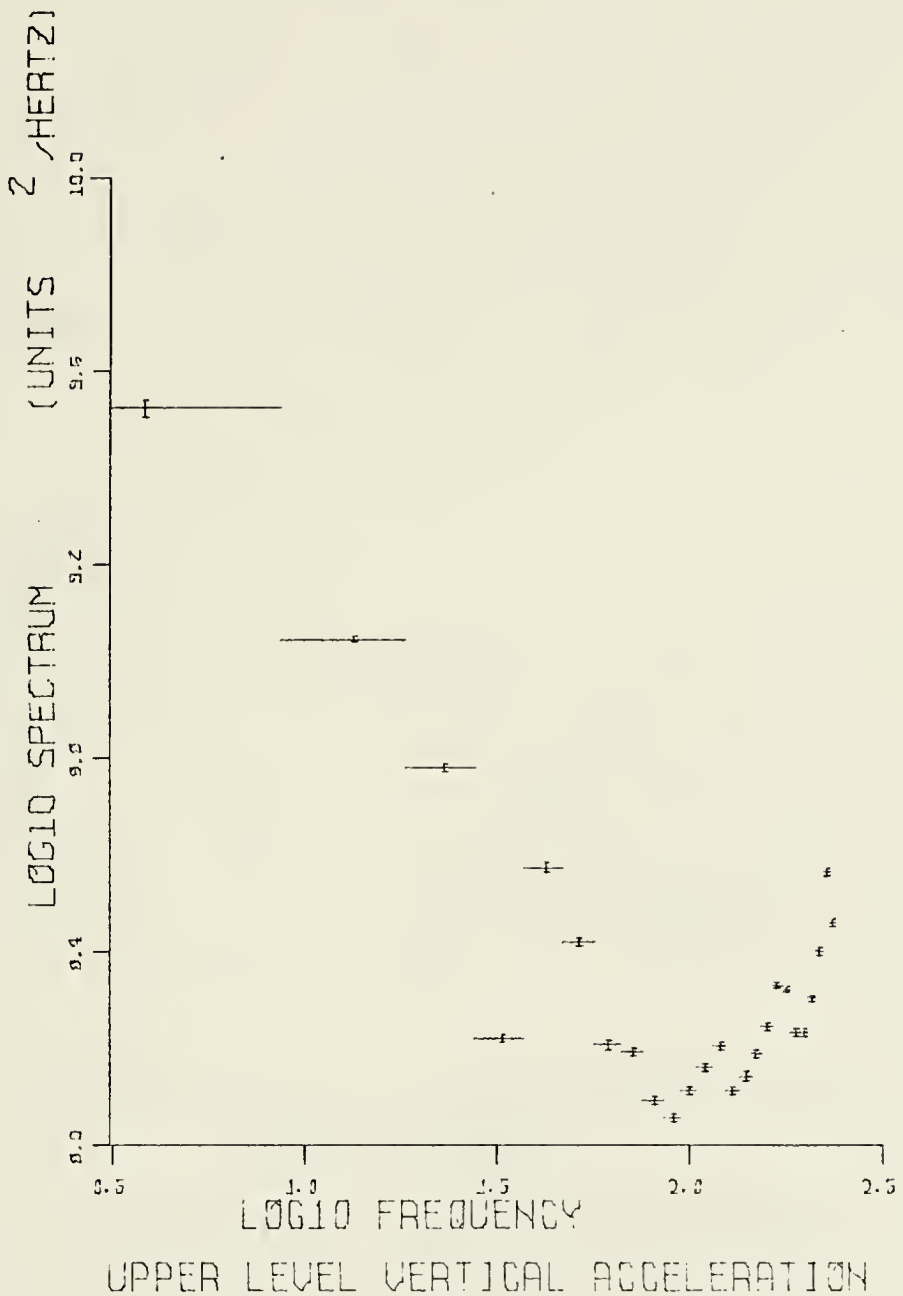
LOG10 SPECTRUM (UNITS 2/HERTZ)
LOG10 FREQUENCY
UPPER LEVEL VERTICAL ACCELERATION

Figure 30.

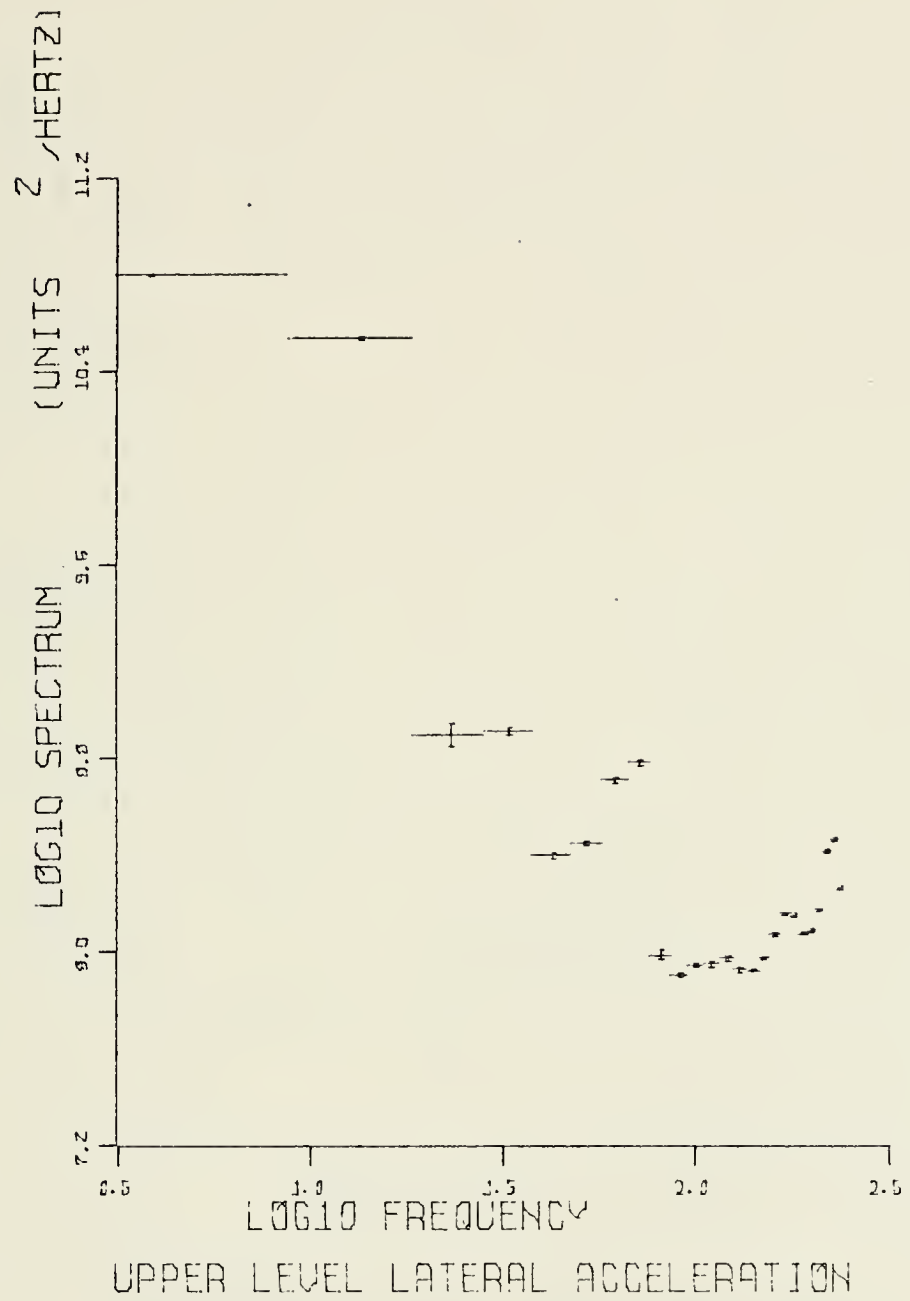
LØG10 SPECTRUM (UNITS 2 /HERTZ)
11.2
10.4
9.6
8.8
8.0
7.2
0.5
1.0
1.5
2.0
2.5
LØG10 FREQUENCY
UPPER LEVEL LATERAL ACCELERATION

Figure 31.

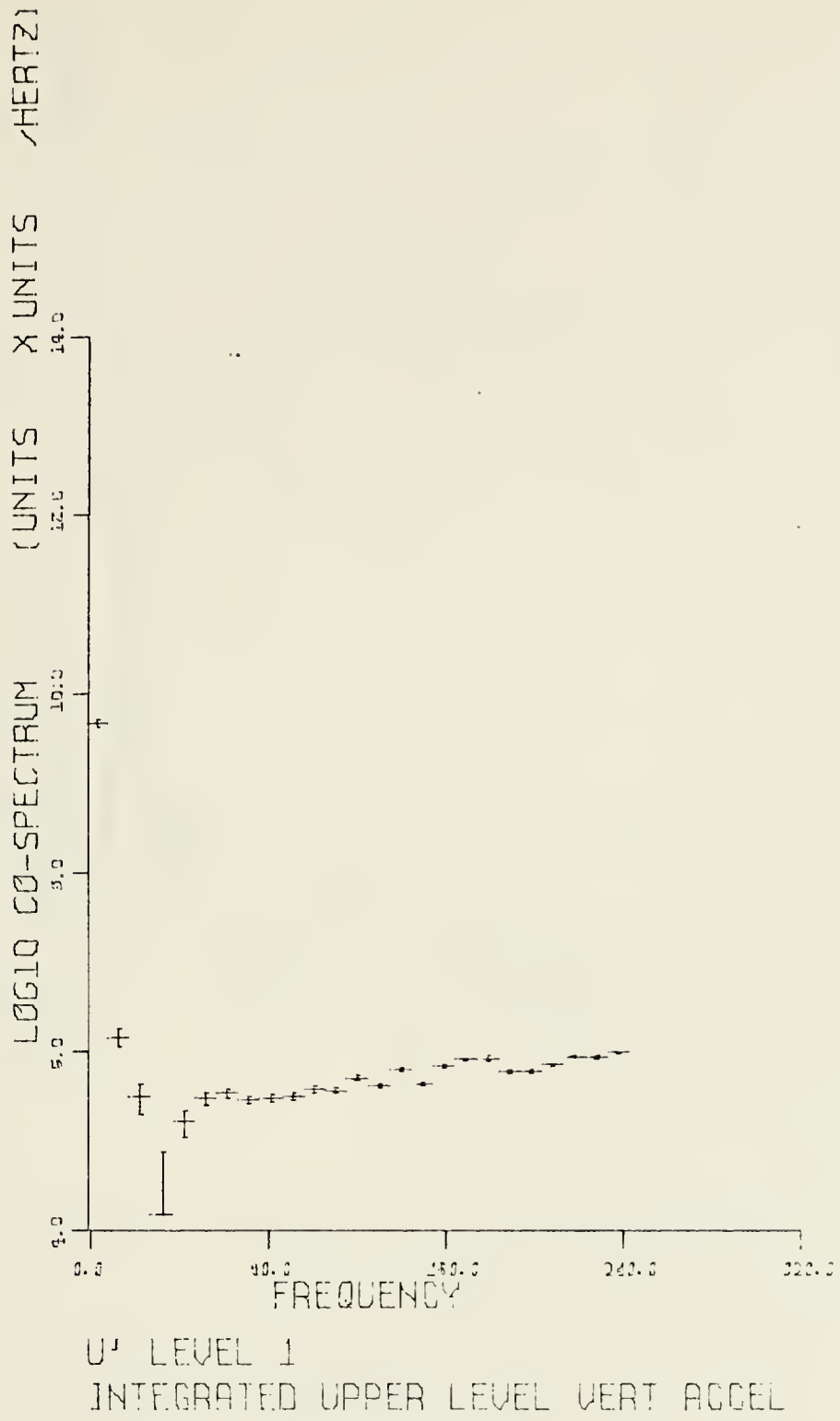
LOG10 CO-SPECTRUM (UNITS X UNITS /HERTZ)
FREQUENCY
U' LEVEL 1
INTEGRATED UPPER LEVEL VERT ACCEL

Figure 32.

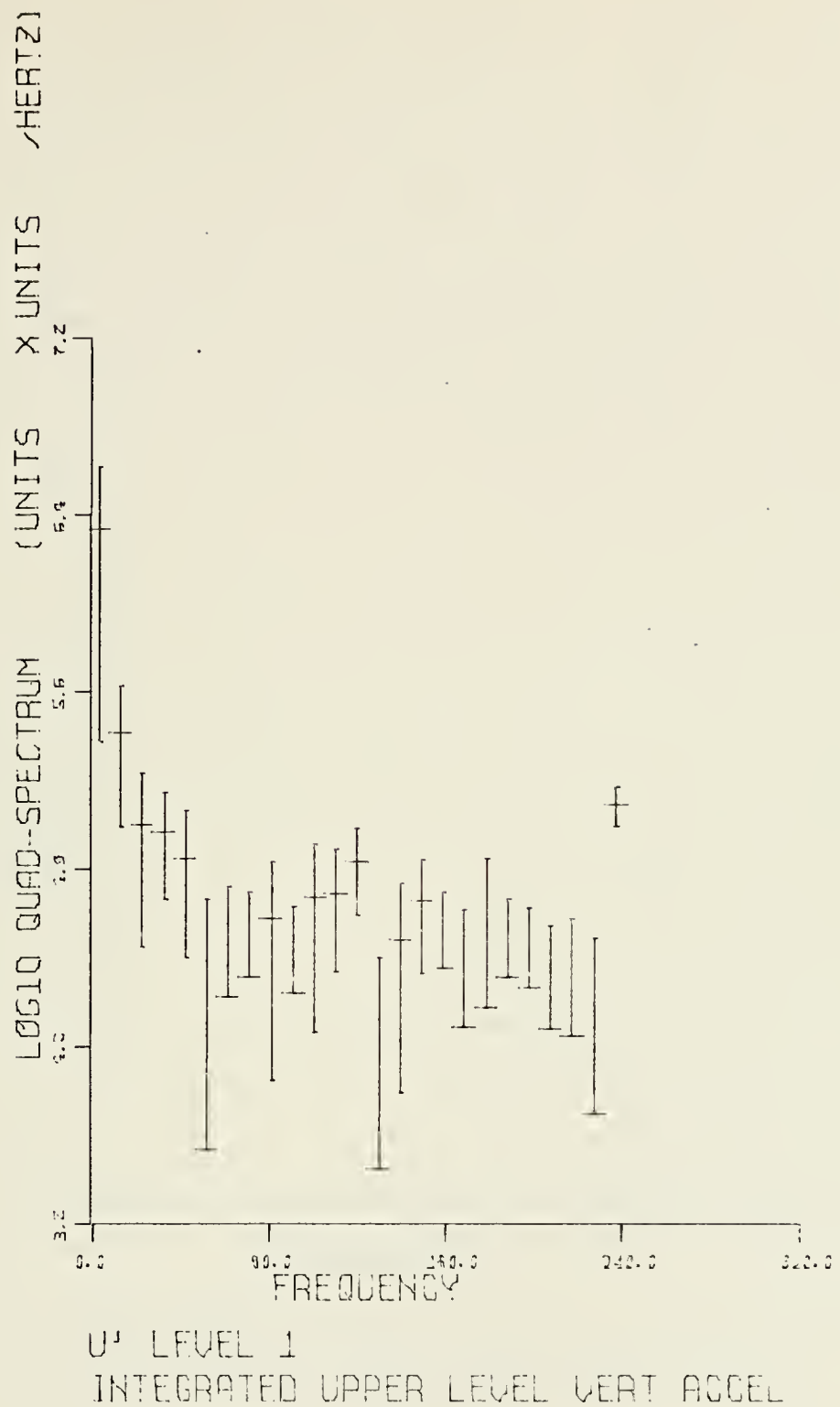
LØG10 QUAD-SPECTRUM (UNITS X UNITS /HERTZ)
7.2
5.9
5.6
3.3
0.0
90.0
180.0
240.0
320.0
FREQUENCY
U' LEVEL 1
INTEGRATED UPPER LEVEL VERT ACCEL

Figure 33.


PHASE (X10¹)
90.0
50.0
FREQUENCY
U³ LEVEL 1
INTEGRATED UPPER LEVEL VERT ACCEL

Figure 34.

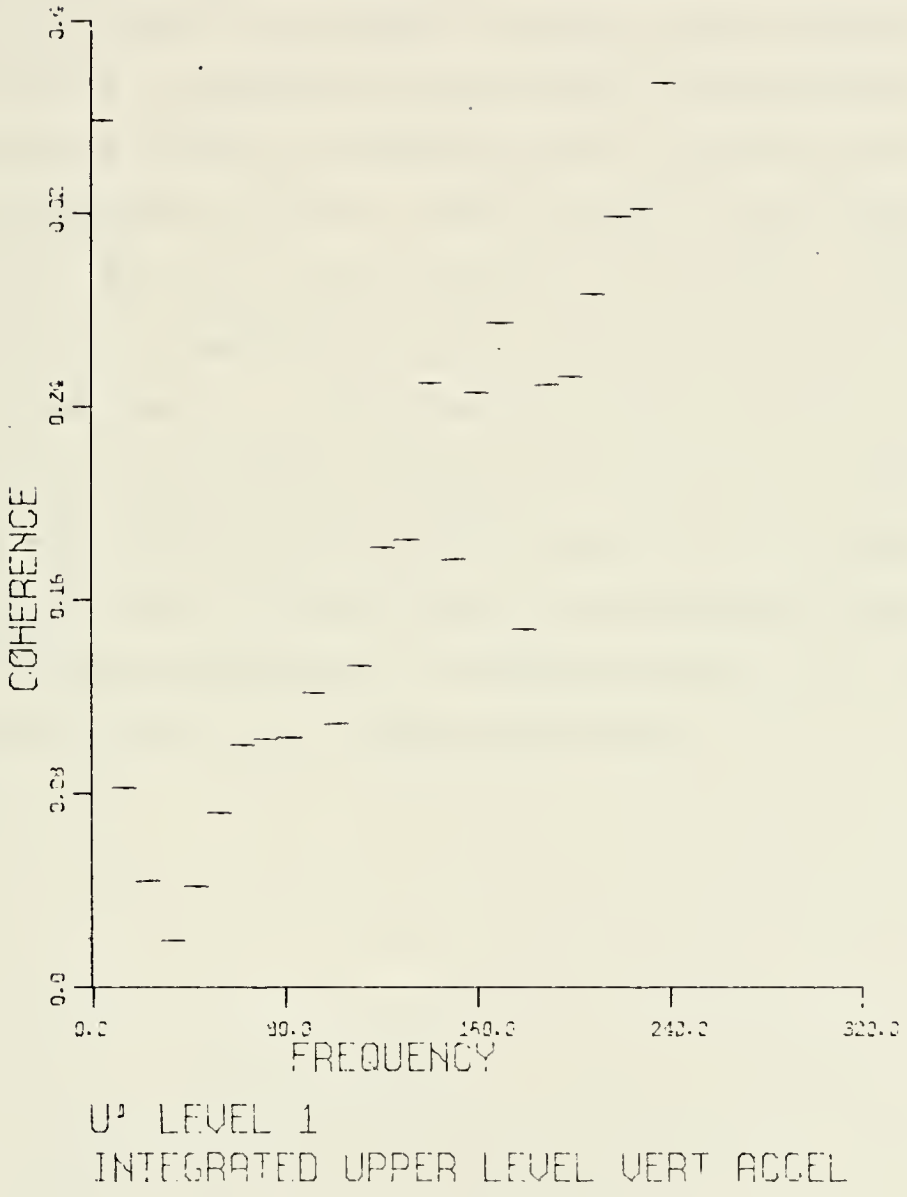
COHERENCE
0.0
0.08
0.16
0.24
0.32
0.0
90.0
160.0
240.0
320.0
FREQUENCY
U³ LEVEL 1
INTEGRATED UPPER LEVEL VERT ACCEL

Figure 35.

linearly with frequency beyond 60 Hz. This is interpreted as either noise intrusion into both spectra, or the effect of the wind energy spectrum decreasing (-5/3 law) until the motion effect gradually becomes more evident.

Consideration of these same plots for the upper triad of accelerometers firther supports a conclusion of isotropy at high frequencies, Figures 36 to 43. The similarity of the co-spectra and quad-spectra shapes as well as the phase and coherence plots for the lateral and vertical accelerometers show that a single instrument could probably suffice for all but the most exact description of the motion. The fore-aft motion and its relationship to vertical motion is more complex. The co-spectra plot shows a strong similarity with the previous co-spectral plot, but the quadrature spectrum show two distinct minima near 80 and 200 Hertz which also show on the coherence plot. A possible explanation for this is vibrations due to rotating machinery aligned fore-aft. These vibrations would be sensed by both vertical and lateral accelerometers but not the one aligned with the shaft.

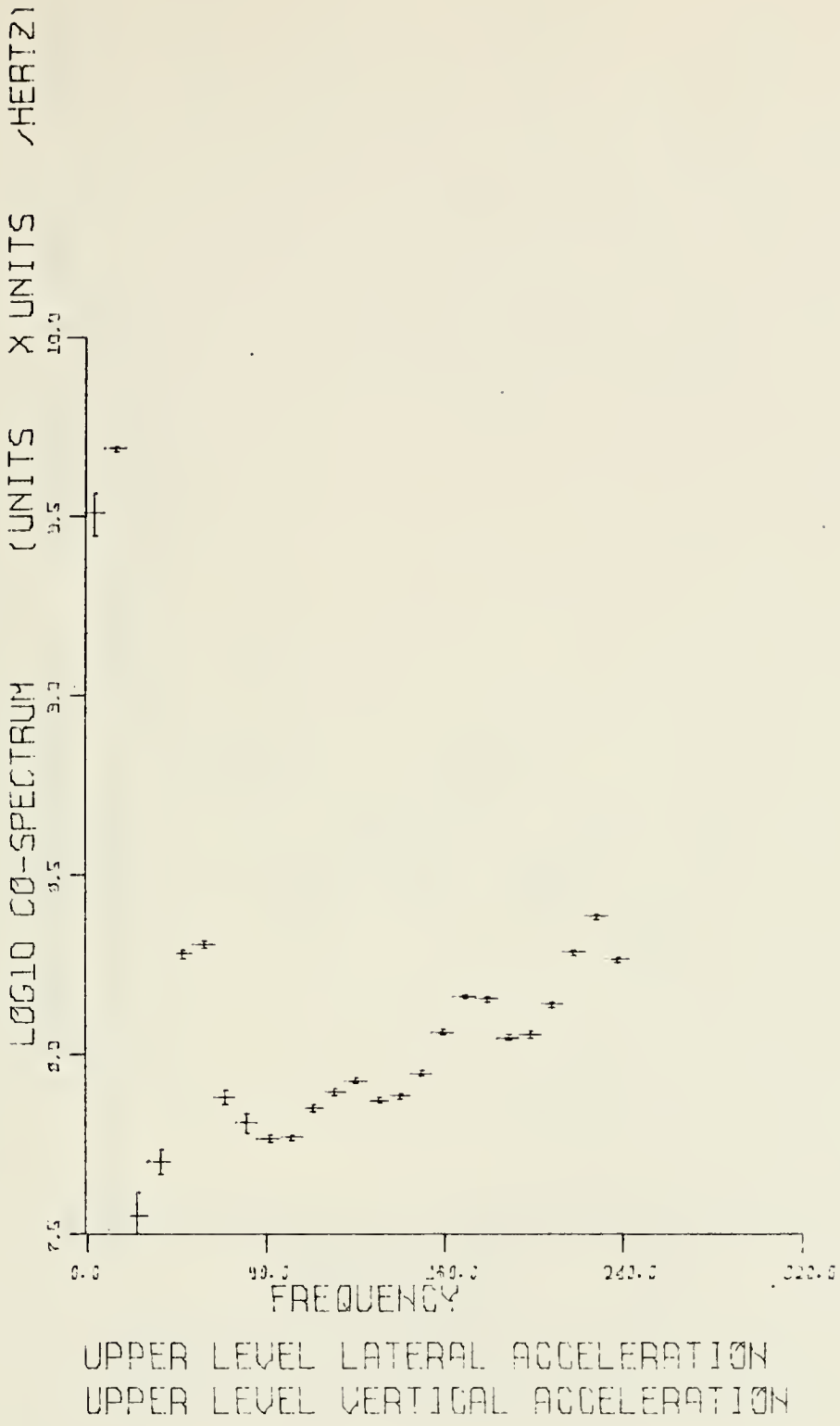
LOG10 CO-SPECTRUM (UNITS X UNITS /HERTZ)
FREQUENCY
UPPER LEVEL LATERAL ACCELERATION
UPPER LEVEL VERTICAL ACCELERATION

Figure 36.


LØG10 QUAD--SPECTRUM (UNITS X UNITS /HERTZ)
FREQUENCY
UPPER LEVEL LATERAL ACCELERATIØN
UPPER LEVEL VERTICAL ACCELERATIØN

Figure 37.

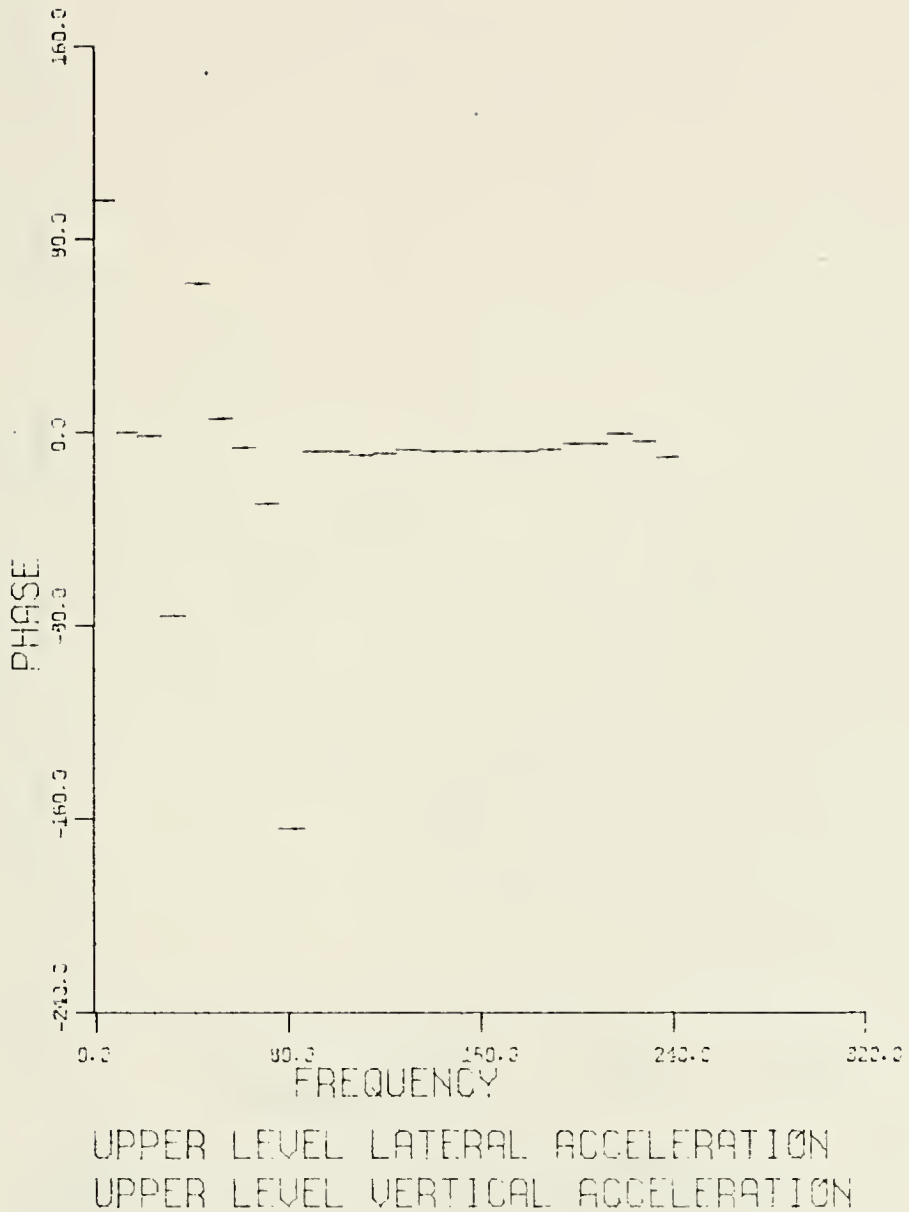
PHASE
FREQUENCY
UPPER LEVEL LATERAL ACCELERATION
UPPER LEVEL VERTICAL ACCELERATION

Figure 38.

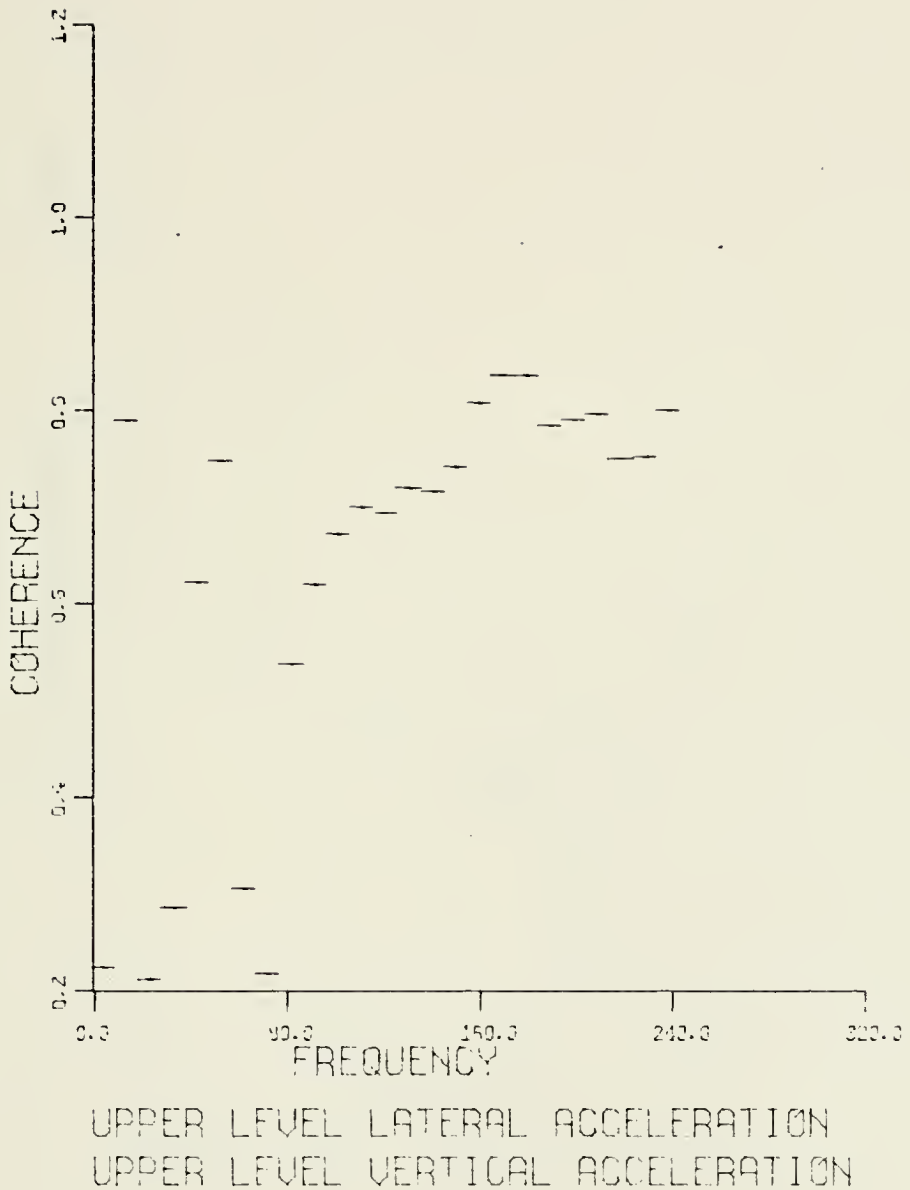
COHERENCE
1.2
1.0
0.5
0.2
0.0
150.0
FREQUENCY
UPPER LEVEL LATERAL ACCELERATION
UPPER LEVEL VERTICAL ACCELERATION

Figure 39.

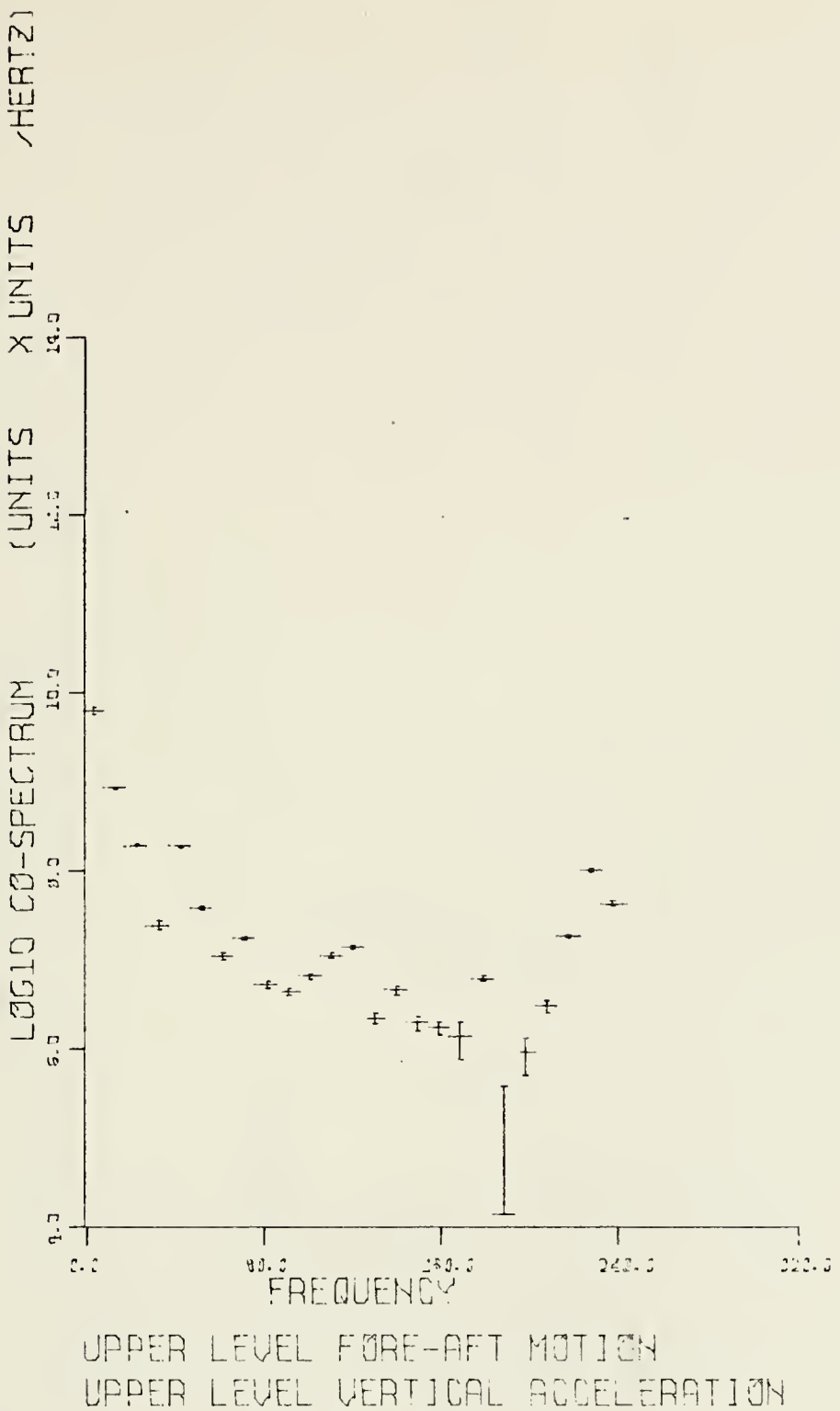
LØG10 CØ-SPECTRUM (UNITS X UNITS /HERTZ)
FREQUENCY
UPPER LEVEL FØRE-AFT MØTIØN
UPPER LEVEL VERTICAL ACCELERATIØN

Figure 40.

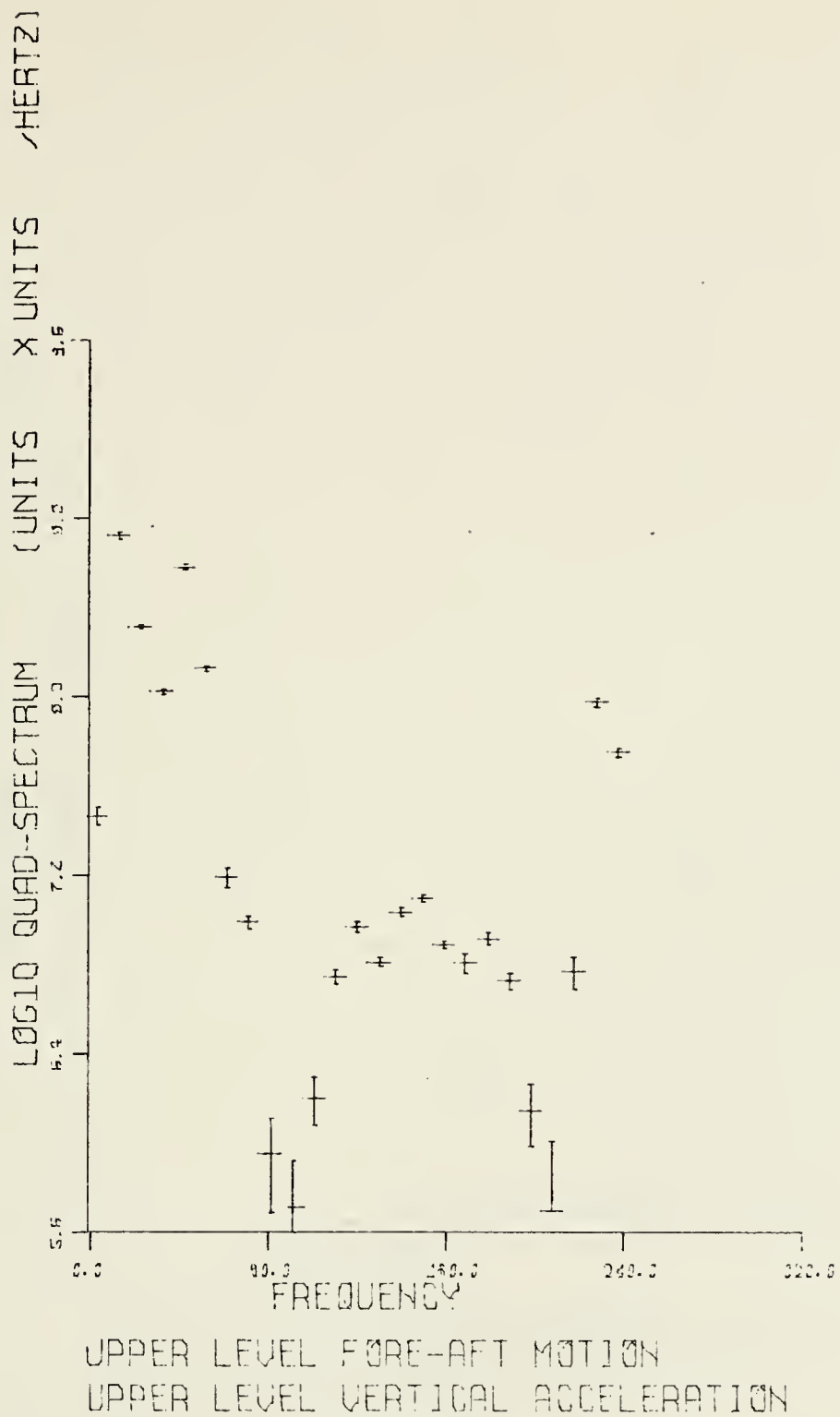
LØG10 QUAD--SPECTRUM (UNITS X UNITS /HERTZ)
FREQUENCY
UPPER LEVEL FØRE-AFT MØTIØN
UPPER LEVEL VERTICAL ACCELERATIØN

Figure 41.

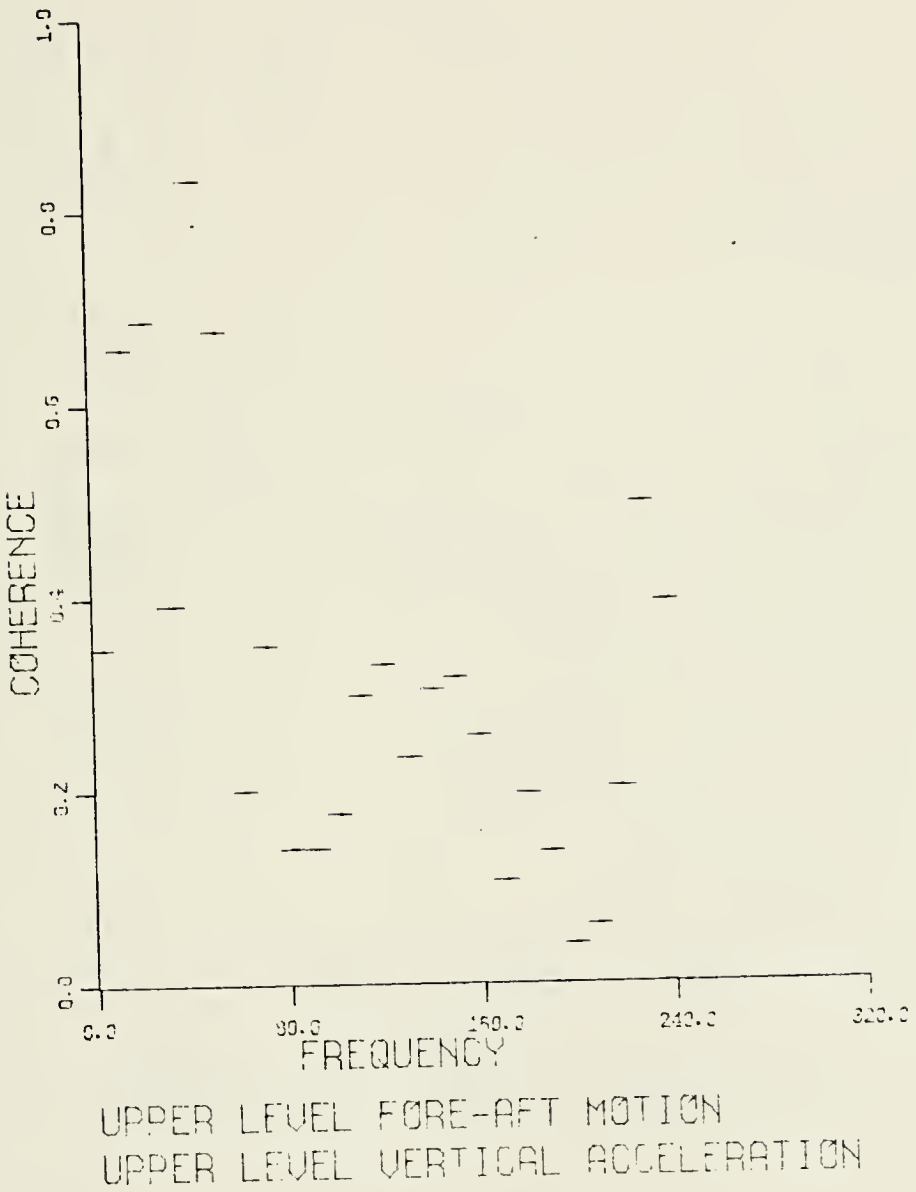
1.0
0.8
0.6
0.4
0.2
0.0
COHERENCE
0.0
80.0
160.0
240.0
320.0
FREQUENCY
UPPER LEVEL FORE-AFT MOTION
UPPER LEVEL VERTICAL ACCELERATION

Figure 42.

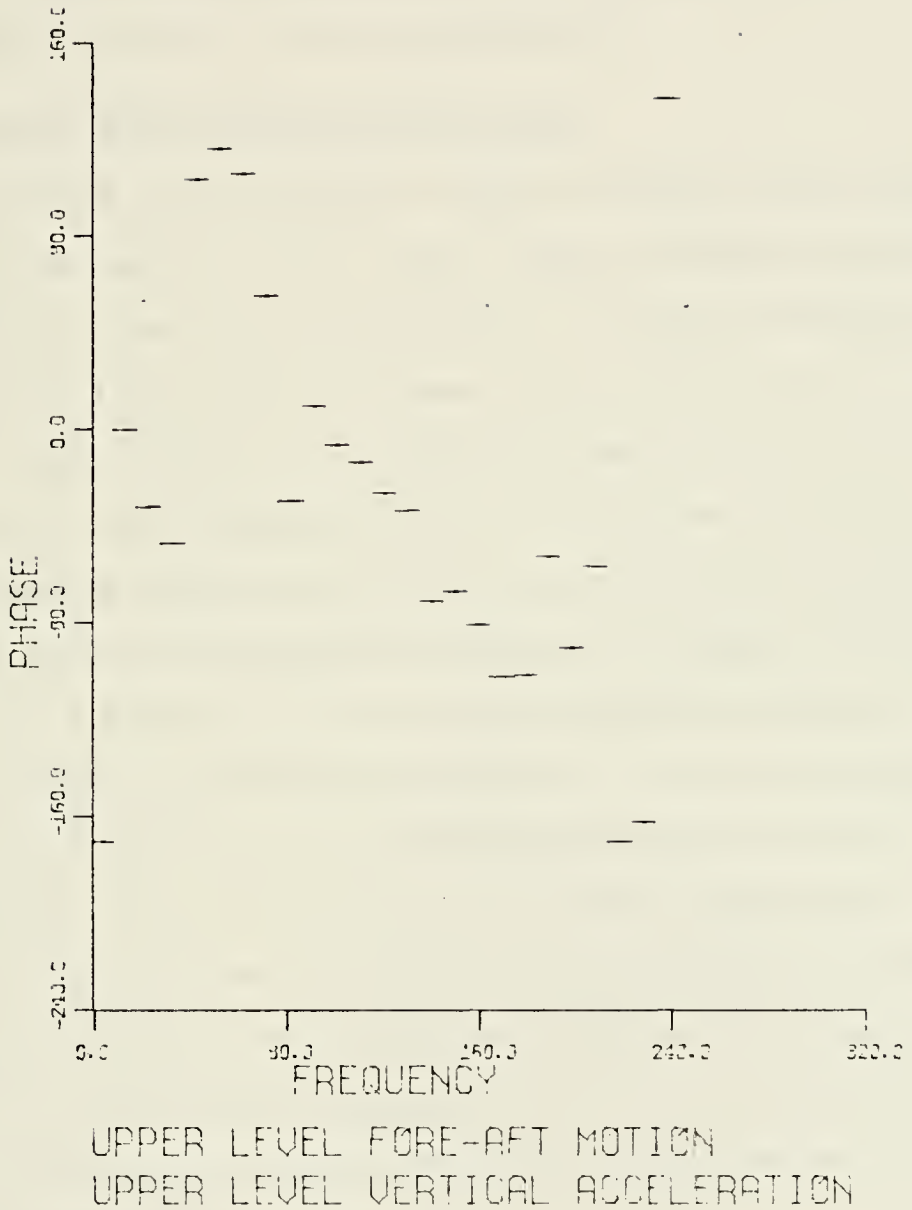
PHASE
FREQUENCY
UPPER LEVEL FORE-AFT MOTION
UPPER LEVEL VERTICAL ACCELERATION

Figure 43.

VI. CONCLUSIONS

A. ABOUT THE MOTION MEASUREMENT SYSTEM

The accelerometer system developed in this study was found to be sufficiently adapted for shipboard application.

B. ABOUT TURBULENCE MEASUREMENTS FROM SHIPS

The results of the experiment indicate that small scale turbulence measurements can be made from a ship. This is a qualified result due to the lack of data during low wind speeds. During the experiment mean winds ranged from about 10 to 20 knots with the latter being most frequent. These velocities are sufficient to give well developed turbulence and a fairly broad inertial subrange. It is apparent from Figures 45 and 46 showing turbulent wind fluctuation spectra and accelerometer spectra that the inertial subrange is generally unaffected by motion between 20 and 50 Hertz. Thus the viscous dissipation parameter (ε) can be estimated from this spectral region. Part of this insensitivity to motion may have been due to the differing nature of the wind fluctuation spectral form and the spectral form of the accelerometers.

At frequencies above and below the inertial subrange the motion of the platform affected the turbulence measurements. Low frequency components in the strip chart segments indicate that there was certainly some fictitious wind induced as the sensor followed the ship's pitching motion through the wind profile.

The results by Kasales (1973) show a consistent energy peak in the vicinity of two Hertz. This was one of the aspects to be explored. It was at one time thought that this was due to a vane assembly oscillation.

However, this was not the case since two analog spectra from this study show similar energy peaks in the region of five Hertz. A significant fact was that the accelerometers had a minimum of energy in the same frequency band. Figure 44 is one of the spectra. This experimenter can only conclude that is a real property of atmospheric turbulence, but not a consistent one.

The high frequency end of the spectrum was dominated by a single spike near 54 Hz, which is thought to have been the frequency of the shipboard power supply. This same contamination appears in u' spectra Figures 45 and 46. This noise, however, is not very significant since it occurs at a distinct frequency.

Other high frequency noise affects the dissipation end of the inertial subrange and ultimately limits a vital cross check on the value of the stress parameter (U_*), as discussed in the background section. It is difficult to select the proper wave number (k_o) for viscous drop-off with such noise in the spectra. Shock mounting of the sensors would decrease the high frequency contamination.

Spectral analysis from both analog or digital means revealed that though the amplitude varies greatly for different members of the upper triad the frequencies remain the same. There were temporal variations in frequency of the spikes, but spatial consistency among the triad appeared to hold in general. With respect to spectral consistency between sensors accelerometers at each level appear to be sufficient to define the high frequency deviations at the dissipation end of the inertial subrange.

Figure 44.

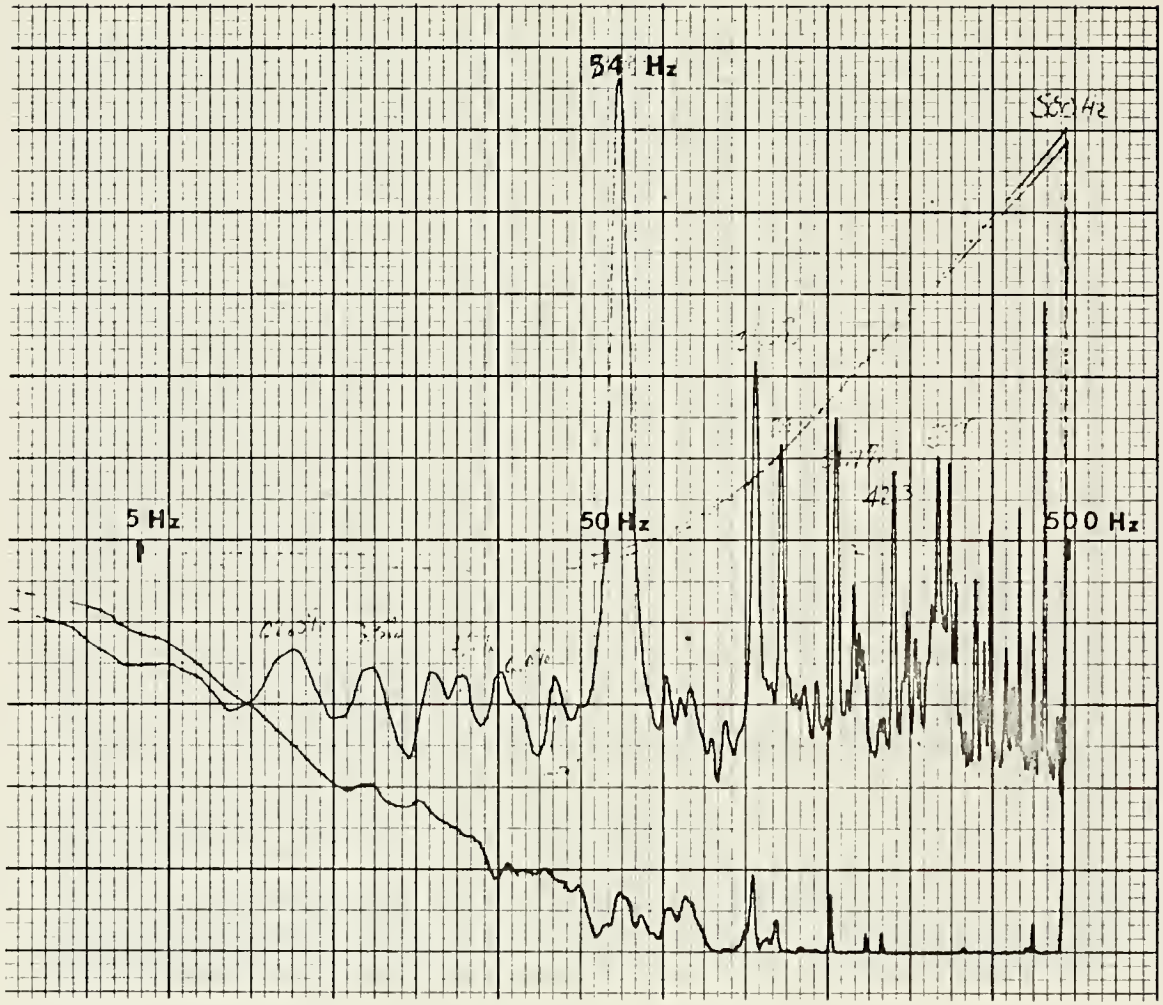

Figure 45.

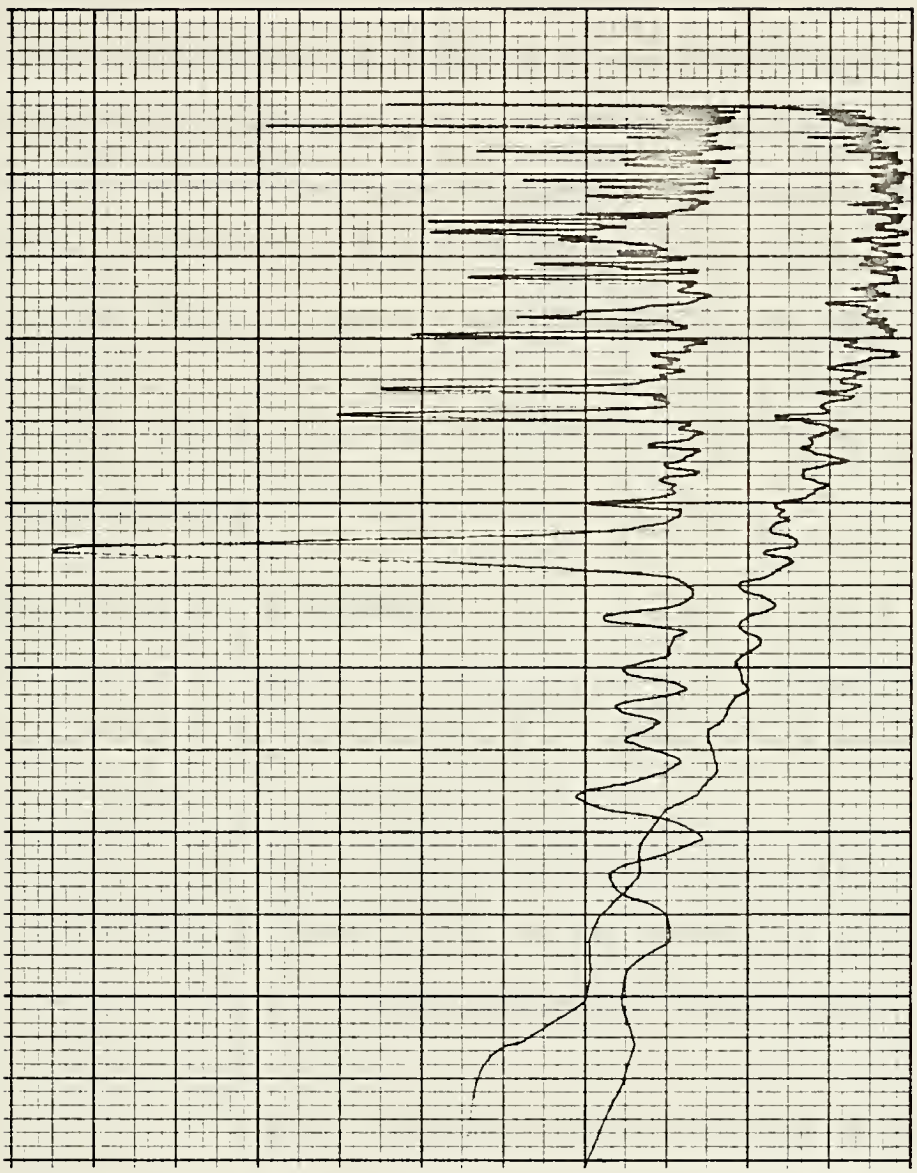

Figure 46.

C. CONSIDERATIONS ON MEAN MEASUREMENTS FROM SHIPS

The mean sensors also showed an effect due to the ship's motion. The pitching of the vessel is the logarithmic wind profile and could produce the observed deviations. The greatest deviations occur at lower heights and would result in an apparent lowering of the sensor, Figure 47. The profile results described by Cavanaugh (1974) showed consistently high values of the drag coefficient, C_D. It is possible that an empirical correction could be determined for this based on the measured shear and the magnitude of the vertical motions which cause this effect.

In shipboard studies of these parameters Denman (1973), did not examine this factor. It is felt that the increase in ship motion during increasing winds may well cause over-estimates of shear, resulting in larger drag coefficients.

D. SUGGESTIONS FOR FUTURE RESEARCH

Specific change recommendations are to increase excitation voltage in the bridge circuit top to the rated level and to use single vertically stabilized accelerometers at each sensor level.

A bottom mounted pressure sensor for wave field data would be useful in describing ship response to the wave field, and also the wave field effects on turbulence. Digitization should be performed to examine low frequency information.

An analog spectrum analyzer should be acquired and used to obtain immediate spectra. This would allow in situ evaluation of the data with more data runs.

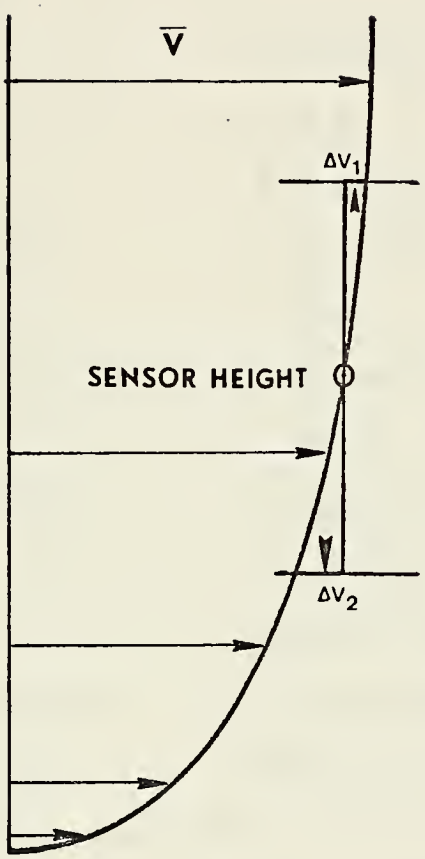

Figure 47. Sensor height variation produces biased mean wind and wind shear values.

APPENDIX A

SENSOR CHARACTERISTICS AND CALIBRATION RESULTS

TYPE: Piezoresistive accelerometer, Model 2265-20 half bridge type.

MANUFACTURER: Endevco

CHARACTERISTIC DATA:

Excitation	10 volts DC
Range	± 20 g
Shock limits	± 80 g, 2000 g pulsed maximum
Frequency response	± 5%, steady state to 200 Hz.
Weight	6 grams
Transverse sensitivity	Less than 5%
Warmup time	1 minute
Resistance (each arm)	Nominal 1800 ohms
Ground	Inner shield connected to cable shield
Signal level	Nominal 30 millivolts/g
Linearity and hysteresis	± 2% over range
Humidity protection	Epoxy and silicone rubber sealed

FACTORY CALIBRATION: 21 August 1973

Serial	Color	Signal	Maximum Transverse Sensitivity	Zero Measured Output	Resonant Frequency
BC 25	Red	34.4 mv/g	.3%	+13.5 mv	1.11 KHz
BC 50	White	33.5	1.9	+14.3	1.13
BC 65	Blue	36.8	3.0	+ 8.8	1.12
BC 28	Cromate	37.5	2.4	-19.7	1.08
BC 18	Grey	33.0	1.6	+19.0	1.08
BC 43	Gold	31.4	2.5	+ 9.5	1.13

FREQUENCY RESPONSE:

	50 Hz	100 Hz	150 Hz	200 Hz
Red	0	0	+1%	+2.5%
White	0	0	+1	+2
Blue	0	0	+1	+2.5
Chromate	0	0	+1	+2.5
Grey	0	0	+1	+3
Gold	-.5	0	+1	+2

PRESAIL CALIBRATION (with amplifier):

The presail calibration was limited to a signal output level measurement. The accelerometers were connected to 200 feet of cable and both were color-coded to a specific amplifier. The bridge was then balanced to $\pm$0.0001 volt on a recently calibrated Simpson digital voltmeter. Sensors were attached to a vane and positioned to measure the earth's gravitational field. Measurements were also taken at ninety degree increments. These measurements were all completed at least twice.

TABLE A-1

AMP	COLOR LEVEL(H/L) AXIS	Volts -1g	ΔV	0g	ΔV	+1g
6	Red H.L. (Lateral)	+0.027 +0.028	0.347	-0.320 -0.319	0.378	-0.698 -0.697
5	White L.L. (Pitch)	+0.205 +0.208 +0.211	0.395	-0.188 -0.187 -0.186	0.416	-0.605 -0.603 -0.602
4	Blue H.L. (Vertical)	+0.063 +0.063	0.329	-0.266 -0.267	0.370	-0.636 -0.635

TABLE A-1 (con)

AMP	COLOR LEVEL (H/L) AXIS	volts -1g	ΔV	0g	ΔV	+1g
3	Gray L.L. (failed)	-0.030 -0.030	0.344	-0.374 -0.373	0.394	-0.769 -0.768
2	Chromate H.L. (fore-aft)	+0.475 +0.478	0.629	-0.153 -0.153	0.646	-0.799 -0.798
1	Gold L.L. (roll)	-0.196 -0.192	0.391	+0.200 +0.195	0.387	+0.582 +0.586

INSTALLATION CHECK-OUT:

On completion of installation sensors were checked for operation during a calm night with R/V Acania moored pierside prior to getting underway.

SHIP'S CLINOMETER READING

List: 0.5 degree starboard

Roll: 1 degree peak

TABLE A-2

Sensor	Mean Voltage	Deviation
Red	0.243	0.004
White	0.371	0.001
Blue	0.240	0.002
Gray	2.485	Steady
Chromate	0.195	0.002
Gold	0.258	0.003

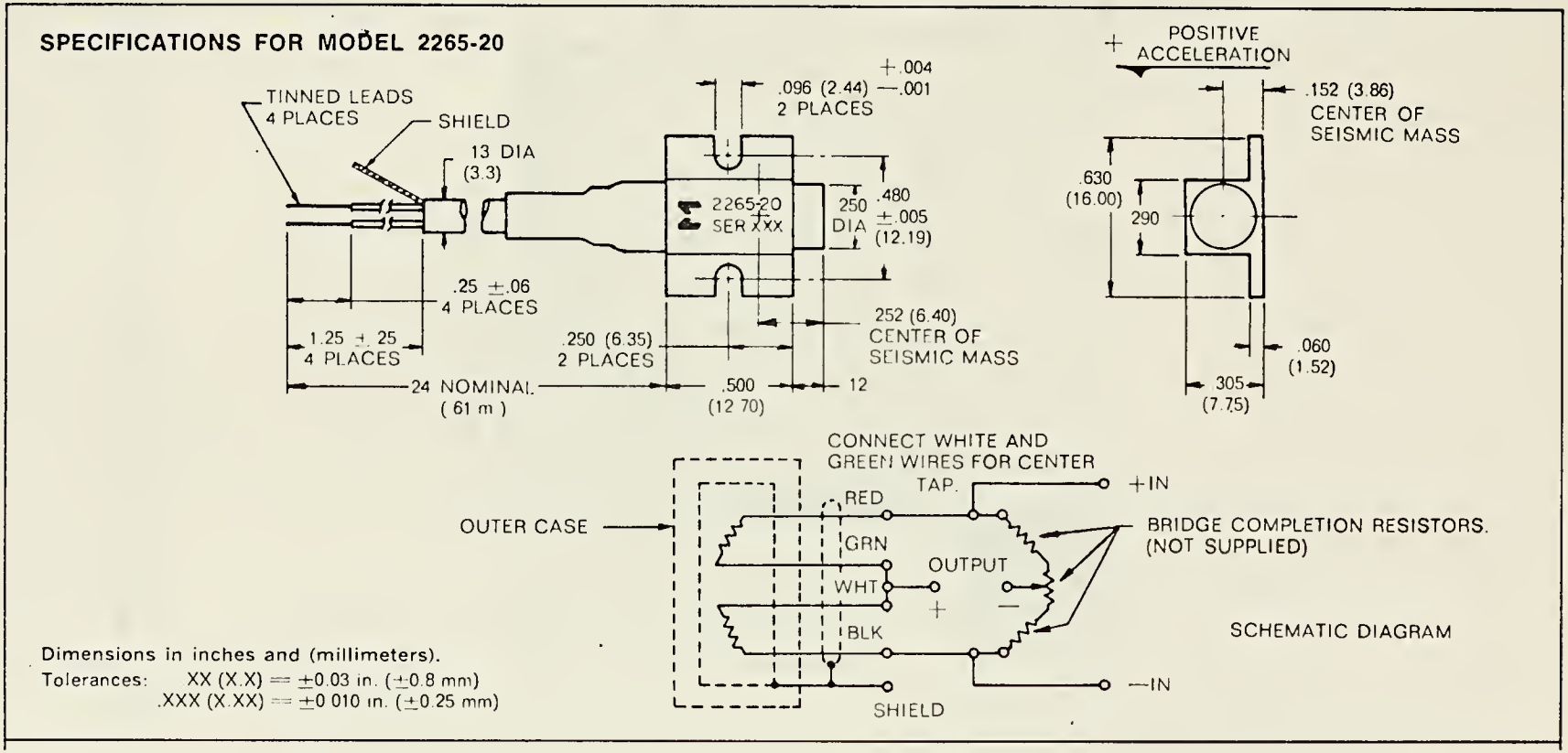

Figure A-1. Schematic of a piezoresistive accelerometer (from manufacturer).

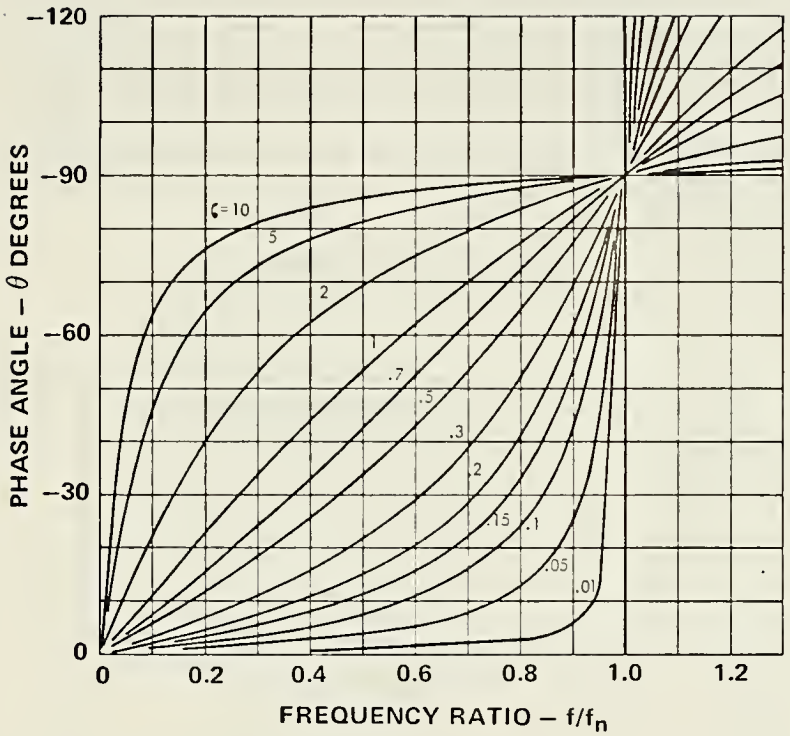

Figure A-2. Phase shift as a function of damping (from manufacturer).

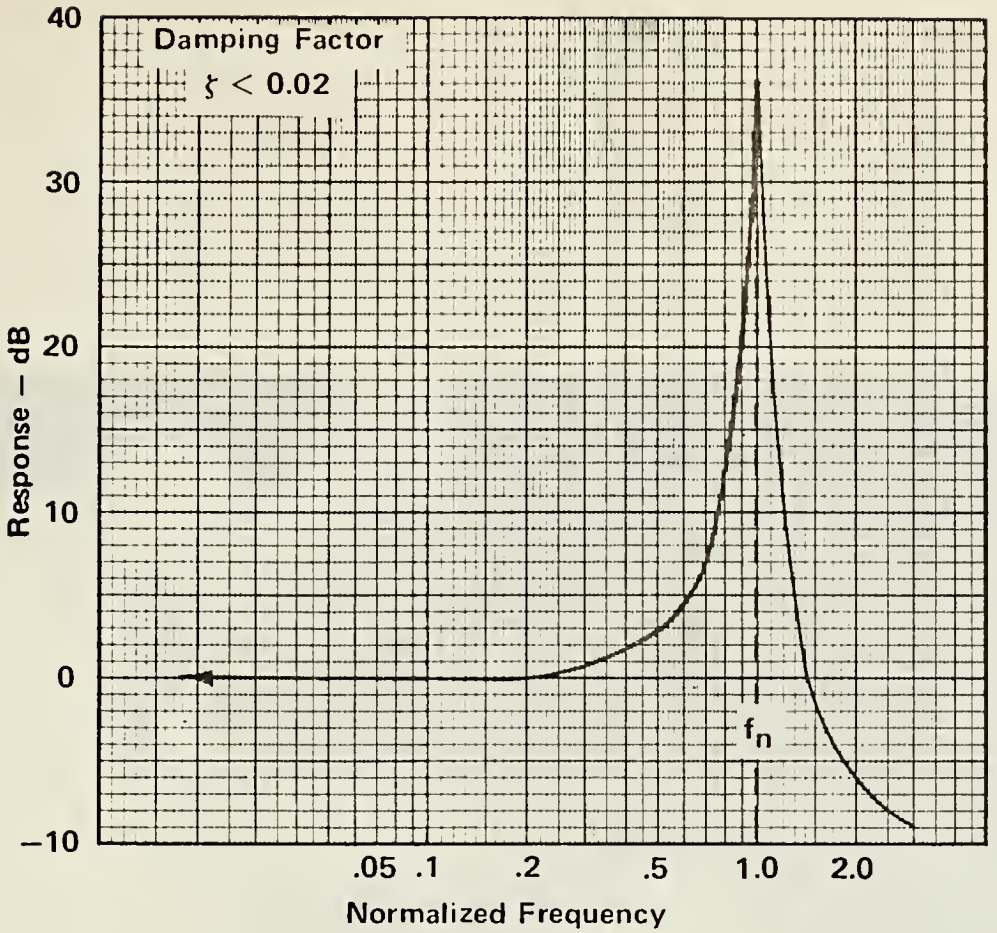

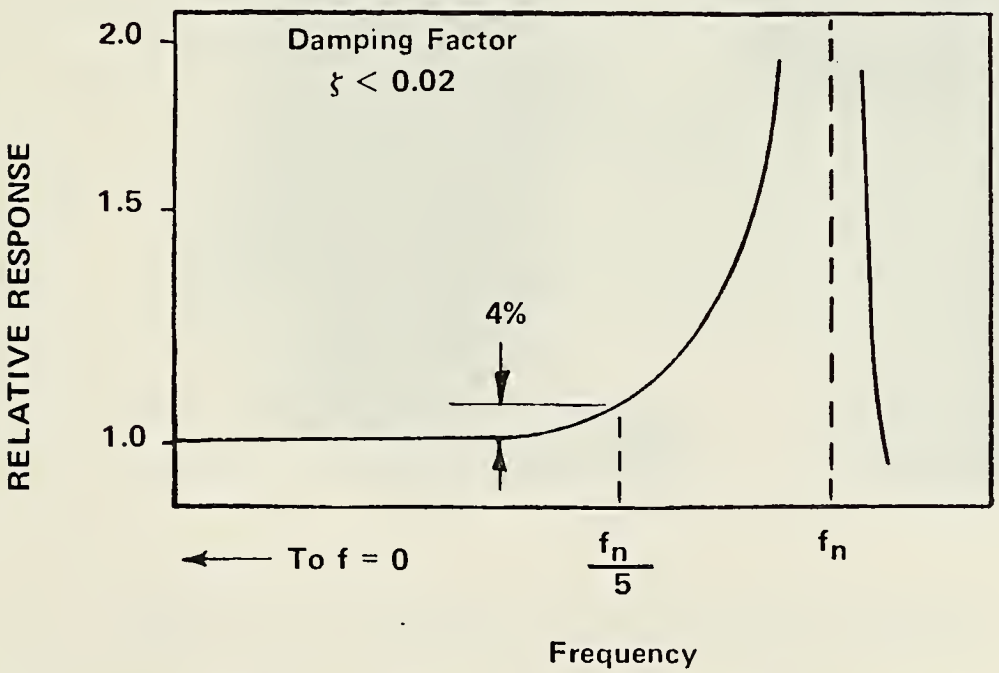

Figure A-3. Frequency response curves (from manufacturer).

Figure A-4. Disassembly of the lower sensor mounting.

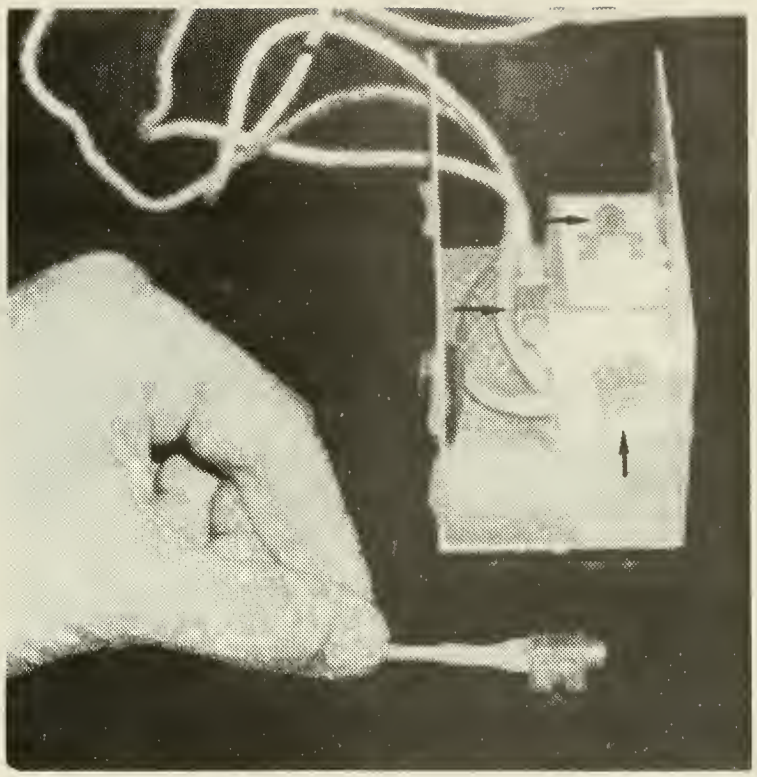

Figure A-5. Upper mounting after disassembly. Arrows indicate sensors.

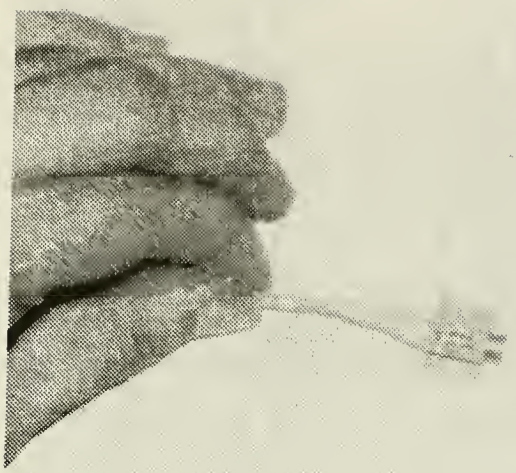

Figure A-6. Typical sensor.

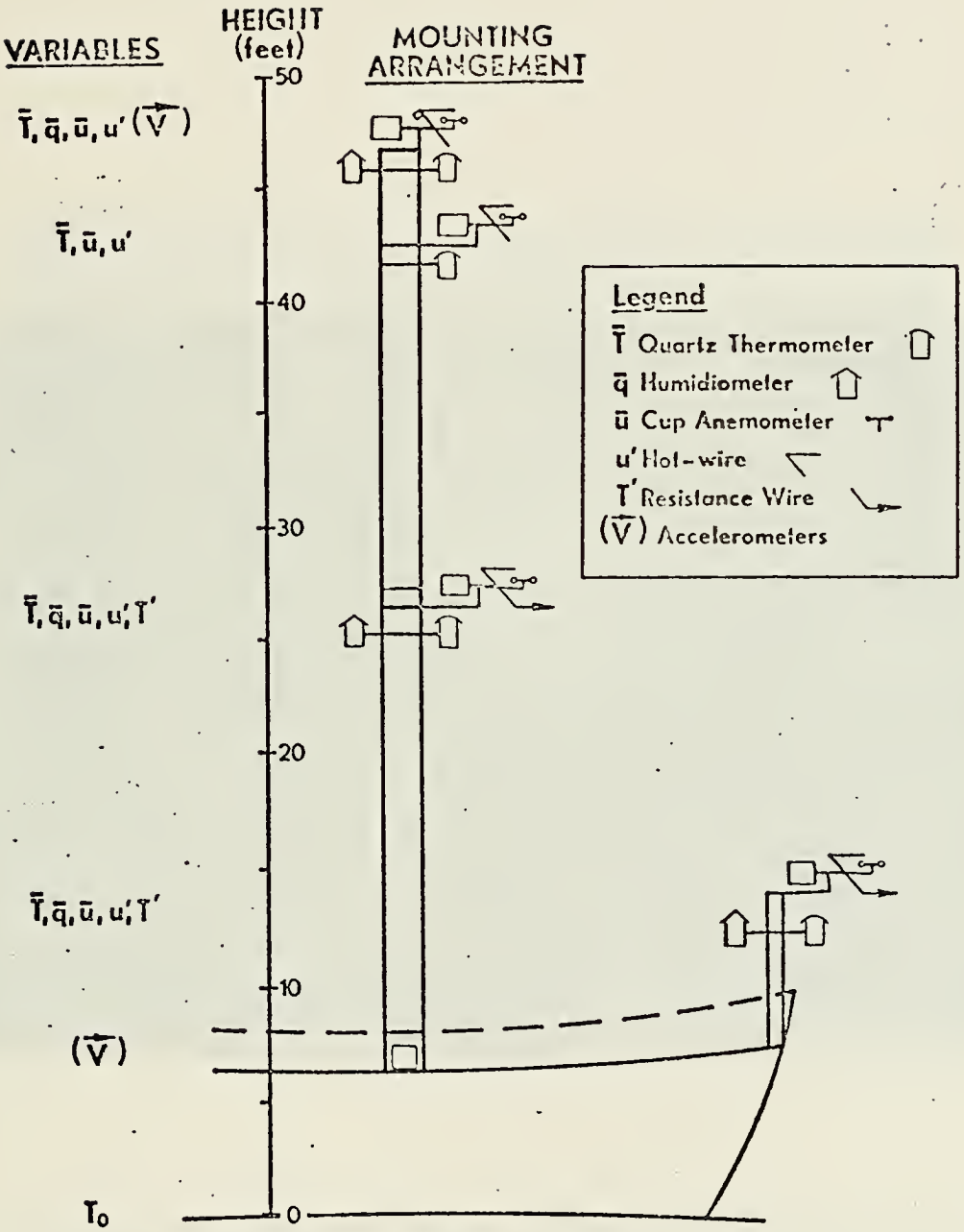

Figure A-7. Sensor schematic.

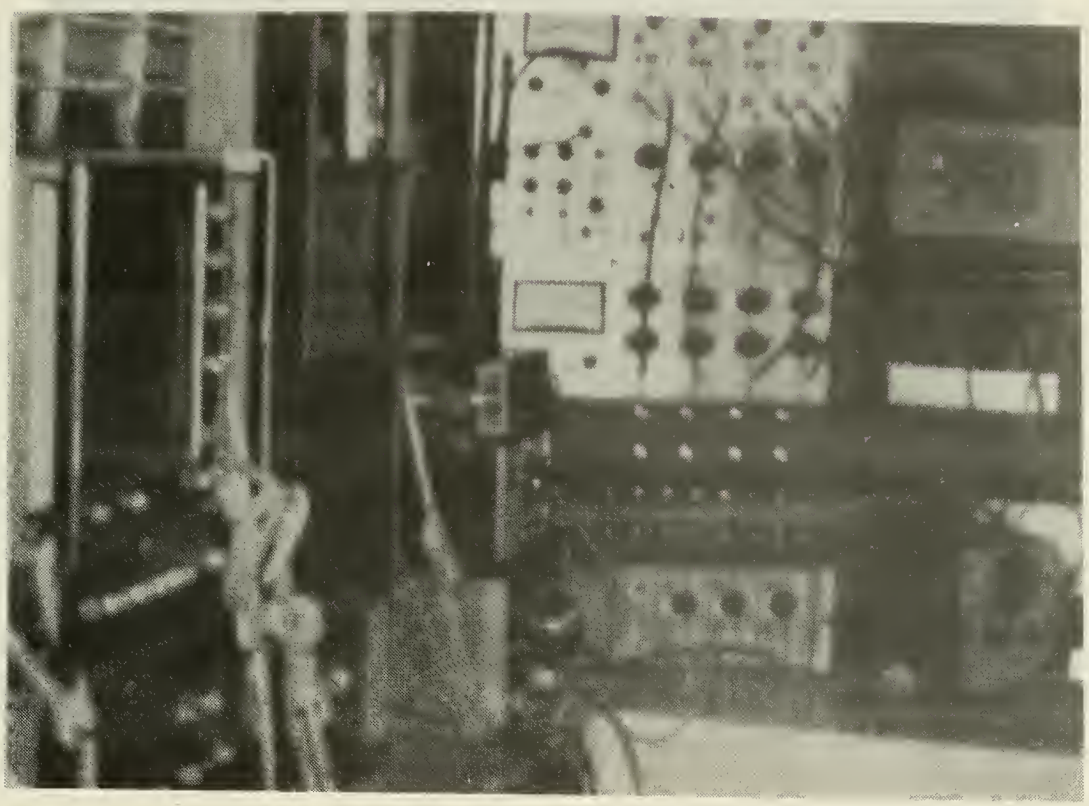

Figure B-1. Dry laboratory array. From left, spectrum analyzer, tape recorder, fluctuation conditioning panels, oscilloscope monitor.

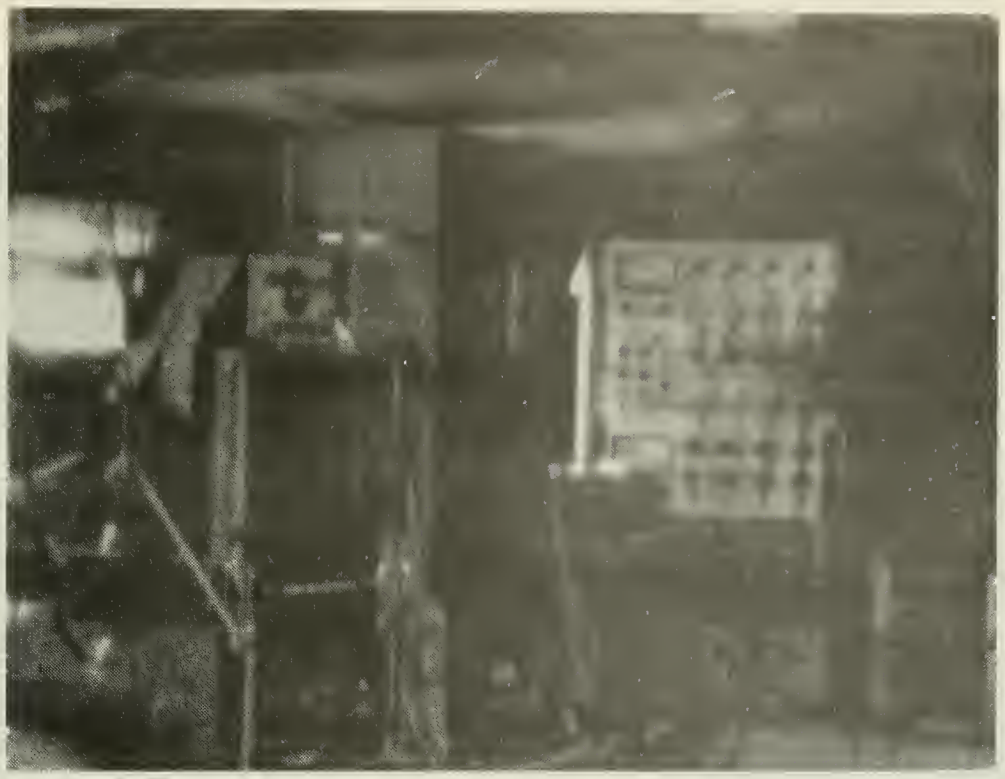

Figure B-2. Dry laboratory second view.

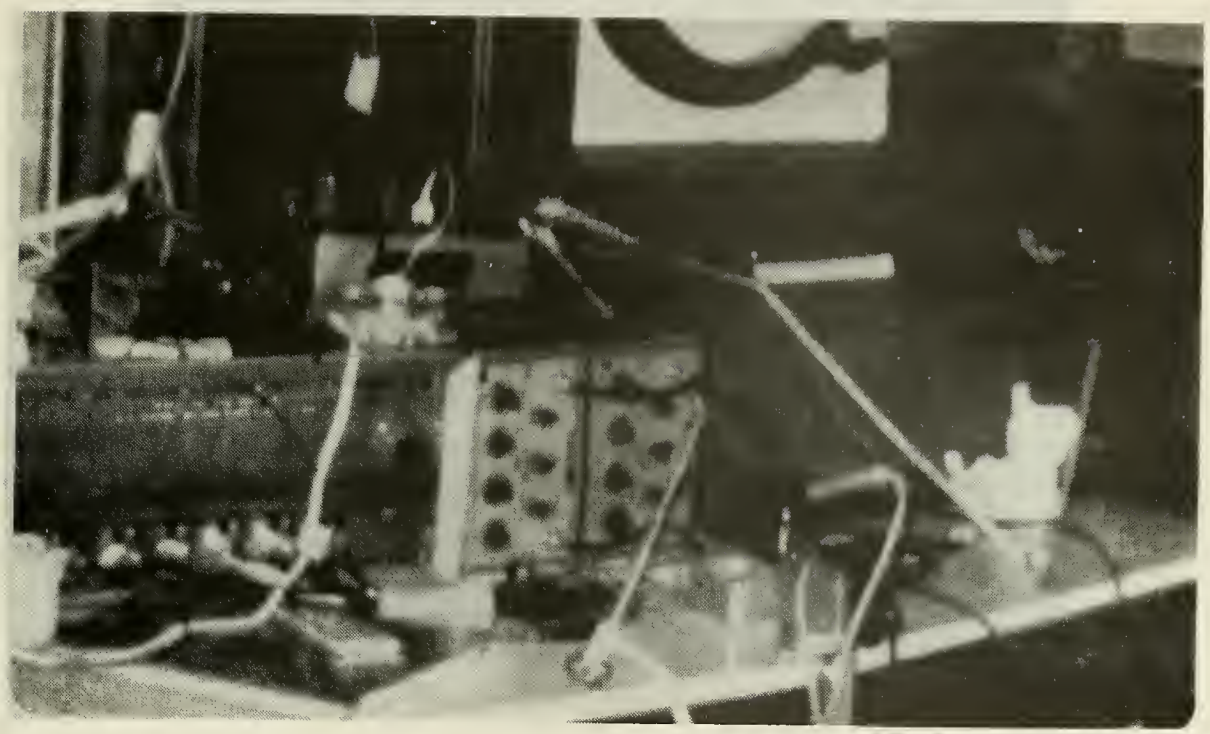

Figure B-3. Dry laboratory array. From left, accelerometer conditioning unit, filters, tape recorder.

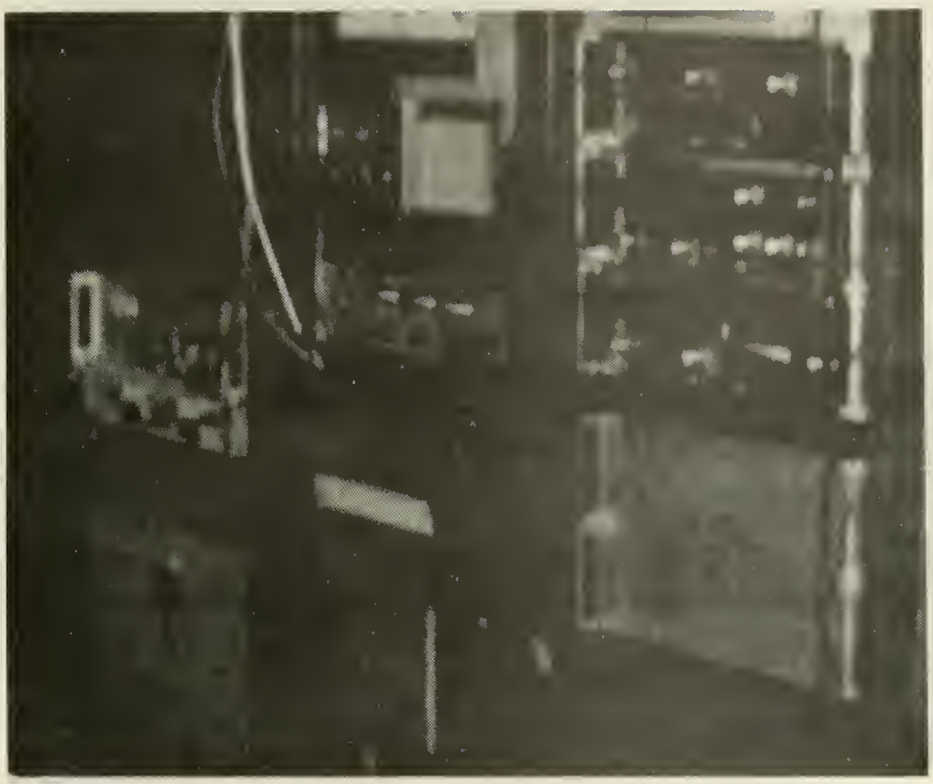

Figure B-4. Dry laboratory array. Items included; temperature array monitor, humidity array monitor, wind speed counter indicators.

Figure B-5. LT W.E. Johnston checks probe assembly on stem mast.

Figure B-6. LT M.P. Cavanaugh climbs the main instrument mast to Connect cables.

Figure B-7. Highest level of mast, note accelerometer and blank casings on probe assembly.

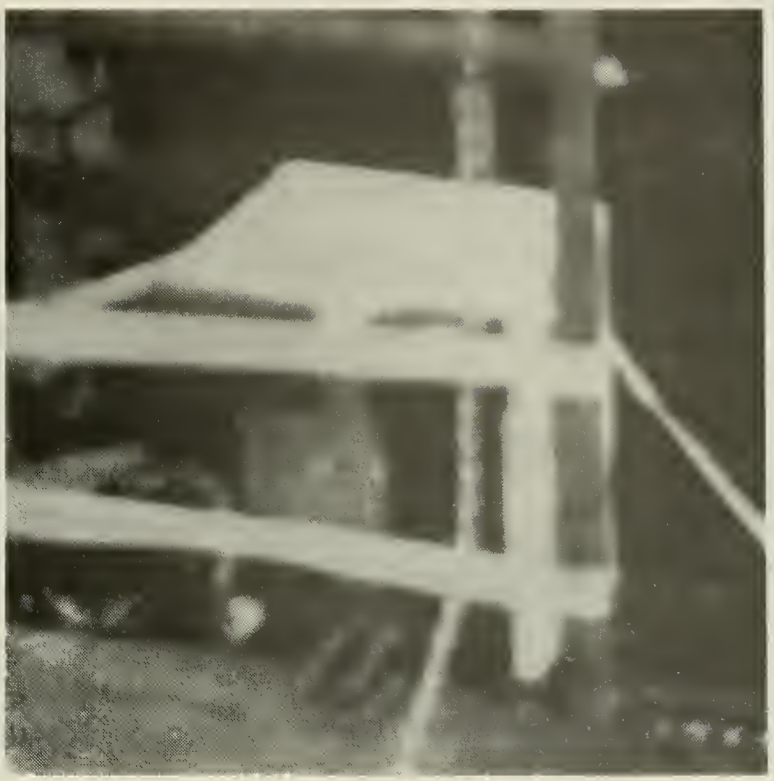

Figure B-8. Lower mounting.

Figure B-9. Sea surface temperature probe.

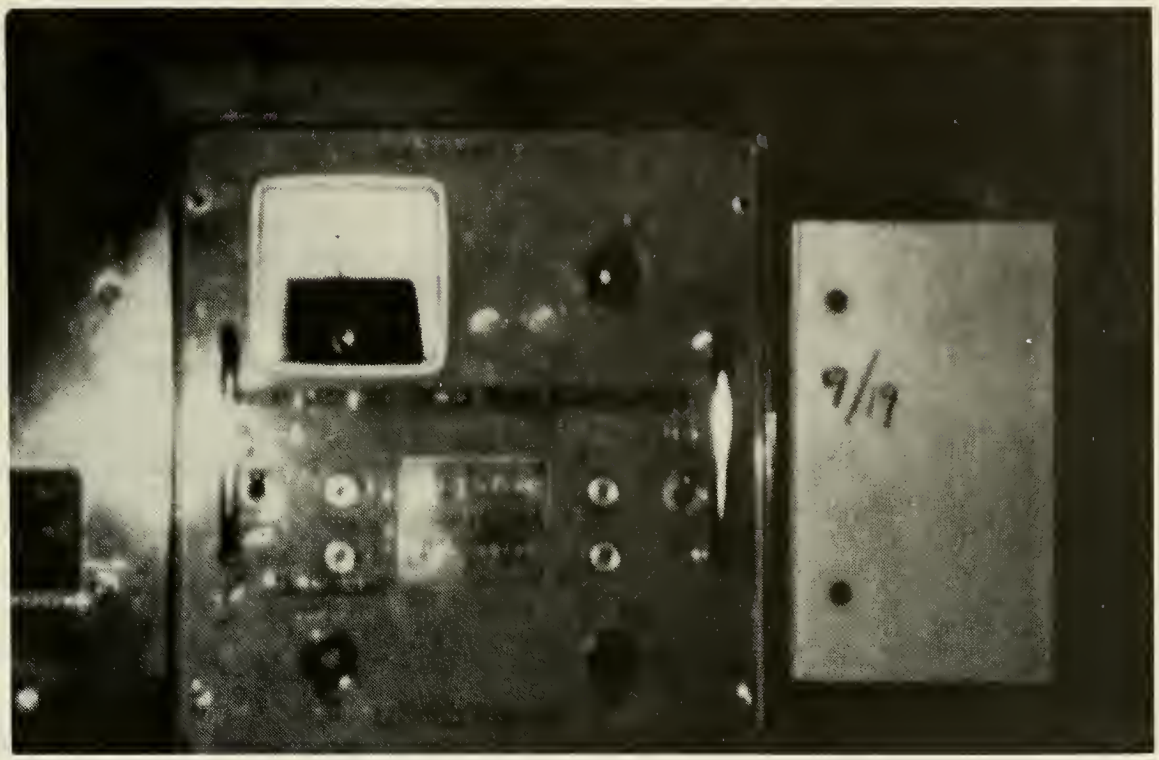

Figure B-10. Close-up of wind speed counter indicator.

APPENDIX C

SUMMARY OF MEASUREMENTS AND ANALYSIS

DIGITIZED DATA PERIODS:

TIME	*FLUCTUATION VARIABLES	**MEAN VARIABLES	DIGITAL TAPES
2000 Sept. 20	u'(4), A, INTA	$\bar{u}(3), \bar{t}(4), T_o, q(3)$	2
2323 Sept. 20	u'(4), A, INTA	$\bar{u}(3), \bar{t}(4), T_o, q(3)$	2
0637 Sept. 21	u'(4), A, INTA	$\bar{u}(3), \bar{t}(4), T_o, q(3)$	2

* A = Accelerometer data

INTA = Integrated upper vertical accelerometer

u'(3) = Wind fluctuation at three levels

** $\bar{u}(2)$ = mean (10 minute) wind at two levels

$\bar{t}(4)$ = mean temperature at four levels

T_o = sea surface temperature

q(2) = humidity at two levels

SPECTRAL ANALYSIS:

TIME	VARIABLES	REMARKS
2000 Sept. 20	u'(4), A(3), INTA	Run 2. Spectra of inertial subrange and accelerometers (Stable).
2323 Sept. 20	u'(4), A(3), INTA	Run 8. Spectra of inertial subrange and accelerometers by both analog and digital means. u'_1 was the only very low frequency u' signal. Selected for co-spectra, quad-spectra, phase, and coherence studies. (Neutral)
0637 Sept. 21	u'(4), A(3), INTA	Run 3. Spectra of Inertial subrange and accelerometers. Integrated accelerometers suffered poor null adjust (Unstable).

LIST OF REFERENCES

1. Cavanaugh, M. P., 1974: Examination of Shipboard Measurements of the Vertical Profiles of Mean Temperature, Humidity, and Wind Speed. M.S. Thesis, Naval Postgraduate School, Monterey, California.

2. Denman, K. L., and Miyake, M., 1973: Behavior of the Mean Wind, the Drag Coefficient, and the Wave Field in the Open Ocean, J. Geophys. Res., 78(12), 1917-1932.

3. Johnston, W. E., 1974: Estimating Boundary Layer Fluxes from Dissipations of Turbulent Kinetic Energy and Temperature Variance. M.S. Thesis, Naval Postgraduate School, Monterey, California.

4. Jones, R. D., 1971: Time Series Analysis of Analog Data by Analog-to-Digital and Digital Data Processing Methods at the Naval Postgraduate School, Monterey, California.

5. Kasales, J. A., 1973: Properties of Velocity Spectra Obtained from Shipboard Measurements, unpublished.

6. Miyake, M., M. Donelan, and M. Mitsuta, 1970: "Airborne Measurement of Turbulent Fluxes", J. Geophys. Res., 75(24), 4506-4518.

INITIAL DISTRIBUTION LIST

No. Copies

~~1. Defense Documentation Center~~ ~~2~~
~~Cameron Station~~
~~Alexandria, Virginia 22314~~

2. Library (Code 0212) 2
Naval Postgraduate School
Monterey, California 93940

3. Naval Oceanographic Office 1
Library (Code 3330)
Washington, D. C. 20373

4. Commander, Naval Weather Service Command 1
Naval Weather Service Headquarters
Washington Navy Yard
Washington, D. C. 20390

5. Professor Kenneth L. Davidson, Code 51Ds 5
Department of Meteorology
Naval Postgraduate School
Monterey, California 93940

6. Professor Thomas M. Houlihan, Code 59Hm 3
Department of Mechanical Engineering
Naval Postgraduate School
Monterey, California 93940

7. Mr. P. Vial, Code 048 1
Naval Ordnance Laboratory
White Oak
Silver Spring, Maryland 20910

8. Mr. E. Boudreaux, Code 048 1
Naval Ordnance Laboratory
White Oak
Silver Spring, Maryland 20910

9. Dr. P. Livingston 1
Applied Optics Branch, Bldg. 30
Naval Research Laboratory
Washington, D. C. 20390

10. Lieutenant William E. Johnston 1
c/o Mr. Lou Hanna
33 East Bond Street
Corry, Pennsylvania 16407

		No. Copies
11.	Mr. Steve Rinard Department of Meteorology Naval Postgraduate School Monterey, California 93940	1
12.	Mr. Robert Smith Department of Research, Code 023 Naval Postgraduate School Monterey, California 93940	1
13.	Professor Dale F. Leipper Chairman, Department of Oceanography Naval Postgraduate School Monterey, California 93940	1
14.	Lieutenant Michael P. Cavanaugh c/o Mr. James A. Cavanaugh 3607 Husted Drive Chevy Chase, Maryland 20015	1
15.	Lieutenant Patrick T. Welsh Student, Naval Destroyer School Naval Station Newport, Rhode Island 08240	3
16.	R/V ACANIA Department of Oceanography Naval Postgraduate School Monterey, California 93940	1
17.	Professor Charles L. Taylor, Code 35A Department of Meteorology Naval Postgraduate School Monterey, California 93940	1

UNCLASSIFIED
SECURITY CLASSIFICATION OF THIS PAGE (When Data Entered)

REPORT DOCUMENTATION PAGE		READ INSTRUCTIONS BEFORE COMPLETING FORM
1. REPORT NUMBER	2. GOVT ACCESSION NO.	3. RECIPIENT'S CATALOG NUMBER
4. TITLE (and Subtitle) AN INVESTIGATION OF SHIP RELATED MOTION AND ITS EFFECT ON TURBULENCE MEASUREMENTS		5. TYPE OF REPORT & PERIOD COVERED Master's Thesis; March 1974 6. PERFORMING ORG. REPORT NUMBER
7. AUTHOR(s) Patrick Timothy Welsh		8. CONTRACT OR GRANT NUMBER(s)
9. PERFORMING ORGANIZATION NAME AND ADDRESS Naval Postgraduate School Monterey, California 94930		10. PROGRAM ELEMENT, PROJECT, TASK AREA & WORK UNIT NUMBERS
11. CONTROLLING OFFICE NAME AND ADDRESS Naval Postgraduate School Monterey, California 93940		12. REPORT DATE March 1974 13. NUMBER OF PAGES 108
14. MONITORING AGENCY NAME & ADDRESS(if different from Controlling Office) Naval Postgraduate School Monterey, California 93940		15. SECURITY CLASS. (of this report) Unclassified 15a. DECLASSIFICATION/DOWNGRADING SCHEDULE

16. DISTRIBUTION STATEMENT (of this Report)

Approved for public release; distribution unlimited.

17. DISTRIBUTION STATEMENT (of the abstract entered in Block 20, if different from Report)

18. SUPPLEMENTARY NOTES

19. KEY WORDS (Continue on reverse side if necessary and identify by block number)

Atmospheric Turbulence
Turbulence Measurements
Accelerometer
Ship Motion

20. ABSTRACT (Continue on reverse side if necessary and identify by block number)

This study follows the development and initial employment of piezo-resistive accelerometers as ship motion sensors. The spectral results are discussed as they relate to concurrent measurements of wind fluctuation and temperature variance data. Both analog and digital Fourier analysis were performed. Results include co-spectra, quad-spectra, and phase and coherence plots. Biasing of mean parameters by pitching effects are also discussed.

DD FORM 1 JAN 73 1473 EDITION OF 1 NOV 65 IS OBSOLETE
S/N 0102-014-6601
(Page 1)

UNCLASSIFIED
SECURITY CLASSIFICATION OF THIS PAGE (When Data Entered)

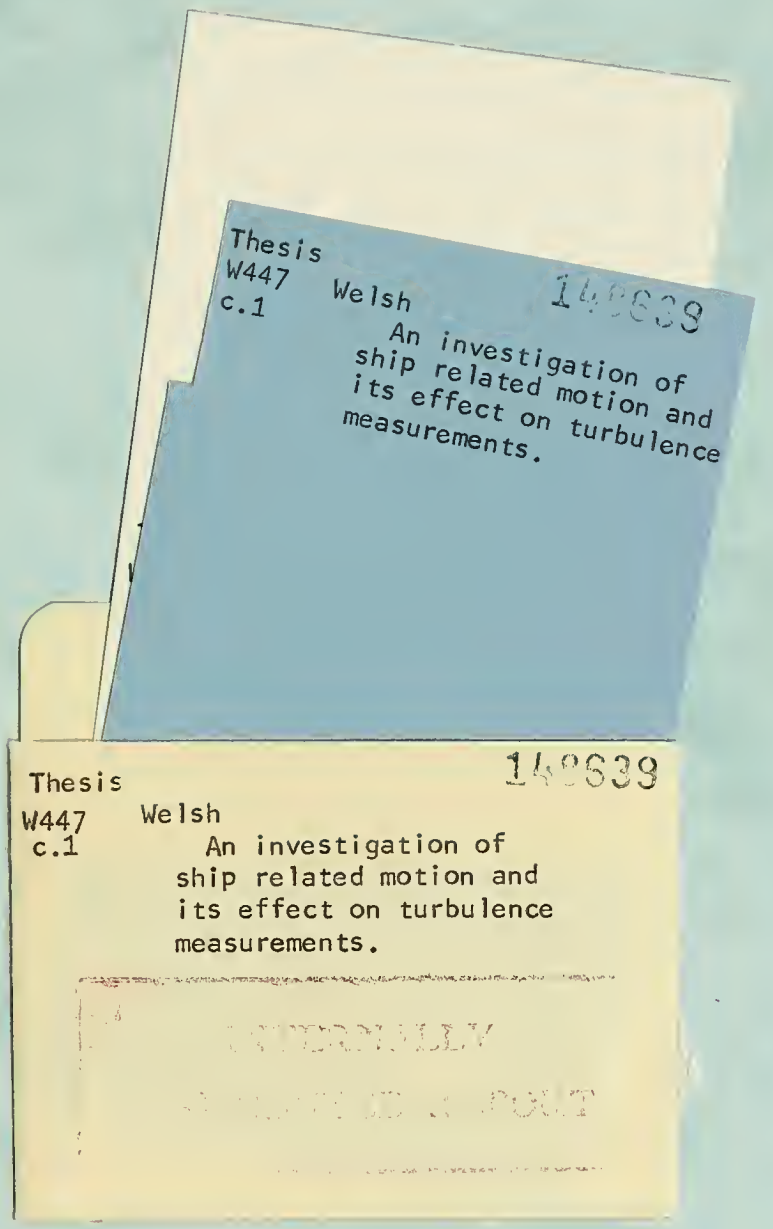
Thesis
W447
c.1
Welsh
An investigation of ship related motion and its effect on turbulence measurements.
Thesis
W447
c.1
Welsh
An investigation of ship related motion and its effect on turbulence measurements.